ANNUAL REPORT

2001

CORROSION RESEARCH

Materials Science and Engineering

Published

by

THE CORROSION RESEARCH GROUP HOKKAIDO UNIVERSITY For additional copies and more information, please write to the group members

Prof. T. Ohtsuka; CORROSION ENGINEERING LABORATORY

Prof. M. Seo; INTERFACIAL ELECTROCHEMISTRY LABORATORY

Prof. T. Narita; DISSIMILAR MATERIALS INTERFACE ENGINNEERING LABORATORY

Prof. H. Takahashi; INTERFACE MICRO-STRUCTURE ANALYSYS LABORATORY

Prof. H. Konno: LABOLATORY OF ADVANCED MATERIALS CHEMISTRY

Assoc. Prof. Hiroki Tamura

Graduate school of Engineering, Hokkaido University Kita 13 Nishi 8, Kita-ku, Sapporo 060-8628, Japan

Prof. F. Watari; DENTAL MATERIALS AND ENGINEERING LABORATORY

Graduate School of Dental Medicine, Hokkaido University

Kita 13 Nishi 7, Kita-ku, Sapporo 060-8586, Japan

Prof. Emeritus Norio Sato

Hanakawa-Kita 1-3, Ishikari 061-8211, Japan

CONTENTS

Page
CURRENT ACTIVITIES and PRESENTATIONS
CORROSION ENGINEERING LABORATORY 3
INTERFACIAL ELECTROCHEMISTRY LABORATORY · · · · · · · · · 11
DISSIMILAR MATERIALS INTERFACE ENGINEERING LABORATORY · · · · · · 21
INTERFACE MICRO-STRUCTURE ANALYSYS LABORATORY · · · · · · · · 29
DENTAL MATERIALS AND ENGINEERING LABORATORY · · · · · · · 44
LABOLATORY OF ADVANCED MATERIALS CHEMISTRY · · · · · · · · · · · · · · · · · · ·
OTHER CORRESPONDING MEMBERS
NS ELECTROCHEMICAL LABORATORY
ABSTRACTS of PUBLICATIONS
CORROSION
Synergistic Effect of Three Corrosion-Resistant Elements on Corrosion Resistance in Concentrated Hydrochloric Acid
An Attempt at Preparation of Corrosion-Resistant Bulk Amorphous
Ni-Cr-Ta-P-B Alloys · · · · · · · · · · · · · · · · · · ·
Preparation of Corrosion-Resistant Amorphous Ni-Cr-P-B Bulk Alloys
Containing Molybdenum and Tantalum
Highly Corrosion-Resistant Ni-Based Bulk Amorphous Alloys · · · · · · · · · · · · 74
Effects of Nanoscale Heterogeneity on the Corrosion Behavior of
Non-Equilibrium Alloys · · · · · · · 75

Corrosion Behavior of Amorphous Ni-Cr-Nb-P-B Bulk Alloys in 6M HCl Solution · · · 76
Extremely Corrosion-Resistant Bulk Amorphous Alloys · · · · · · · · · · · · · · · · 77
Corrosion of Metals by Contact with Metal Oxides · · · · · · · · · · · 78
Surface Oxides Affecting Metallic Corrosion · · · · · · · · · · · · · · · · · · ·
Potential-Dimension Diagram of Localized Corrosion · · · · · · · 80
DA GORMATION - DA MODIC OVIDE BILM
PASSIVATION and ANODIC OXIDE FILM Measurement of Surface Thin Films on Electrodes by Ellipsometry
Luminescence with Band-Gap Energy by UV-Light Excitation to
Anodic Oxide Films on Titanium · · · · · 82
Nano-Mechano-Electrochemical Aspect of Passive Metal Surfaces · · · · · · · · · 83
Stress Generation During Anodic and Cathodic Polarization of
a Titanium Thin Film Electrode in pH 8.4 Borate Buffer Solution
Transport of Alkaline Cation and Neutral Species through
the α -Ni(OH) ₂ / γ -NiOOH Film Electrode · · · · · · · · · · · · · · · · · · ·
Nano-mechano-electrochemistry of Passive Metal Surfaces · · · · · · · · · · · · · · · · · · ·
Susceptibility of Local Breakdown of Passive Film Formed on Iron · · · · · · 87
Initiation of a Local Breakdown of Passive Film on Iron due to
Chloride Ions Generated by a Liquid-Phase Ion Gun · · · · · · · · · · · · · · · · · · ·
Double Zincate Pretreatment of Sputter Deposited Al Films89

Formed on Titanium During Potential Sweep · · · · · · · · · · 90	
Effect of Anodic Oxide Film Structure on The Prevention of Electroless Ni-P Deposition on Al 5052 Alloy	
Repairing of Anodic Oxide Films on Al - Zn Alloy Coated Steel After Removal with Photon Rupture in Solution	
Morphology and Composition of Layered Anodic Films on InP93	
Enrichment of Alloying Elements Beneath Anodic Oxides: Investigation of Ta-1.5 at.% Cu Alloy	
Behaviour of Bismuth During Simulated Processing of Model Aluminium Capacitor Foils	
History Effects in Anodic Oxidation of Al-W Alloys96	
Role of Oxygen Bubble Generation in Anodic Film Growth on InP97	
Influence of Current Density in Anodizing of an Al-W Alloy	
Influence of Surface Treatment on Detachment of Anodic Films from Al-Mg Alloys · · 99	
Influence of Interfacial Depth on Depth Resolution During GDOES Depth Profiling Analysis of Thin Alumina Films	
Migration of Oxalate Ions in Anodic Alumina · · · · · · · · · · · · · · · · · · ·	
Reproducibility in r.fGDOES Depth Profiling Analysis of Thin Films	

The Stability and Breakdown of Passive Oxide Films on Metal Anodes · · · · · · · · 103
Ion Selective Lust Layers and Passivation of Metals · · · · · · · · · · · · · · · · · · ·
Surface Oxide Films Affecting Metallic Corrosion
The Stability and Breakdown of Passive Oxide Films on Metals · · · · · · · · 106
On Long-Term Extrapolation of Passive Behavior · · · · · · 107
The Behaviour of Iron During Anodic Oxidation of Sputtering-Deposited Al-Fe Alloys 108
CHARACTARIZATION of SURFACE and INTERFACE
Water Layer in Course of Corrosion of Copper in Humid Air Containing SO ₂ ······ 109
and any or the Common of Company of the Common of the Comm
Durable Al-Zn Coating on Steels by Two-step Hot Dipping · · · · · · · · · · · · 110
Anodizing of Aluminum Coated with Silicon Oxide by a Sol-Gel Coating
Anodizing of Aluminum Covered with SiO ₂ by Sol-Gel Coating - Formation
Mechanism of Composite Oxide Films with High Potential Sustainability
Formation of Nickel Dispersed Carbon Spheres from Chelate Resin
and Their Magnetic Properties · · · · · · · · · · · · · · · · · · ·
Synthesis and Structure of Novel Cr ^V -Cr ^{VI} Mixed Valence Compounds,
Nd _{1-x} Ca _x CrO ₄ (x=0.02-0.20) · · · · · · · · · · · · · · · · · · ·
Characterization of Rust Layers of Weathering Steels Exposed to
the Atmosphere for 17 Years · · · · · · · · · · · · · · · · · · ·
Mechanism of Hydroxylation of Metal Oxide Surfaces

A Kinetic Model of the Dissolution of Copper(II) Oxide in EDTA Solutions
Considering the Coupling of Metal and Oxide Ion Transfer
Modeling of the Kinetics of Metal Oxide Dissolution with Chelating agents
Glow Discharge Optical Emission Spectroscopy – a Powerful Tool
for the Study of Compositional Non-Uniformity in Electrodeposited Films · · · · · · · 119
ELECTROCHEMISTRY
Electron Transfer of Mangnese Hologenayed Tetraphynilporphyrin
Derivatives Assembled on a Gold Electrode
A Bipolar Electrode Cell for Aluminum Electrorefining
Cathodic Decomposition and Changes in Surface Morphology of InP in HCl · · · · · · 122
Cathodic Decomposition and Anodic Dissolution and Changes in
Surface Morphology of n-Type InP in HCl
Analysis of Anodic Current Transient and Beam Deflection Transient
Simultaneously Measured from Pd Foil Electrode Pre-charged with Hydrogen · · · · · · 124
Analysis of Stresses Generated during Hydrogen Transport through
a Pd Foil Electrode under Potential Sweep Conditions
Characterization of Pd Electrode Surface Modified by Phase
Transformation-induced Plastic Deformation using Fractal Geometry · · · · · · · 126
An SECM Observation of Dissolution Distribution of Ferrous or
Ferric Ion from a Polycrystalline Iron Electrode · · · · · · · · · · · · · · · · 127
In-situ Glow Discharge Spectroscopy of Stainless Steel in Electrolyte···········128

Application of Resistmetry to the Corrosion Study of Metals
HIGH TEMPERATURE OXIDATION and SULFIDATION
Effect of Water Vapor on the Oxidation Properties of Sintered
Fe-3mass%SiO ₂ in air at 1273K······130
Effect of Water Vapor on the Oxidation Behavior of Fe-1.5mass%Si Alloy
in Air at 1073 and 1273K · · · · · · 131
Oxidation Behavior of Sulfidation Processed TiAl-2at%X
(X=V, Fe, Co, Cu, Nb, Mo, Ag, and W) Alloys at 1173K in air · · · · · · · · · · 132
Competitive effect of water vapor and oxygen on oxidation of
Fe-5mass%Al alloy at 1073K · · · · · · 133
Effects of Temperature and Atmosphere for Dissolution of Cr Carbide
Precipitate near the Surface on Fe-Cr-C alloy · · · · · · · · · · · · · · · · · · ·
Sulfidation Behavior of a Thermal Barrier Coating at 1173K in H ₂ S-H ₂ Gas
Mixture with a 10 ^{-0.65} Pa Sulfur Partial Pressure
Application of Rhenium Coating as a Diffusion Barrier to Improve
the High Temperature Oxidation Resistance of Nickel-Based Superalloy · · · · · · · 136
Oxidation Behavior of Plasma Sprayed Co Ni Cr Al Y/YSZ Film at
1173K and 1273K in Air137
Effect of Water vapor on the Oxidation Behavior of Fe-0.5 and 5 mass%
Ni Alloys in air at 1273K · · · · · · 138
High-Temperature Corrosion Resistance of Al-Re and Re Coating · · · · · · · · 139
Synthesis and Oxidation Resistance of a Re Silicide140

Silicides as Coatings Having High Oxidation Resistance · · · · · · · · · · · · · · · · · · ·
The Sulfidation and Oxidation Behavior of Sputter-Deposited
Nb-Al-Cr Alloys at High Temperatures · · · · · · · · · · · · · · · · · · ·
SURFACE FINISHING and MICRO FABRICATION
Local Surface Modification of Aluminum by Laser Irradiation · · · · · · · · · · · · · · · · · 143
Formation of Composite Oxide Films on Aluminum by Sol-Gel Coating
and AnodizingFor the Development of High Performance Aluminum
Electrolytic Capacitors-**** 144
Fabrication of Micropores and Grooves on Aluminum by
Laser Irradiation and Electrochemical Technique · · · · · · · · · · · · · · · · 145
Fabrication of Grooves on Aluminum Surface with Atomic Force Microscope Probe Processing · · · · · · · · · · · · · · · · · · ·
Fabrication of Grooves on Aluminum Surface with Atomic
Force Microscope Processing · · · · · · 147
Fabrication of Fine Pattern Coils by Anodizing, Laser Irradiation,
and Metal Deposition · · · · · · · · · · · · · · · · · · ·
Fabrication of Printed Circuit Board by Anodizing of Aluminum · · · · · · · · · 149
Fabrication of New Type Plastic Injection Mold by Anodizing,
Laser Irradiation and Ni-P Electroless Plating · · · · · 150
Formation of B/C Composites Containing B ₄ C from Sugar-organoborane Complexes · 151

Formation of Graphite Crystals at 1000-1200°C from Mixtures of
Vinyl Polymers with Metal Oxides · · · · · · · 152
The Electronic and Magnetic Properties of LaCrO ₄ and Nd _{1-x} Ca _x CrO ₄ (x=0-0.2)
and Their Conduction Mechanism · · · · · · · · · · · · · · · · · · ·
Synthesis, Structure and Defects of Rare Earth Chromates(V),
RE _{0.9} CrO _{3.85} (RE=Gd, Yb and Y) · · · · · · · · · · · · · · · · · ·
Carbonization and Graphitization of the Kapton-type Polyimide Film
with Boron-bearing Functional Groups
Formation of β -SiC from Exfoliated Graphite and Silicone
Structure of EuCrO ₄ and Its Electronic and Magnetic Properties · · · · · · · 157
Nanocrystalline Manganese-Molybdenum-Tungsten Oxide Anodes
for Oxygen Evolution in Seawater Electrolysis · · · · · · · · 158
Composition and Structure of Enriched Alloy Layers in
Filmed Al Alloys Studied by Medium-Energy Ion Scattering · · · · · · · 159
Advanced Materials for Global Carbon Dioxide Recycling · · · · · · · 160
Compositional and Morphological Imaging of Laser Irradiated Human Teeth
by Low Vacuum SEM, Confocal Laser Scanning Microscopy and Atomic
Force Microscopy · · · · · · · · · · · · · · · · · · ·
Gradient Tissue Reaction Induced by Functionally Graded Implant
Tissue Reaction around Metal Implants Observed by X-ray
Scannning Analytical Microscope · · · · · · · 163

Visualization and Detectability of Rarely Contained Elements in Soft Tissue
by X-ray Scanning Analytical Microscopy and Electron Probe Micro Analysis · · · · · · 164
Biocompatibility and Osteogenesis of Refractory Metal Implants,
Titanium, Hafnium, Niobium, Tantalum and Rhenium · · · · · · · · · · · · · · · · · · ·
The Size Dependences and Vital Reaction against Minute Particles of
Titanium in vivo and in vitro · · · · · · · · · · · · · · · · · · ·
Fabrication of a Functionally Graded Dental Composite Resin Post and
Core by Laser Lithography and Finite Element Analysis of its Stress
Relaxation Effect on Tooth Root · · · · · 167
Radiation Effects of Carbon Ions and Gamma Ray on UDMA Based Dental Resin · · · · 168
SOLIDIFICATION
Effect of Cooling Rates on Microstructures of Binary Sn-Ag Solder · · · · · · · · 169
Aging Behavior of a Sn-Bi Eutectic Solder at Temperature between 233 and 373 K · · · 170
Isothermal Solidification Behavior During the Transient Liquid
Phase Bonding Process of Nickel Using Binary Filler Metals · · · · · · · 171
Numerical Simulation of Solidification for Aluminum Base Multi-Component Alloy · · 172
Application of Thermodynamics Analysis to the Heat Transfer Simulation
for Multi-Component Alloy Casting · · · · · · · · · · · · · · · · · · ·





CORROSION ENGINEERING LABORATORY

Prof. Dr. Toshiaki Ohtsuka

TEL/FAX: +81-11-706-6351

E-mail: ohtsuka@elechem1-mc.eng.hokudai.ac.jp

Assoc. Prof. Dr. Takeshi Sasaki

TEL: +81-11-706-6352

FAX: +81-11-706-7813

E-mail:txsasaki@eng.hokudai.ac.jp

Lecturer Dr. Takenori Notoya

TEL/FAX: +81-11-706-6353

E mail: tnotoya@eng.hokudai.ac.jp

Res. Assoc. Dr. Mikito Ueda

TEL: +81-11-706-6354

FAX: +81-11-706-7813

E mail: mikito@eng.hokudai.ac.jp

Technician Dr. Shoichi Konda

TEL: +81-11-706-7236

FAX: +81-11-706-7813

E mail: konda@eng.hokudai.ac.jp

Students

M. Nagata, T.Yamada, M. Kondo, M. Satake, D. Susukida. K. Hayakawa, K. Hioki, T. Domyo, H. Ohsaki, M. Ito, H. Kikawa, M. Matsuda, T. Komatsu

Our research activities are concerned with corrosion and corrosion prevention of metals and modeling of artificial photosynthesis system.

Research programs in progress are as follows:

(1) New corrosion resistive films consisting of conductive polymers

A composite film consisting of poly-pyrrol and polymolibdate acid was electrochemically formed on steel electrodes. The poly-pyrrol films functions as an anodic protective films on which oxygen reduction is accelerated and the passivation oxide is formed at the steel/ polypyrrol interface. The poly-molibdate anion incorporated in the films facilitates the formation of the oxide film.

A corrosion test was done for the steels coated by the composite films in 3% NaCl aqueous solution. The pitting potential estimated from the anodic sweep measurement in the NaCl solution shifts to the positive potential by 0.2 to 0.4 V with the coating. The degradation of the composite film was measured by potential decay and change of impedance spectra during immersion in the NaCl solution. It is estimated that the degradation is caused by reduction of the polypyrrole accompanied by dissolution of polymolibdate anion to the aqueous solution.

(2) Artificial model for photosynthesis

In the bioreaction, the quinone and porphyrin derivatives play a large role in electron and /or proton transfer for energy production. Electron transfer from Mn porphyrins in the self-assembled monolayer (SAM) to gold electrodes was studied by cyclic voltammogram and potential modulation reflectance or electroreflectance (ER). The rate constants (ie., the turn-over number of electron transfer) of the redox reaction of Mn(II) and Mn(III) in the various porphyrin derivatives was measured from the relation between complex ER signal and AC frequency. The rate constant thus estimated greatly depends on the association between the porphyrin units. For example, introduction of Cl species around the porphyrin induces relatively high rate constant, probably because the steric hindrance of the large size of Cl species weakens the association between the porphyrins.

(3) Monitoring of corrosion layer on zinc by Raman spectroscopy

Formation of the corrosion layer on zinc in a model atmosphere was monitored by Raman scattering spectroscopy. Under the presence of NaCl, aqueous ZnCl₂ layer is at first formed by the electrochemical reaction between zinc and oxygen in the water layer adsorbed from the humid air. When the concentration of ZnCl₂ in the aqueous surface layer increases and reaches the saturation, simonkolleite begins to form. The transient in the Raman peak intensities of the aqueous ZnCl₂ layer and simonkolleite was measured. It is found that the time until the formation of simonkolleite largely depends on the humidity in the surrounding air.

(4) Evaluation of corrosion rate of steels in solutions containing snow-melt salts

Corrosion Rate of Steels was evaluated in solutions containing snow-melt salts of NaCl-CaCl₂ and NaCl-MgCl₂ by an electrochemical polarization technique. To prevent the corrosion, various inhibitors were added to the salts. The poly-phosphate salt was found to be an effective candidate of inhibitors for decreasing the corrosion loss in this solution.

(5) Improvement of corrosion resistance of TiAl inter-metallic compound by coating of Al-Cr alloy from a molten salt electrolysis

A coating layer of Al-Cr alloy was cathodically formed at 423 K on the TiAl inter-metallic compound in an AlCl₃-NaCl-KCl molten salt mixture containing CrCl₂. A large improvement for oxidation resistance of the TiAl compound at 1173 K was obtained by the coating of the Al-Cr alloy layer.

(6) Electrophoretic deposition for preparation of functional oxide films

Oxide powder with perovskite structure was deposited electrophoretically in an organic solvent to prepare the oxygen permeability membrane. For estimation of the electrophoretic deposition mechanism, a potential profile in the organic solution containing the oxide powder was measured by a probe electrode the position of which can be controlled. It was found that a potential drop about 15 V

was required for electrophoretic deposition of the oxide powders at the solution/ electrode interfacial layer.

(7) Corrosion products of tin in humid air containing SO₂ and/or NO₂.

Surface layers initially formed on tin in air containing SO_2 and/or NO_2 were investigated by in situ IR-RAS. The XPS and Raman spectroscopic measurements were also carried out for supplementation. The test was carried out in air of $80\sim 90\%$ RH(relative humidity) containing $1\sim 20$ ppm SO_2 and/or NO_2 gases. Corrosion products were rapidly grew in air containing NO_2 , whereas almost no corrosion proceeded in the environment containing SO_2 . The corrosion products in air containing NO_2 were nitrate, hyponitrite and tin oxides. The synergistic effect of SO_2 and NO_2 on the corrosion rate was not observed.

(8) Adsorption of water on Fe(III) oxyhydroxide.

For the fundamental understanding of corrosion process of steel, the interaction between Fe(III) oxyhydroxide and water vapor was investigated by measuring the mass change with time with QCM. The α -, β - and γ - oxyhydoxides, which were synthesized by usual way, were coated on the surfaces of QCM elements, and the resonance frequency was followed in air with various amounts of humidity. The amount of adsorbed water per mass of the α -, β - and γ - oxyhydoxides increased in that order. The crystallographic property and the physicochemical property of the surface of the oxyhydoxides were under investigation.

(9) Adsorption of thiourea on a gold electrode in perchloric acid.

Adsorption of thiourea on gold in perchloric acids and its structure changes with potential variation were investigated using in situ surface-enhanced infrared absorption spectroscopy (SEIRAS) together with the electrochemical technique. Ab initio molecular orbital (MO) calculation was also conducted to assist the estimation of the molecular structure from the spectra. Infrared spectra obtained in the range under 0.4V showed that there were two kinds of adsorbed states of thiourea; one was specifically adsorbed thiourea through sulfur atom and the other was molecules forming mercaptide bond with gold. In the potential from 0.4V to 0.6V, specifically adsorbed thiourea molecules were subjected to one-electron oxidation. On the other hand, the adsorbed molecules originated from thiol type

were unchanged. In the range over 0.6V, both adsorbed species were subjected to four-electron oxidation to form the same chemical species.

Other activities

Prof. Ohtsuka attended the 2nd Intern. Conf. on Environment Sensitive Cracking and Corrosion Damage, Hiroshima, 29 Oct.-2 Nov., 2001 and presented a paper entitled by Luminescence with Band Gap Energy by UV-Light Excitation to Anodic Oxide Films on Titanium. Prof. Sasaki and Mr. Domyo attended the 3rd International Conference on Application of Conducting Polymers (3rd ICCP), Mishima/ Japan, 26 - 28 November 2001 and presented a paper entitled by Polypyrrole-polymolybdate Composite Film for the Corrosion Protection of Steels. Prof. Sasaki attended the 12th Asian-Pacific Corrosion Control Conf. 2001, Seoul/Korea, October 2001 and presented a paper entitled by Water Layer in Course of Corrosion of Copper in Humid Air Containing SO₂.

Dr. Ueda had visited the laboratory of Prof. Plieth in TU-Dresden/ Germany since November 2000 as a Monbusho fellowship researcher. He studied a theme on preparation of silver nano-particles by electrodeposition and returned in November 2001.

Presentations

Recovery of Aluminum Metal from Aluminum Dross by Molten Salt Electrolysis; S. Tsukamoto, M. Ueda, S. Konda, T. Ohtsuka: The Joint Meeting of The Hokkaido Sections of ECS Jpn, Surf. Finish. Soc. Jpn, and Jpn Soc. Corros. Eng., Sapporo, Jan., 2001.

1-[(2-ethylhexilamino)methyl]benzotriazole as a Film Forming Inhibitor of Copper; M. Satake, T. Notoya, and T. Ohtsuka: The Joint Meeting of The Hokkaido Sections of ECS Jpn, Surf. Finish. Soc. Jpn, and Jpn Soc. Corros. Eng., Sapporo, Jan., 2001.

Rust of the Steels; T. Ohtsuka: Annual Meeting of Hokkaido Section of Soc. of Material Sci. Jpn, Sapporo, March, 2001.

Self-organization of Mn Porphyrin Derivatives and their Electron Transfer; T. Yamada, M. Nango, and T. Ohtsuka, The 79th Spring Meeting of Chem. Soc. Jpn Kobe, March, 2001.

Self-organization of Porphyrin Derivatives Bound to Polyechileneimin and their Electron Transfer; M. Nagata, T. Ohtsuka, M. Kondo, and M. Nango: The 79th Spring Meeting of Chem. Soc. Jpn, Kobe, March, 2001.

Potential Modulation Reflectance of Self-organized Porphyrin Monolayer Electrocde; T. Yamada, M. Nango, T. Ohtsuka: The 68th Annual Meeting of Electrochem. Soc. Jpn., Kobe, April, 2001.

Luminescence from Titan Anodic Oxide Films by Band-Gap Photo-Excitation: M. Ueda and T. Ohtsuka, The 68th Annual Meeting of Electrochem. Soc. Jpn., Kobe, April, 2001.

Oxidation Behavior of Al-Ti Coated by Al-Cr Alloy in AlCl₃-NaCl Molten Salt: D. Susukida, M. Ueda, S. Konda, and T. Ohtsuka, The 68th Annual Meeting of Electrochem. Soc. Jpn., Kobe, April, 2001.

1-[(2-ethylhexilamino)methyl]benzotriazole as an Inhibitor for Copper and Copper Alloys: M. Satake, T. Notoya, and T. Ohtsuka, The 2001 Annual Meeting of Jpn Soc. Corros. Eng., Tsukuba, May, 2001.

Electron Transfer in Various Mn Porphyrin Monolayers on Gold Electrodes: T. Yamada, T. Ohtsuka, and M. Nango, The 2001 Fall Annual Meeting of Electrochem. Soc. Jpn., Tokyo, Sept., 2001.

Raman Spectra of Atmospheric Corrosion Products on Zn in the presence of NaCl: T. Ohtsuka and K. Shoji, The 48th Discussion Meeting of Jpn. Soc. Corros. Eng. Sapporo, Sept. 2001.

Corrosion of Tin in Air Containing NO₂ and SO₂: T. Sasaki, R. Kanagawa, T. Ohtsuka, and K. Miura, The 48th Discussion Meeting of Jpn. Soc. Corros. Eng. Sapporo, Sept. 2001.

Water Layer for Corrosion Progress of Copper in Air Containing SO₂: J. Ito, T. Ssaaki, and T. Ohtsuka, The 48th Discussion Meeting of Jpn. Soc. Corros. Eng. Sapporo, Sept. 2001.

Al-Cr Alloy Electrodeposition on TiAl – The Effect of Deposition Layer on Corrosion Resistance in the High Temperature Environment: D. Susukida M. Ueda, S. Konda, and T. Ohtsuka, The 48th Discussion Meeting of Jpn. Soc. Corros. Eng. Sapporo, Sept. 2001.

Corrosion Prevention of Steel by Polypyrrole-Polymolybdic Acid Composite Coating: T. Domyo and T. Ohtsuka, The 48th Discussion Meeting of Jpn. Soc. Corros. Eng. Sapporo, Sept. 2001.

Current Activities and Presentations

Corrosion Behavior of Carbon Steels in the Solution Containing Chloride Snow-Melting Media: S. Konda, T. Ohtsuka, and M. Kubota, The 48th Discussion Meeting of Jpn. Soc. Corros. Eng. Sapporo, Sept. 2001.

Al-Cr Alloy Electroplationg on TiAl from AlCl₃-NaCl-KCl Molten Salt –Effect on Pretreatment of TiAl: D. Susukida, M. Ueda, S. Konda, and T. Ohtsuka, The 33rd. Symp. On Molten Salt Chemistry of Japan, Niigata, November, 2001.

Raman Spectra of Atmospheric Corrosion Products of Zinc under Chloride Environment: T. Ohtsuka, K. Shoji, M. Matsuda, Symposium on Prevention mechanism of Zinc Coated Steels, Tokyo, Oct., 2001.

Luminescence with Band Gap Energy by UV-Light Excitation to Anodic Oxide Films on Titanium: M. Ueda and T. Ohtsuka, The 2nd Intern. Conf. on Environment Sensitive Cracking and Corrosion Damage, Hiroshima, Oct.-Nov., 2001.

Water Layer in Course of Corrosion of Copper in Humid Air Containing SO₂: T. Sasaki, J. Ito, and T. Ohtsuka, The 12th Asian-Pacific Corrosion Control Conf., Seoul, Korea, Oct., 2001

Polypyrrole-polymolybdate Composite Film for the Corrosion Protection of Steels: T. Domyo, T. Sasaki, and T. Ohtsuka, The 3rd International Conference on Application of Conducting Polymers(3rd ICCP), Mshima, Nov., 2001.

T. Yamada, M. Nango and T. Ohtsuka, Simposium on Monbukagakusho Electron Transfer of Various Manganese Porphyrin Monolayers on Gold Electrodes: 4th Seminar "Organization of Photoenergy Transfer System and Its Function Analysis for Artificial Photosynthesis", Toba, December, 2001.

INTERFACIAL ELECTROCHEMISTRY LABORATORY

Prof. Dr. Masahiro Seo TEL/FAX: +81-11-706-6735

E-mail: seo@elechem1-mc.eng.hokudai.ac.jp

Assoc. Prof. Dr. Kazuhisa Azumi TEL/FAX: +81-11-706-6736

E-mail: azumi@elechem1-mc.eng.hokudai.ac.jp

Res. Assoc. Dr. Koji Fushimi TEL/FAX: +81-11-706-6737

E-mail: fushimi@elechem1-mc.eng.hokudai.ac.jp

Foreign Researcher

Dr. Joong-Do Kim and Dr. Fredrik Falkenberg

Students

M. Chiba, K. Iokibe, H. Mitani, T. Yugiri, T. Ueno, N. Kikuchi, Y. Kurata, T. Kurihara A. Kanada, M. Yamazaki and K. Yamaya

Equipments

Atomic Force Microscope: Digital Instruments Nanoscope-III

Nano-indentation Apparatus: Hysitron Inc.

EQCM System

Laser-Bending Beam Apparatus for Stress Measurement Piezo-detection Apparatus for Surface Stress Measurement Scanning Electrochemical Microsope System

The research activity of the laboratory still continues to be directed towards a better understanding of the interfacial properties of metal and semiconductor electrodes in relation to the interfacial electrochemistry involving adsorption, corrosion, passivation, anodic oxidation, hydrogen adsorption / absorption, and

surface finishing.

Current topics on research are as follows:

(1) Measurement of Changes in Surface Stress of Gold Electrode during Under-Potential Deposition of Pb

The changes in surface stress of gold electrode during under-potential deposition (UPD) of Pb in perchlorate solutions containing Pb^{2+} ions were measured by a bending beam method. The potential of electrocapillary maximum, E_{max} was observed in the course of UPD of Pb and the position of E_{max} was independent of potential sweep rate and electrolyte anion species (chloride or nitrate ions). The relation between changes in surface stress and cathodic charge for UPD showed the linearity with three steps. The deviation from the linearity was ascribed to the structural change of the UPD layer. The research of UPD processes of Pb on Au is still in progress from the view point of surface energetics.

(2) Nano-Mechano-Electrochemistry of Titanium Surfaces

The in-situ and ex-situ nano-indentation and scratching tests were performed to the titanium surfaces anodically oxidized in pH 8.4 borate solution. The hardness of the titanium surface measured under the electrochemical control at 5 V (RHE) after anodic oxidation for 1 h at 5 V (RHE) was significantly larger than that measured in air after anodic oxidation for 1 h at 5 V (RHE). The frictional coefficient of the titanium surface measured under the electrochemical control at 5 V (RHE) after anodic oxidation for 1 h at 5 V (RHE) was also larger than that measured in air after anodic oxidation for 1 h at 5 V (RHE). The increases in hardness and frictional coefficient of the titanium surface due to in-situ nano-indentation and scratching may be explained in terms of the high repassivation rate at the rupture sites of anodic oxide film under the electrochemical control at 5 V (RHE) as compared to in air after the anodic oxidation.

(3) Electrochemo-Mechanical Properties of Passive Nickel Surfaces

The nickel film with a thickness of 250 nm was prepared on one side of a thin glass plate by a magnetron sputtering. The stresses generated during anodic

oxidation of nickel thin film on the glass plate in pH 8.4 borate solution were measured by a bending beam method. The stress changed always to the tensile direction during anodic oxidation in the passive potential region, which may be ascribed to predominant transport of metal ions towards the film / solution interface during oxide film growth. The stress changed to the compressive direction by cathodic potential steps after anodic oxidation. The degree in stress change to the compressive direction was small for the cathodic potential step in the passive region, while it was large for the cathodic potential step in the hydrogen evolution region. The large changes in stress to the compressive direction due to cathodic potential step in the hydrogen evolution region were associated with hydrogen absorption into the oxide film or the nickel substrate.

(4) An EQCM Analysis of Passivation Process of Electroplated Nickel Film.

Nickel thin film was electroplated on a quartz oscillator (AT-cut, 5 MHz). The nickel thin film was anodically polarized by a potential sweep method in deaerated sulfate solutions with different pH values. The changes in current and mass during potentio-dynamic polarization of the nickel thin film were recorded simultaneously. The partial current density of nickel dissolution through the passive film, i_{Ni}^{2+} , and the partial current density of oxygen uptake for film growth, i_{O}^{2-} , could be separated each other by comparing the total current density with the mass change rate, assuming the growth of NiO film in the passive region. The ratio of i_{Ni}^{2+} to i_{O}^{2-} depended on the solution pH, i.e., the lower pH, the ratio was higher.

(5) Formation of Porous Layer on n-Type InP and Its Cathodic / Anodic Treatment The anodic etching of n-type InP (100) wafer in 0.5 M HCl was performed to form a porous layer. The porous layer with a thickness of 1.5 micro-meters, an average pore diameter of 200 nm and an average wall width between pores of 30 nm could be prepared on the InP wafer by anodic etching at 2.2 V (SHE) for 300 s. After the formation of porous layer, the wafer was cathodically polarized to induce a cathodic decomposition (InP+ 3 H⁺ + 3 e⁻ = In + PH₃) of the porous layer and then anodically polarized to induce an anodic dissolution (In = In³⁺ + 3 e⁻) of deposited In. The average pore diameter of the porous layer was increased and the average wall width between pores was decreased by the above cathodic / anodic treatment. The photo-luminescence behaviors of the porous layer before and after the

cathodic / anodic treatment are now being investigated.

(6) Direct Plating of Ni-P onto Al-Ni Alloy Films

Electroless Ni-P plating was achieved onto Al-Ni alloy films deposited on glass substrates using magnetron sputter deposition and ion-beam assisted deposition methods. At the initial stage of plating process dissolution of Al caused enrichment of Ni in the surface of the films. Ni acted as catalysis for electroless plating reaction and thus Ni-P layer was formed on the alloy films without pretreatment such as double zincate process. The quality of Ni-P plating layer depended on the concentration of Ni in the film. For Al-10Ni alloy films Ni-P particles were sometimes formed in the plating bath which grew on Ni detached from the surface of alloy films at the initial stage of plating process. For Al-3Ni and Al-1Ni alloy films smooth plating layers were obtained without formation of Ni-P particles in the plating bath.

(7) Application of Resistometry to Hydrogen Absorption into Ti

Resistometry was applied to several corrosion phenomena. One of the applications was in-situ monitoring of hydrogen absorption into Ti under the cathodic polarization in aqueous solution. Growth of hydride layer with larger electric resistance comparing with metallic Ti from the surface of the Ti specimen caused continuous increase in resistance during cathodic polarization. From the data of resistance change thickness of the Ti hydride layer was estimated. Formation of anodic oxide films did not prevent hydrogen penetration. Anodic oxide films formed at the potentials higher than the breakdown potential of ca. 7.5 V rather promoted absorption of hydrogen, probably due to formation of pathway for hydrogen transfer in the oxide films caused by microcrystallization.

(8) Formation of Metal and Semiconductor Particles from Discharging Electrodes Metal (Ti, Cu) and semiconductor (Si) electrodes were polarized at the cell voltages higher than 100 V to cause spark discharge. At the location where spark discharge occurred electrode material was melted and emitted into solution, cooled immediately to form small particles in a spherical form. The size of particles was distributed in the range from a few tenth nm to a few tenth μ m. From XRD data TiO₂ oxides of rutile, anatase and brockite type nor metallic Ti were detected for Ti

particles and Si nor SiO₂ was detected for Si particles. Suitable range of cell voltage for spark discharge had to be chosen to form such particles. At the cell voltage lower than the spark voltage surface of electrodes was continuously sputtered in a glow discharge sheath covering electrode and thus particles were not formed. If cell voltage for spark discharge was too high, electrodes were melted and deformed due to large heat of spark discharge. Currently controlling the particle size and its distribution is important subjects. It was found that the size of the particles tended to increases with increase in cell voltage.

(9) Initiation of a Local Breakdown of Passive Film on Iron due to Chloride Ions Generated by a Liquid-Phase Ion Gun.

A small amount of Cl could be locally generated from a liquid-phase ion gun (LPIG), which consists of a silver microelectrode covered with silver chloride, by cathodic polarization. The LPIG was employed to induce the local breakdown of the passive films formed on iron in deaerated borate solutions. Drawing the pattern with artificial pits and lines on electrode surface of iron or steel was attempted. A microelectrode for which molten silver chloride is solidified in a quartz glass capillary with a silver wire is developed to generate more amount of chloride ions for longer operation period than a conventional type of microelectrode.

(10) SECM Evaluation of Heterogeneous Electroactivity of Single Crystal Magnetite Electrode after Cathodic Polarization.

Carbon steel is one of the promising candidates for an over-pack in which nuclear wastes are preserved underground for a long time in Japan. However, corrosion of carbon steel accelerates with a galvanic coupling of magnetite. The roles of magnetite electrode in galvanic coupling were analyzed by scanning electrochemical microscopy (SECM). The probe electrode of SECM could successfully detect the hydrogen generated from the single crystal magnetite electrode during the galvanic coupling with carbon steel in deaerated pH 5.8 Na₂SO₄ solution. The detailed analysis indicated that hydrogen evolution and reduction of magnetite itself took place simultaneously with current efficiency of about 50%. The distribution of hydrogen generated on the magnetite electrode surface was observed with the probe current image of SECM and reflected on the heterogeneous reduction of magnetite itself such as appearance of metallic surface

sites.

Other activities

From January 15 to 22, Prof. Su-Il Pyun and Mr. J.-W. Lee (Ph.D. Student), Department of Materials Science and Engineering, Korea Advanced Institute of Science and Technology (KAIST), Korea visited this laboratory to conduct the joint research of the stresses generated on transition metal electrodes during anodic oxidation and hydrogen absorption which was financially supported by JSPS and KOSEF. From February 12 to May 13, Ms. J.-Y. Go (Ph.D. Student, KAIST) visited this laboratory to conduct the research of nano-indentation of the tantalum surface subjected to anodic oxidation. From June 3 to 7, Prof. M. Seo visited Prof. Su-Il Pyun, KAIST, Korea for the joint research. In July 22, Dr. F. Falkenberg left this laboratory to work as research associate, Department of Chemistry, G teborg University, Sweden, In September, Prof. M. Seo, Dr. K. Azumi, Dr. K. Fushimi and Dr. J.-D. Kim participated in the Joint International Meeting of the Electrochemical Society and the International Society of Electrochemistry held from September 2 to 7 in San Francisco, USA. Afterwards, Prof. M. Seo visited Profs. W. H. Smyrl, R. W. Staehle and W. W. Gerberich, Department of Chemical Engineering and Materials Science, University of Minnesota, Minneapolis and was trapped for more three days by the terrible terrorist attack in New York, September 11. From December 19 to 22, Prof. M. Seo visited Profs. C. Levgraf and G. Hultquist, Department of Materials Science and Engineering, Royal Institute of Technology, Stockholm, Sweden to act as a faculty opponent for a doctoral disputation.

The following foreign scientists visited this laboratory: Dr. B. MacDougall, Institute for Chemical Process and Environmental Technology, National Research Council Canada from February 22 to 25, Dr. W. Zidong, Department of Applied Chemistry, Chongqing University, China, Dr. D. S. Mohamed, Dr. M. A. A. El-Neairy, Chemistry Department, Faculty of Science, Cairo University, Egypt, Dr. S. M. M. El-Sheikh, Central Metallurgical Research and Development Institute, Egypt, Dr. M. L. Franco Garcia, Center of Environmental Research and Training, National Institute of Ecology, Mexico and Ms. P. D. L. Payofelin, Rizal Polytechnic College, Philippines, on June 12, Prof. I. Demetrescu, University of Politechnica, Rumania on June 18, Prof. S. G. Park, Department of Industrial and Engineering Chemistry, Chungbuk National University, Korea on June 25, Prof. M.

M. Lohrengel, Institute of Physical Chemistry and Electrochemistry, Heinrich-Heine University Dueseldorf, Germany and Dr. A. W. Hassel, Max-Planck Institute for Iron Research, Germany on October 1, and Prof. S. Hofmann, Max-Planck Institute for Metal Research, Germany on November 26.

Presentations

- M. Aihara, M. Seo and A. W. Hassel: Observation of Changes in Surface Morphology of n-Type InP Due to Cathodic Decomposition and Anodic Dissolution, The 2000 Joint Meeting of Hokkaido Section of Electrochem. Soc. Jpn., Surf. Finish. Soc. Jpn., and Jpn. Corrosion Eng., Sapporo, Jan., 2001.
- M. Kawaguchi, K. Azumi and M. Seo: Application of Glow Discharge Light Emission to the in-situ Measurement Technique, ibid.
- Y. Serizawa and M. Seo: Measurement of Electrocapillary Curve of Platinum Electrode by a Bending Beam Method, ibid.
- M. Chiba and M. Seo: The Effects of Chromate Treatment on the Mechanical Properties of Passivated Iron Surfaces, ibid.
- H. Mitani, M. Seo and S. -I. Pyun: Stress Changes Due to Cation Doping and Undoping During Mutual Conversion Processes of Ni(OH)₂ and NiOOH, ibid.
- T. Ueno, K. Azumi and M. Seo: Evaluation of Non-uniform Dissolution of Iron using Resistometry, ibid.
- Y. Kurata and M. Seo: Nano-indentation to the Titanium Surface Electrochemically Controlled in Solution, ibid.
- K. Fushimi and M. Seo: Estimation of Concentration of Chloride Ion Enriched in Localized Space, The 68th Annual Meeting of the Electrochem. Soc. Jpn., Kobe, April, 2001.
- M. Seo and Y. Serizawa: Changes in Surface Stress and Surface Strain of Platinum Electrode, ibid.

- K. Fushimi and M. Seo: Observation of Dissolution Current Image of Iron by Scanning Electrochemical Microscopy, The 2001 Annual Meeting of Jpn. Soc. Corrosion Eng., Tsukuba, May, 2001.
- M. Chiba and M. Seo: In-situ Nano-indentation to the Single Crystal Iron Surfaces Subjected to Chromate Treatment, ibid.
- K. Azumi, K. Iokibe, T. Ueno and M. Seo: Application of Resistmetry to Corrosion Monitoring, ibid.
- F. Falkenberg, K. Fushimi and M. Seo: Combination of EQCM with Liquid-Phase Ion Gun for Initiation of Local Breakdown of Passive Film on Cu, ibid.
- J.-D. Kim, S.-I. Pyun and M. Seo: Stress Generation During Anodic and Cathodic Polarization of Titanium Thin Film in pH 8.4 Borate Buffer Solution, ibid.
- M. Seo: Stress Generation during Anodic and Cathodic Polarization of Titanium Thin Film Electrode, KAIST Seminar, Taejon, Korea, June, 2001.
- M. Seo, M. Chiba and Y. Kurata: Nano-Mechano-Electrochemical Aspect of Passive Metal Surfaces, The 2001 Joint International Meeting of the Electrochemical Society and the International Society of Electrochemistry, San Francisco, USA, Sept., 2001.
- J.-D. Kim, S.-I. Pyun and M. Seo: Stress Generation During Anodic and Cathodic Polarization of a Titanium Thin Film Electrode in pH 8.4 Borate Buffer Solution, ibid.
- K. Fushimi and M. Seo: Susceptibility of Local Breakdown of Passive Film Formed on Iron, ibid.

- K. Azumi, T. Ueno, K. Iokibe and M. Seo: Application of Resistmetry to the Corrosion Study of Metals, ibid.
- M. Seo: Electrochemo-Mechanical Properties of Passive Metal Surfaces, The 48th Annual Meeting of Jpn. Soc. Corrosion Eng., Sapporo, Sept, 2001.
- H. Mitani, M. Seo and Su-II Pyun: Analysis of Mutual Conversion Processes of Ni(OH)₂/NiOOH by Mass and Stress Measurements, ibid.
- N. Kikuchi and M. Seo: Piezo-electric Detection and EQCM Analysis of Passivation Process of Electroplated Nickel Thin Film, ibid.
- Y. Kurata and M. Seo: Evaluation of Mechanical Properties of Titanium Surface by In-situ Nano-indentation, ibid.
- M. Chiba and M. Seo: Nano-Mechano-Electrochemistry of Passive Iron Surfaces by Cyclic Nano-Indentation, ibid.
- T. Ueno, K. Azumi and M. Seo: Monitoring of Hydrogen Absorption into Ti using Resistometry, ibid.
- K. Fushimi: Pursuit of Initial Local Breakdown Process of Passive Film by Using a SECM, The 134th Symposium of Jpn. Soc. Corrosion Eng. "Corrosion of Thin Metal Films and Measurement of Localized Corrosion", Sapporo, Sept. 2001.
- M. Seo: Changes in Surface Stress of Noble Metal Electrodes and Specific Adsorption of Electrolyte Anions, Seminar of Research Center of Catalysis, Hokkaido University, Sapporo, Nov., 2001.

DISSIMILAR MATERIALS INTERFACE ENGINEERING LABORATORY

Foreign Researchers

Yu Zhiming ,Han Xue, and Zane Zhenyu Liu

Students

F. Lang, S. Gun Su, M. Fukumoto, T.Izumi K.Ono, T.Kobayashi, Y.Natsume, S.Najima, D.Yoshida, H.Shirosawa, S.Tominaga, S.Narita T.Nishimoto Y.Matsumura, D.Iino, and Y.Nishiguchi

The research activities of the laboratory are directed to an understanding of the mechanism of the high temperature corrosion in super alloys, inter-metallic compounds and iron-based alloys, and to the development of the corrosion resistant alloys and corrosion protection of materials with coating and surface modification.

The research activity is also directed to an understanding of the solidification mechanism of metals and Alloys.

Current topics on research are in the following:

(1) High temperature sulfidation of alloys.

Sulfidation properties of stainless steels, nickel alloys, and Ti-Al intermetallic compounds were investigated at relatively low sulfur pressures in H₂S-H₂ atmospheres.

(2) High temperature oxidation resistance of sulfidation processed Ti-Al alloys. High temperature oxidation behavior of sulfidation processed Ti-Al intermetallic compound was investigated. Effect of the third element addition on the oxidation behavior was extensively investigated.

(3) High temperature corrosion under the atmosphere containing water vapor.

Oxidation behavior in Fe-Al and Fe-Si alloys under the atmosphere containing water vapor was studied. Acceleration of the oxidation was observed and its mechanism was investigated.

(4) Effect of Re coating on high temperature oxidation of super alloy.

Re was coated on the surface of a super alloy, and the oxidation behavior of the alloy was examined. A new method for coating Re on the surface of alloys based on electric plating was also investigated.

(5) Characterization of thermal barrier coatings

Thermal barrier coatings of the NiCrAlY-Zirconia composite were prepared by using Plasma Splay Coating Method and their mechanical and physical properties were investigated.

(6) Galvanizing process of steels by two step hot dipping.

Galvanizing of steels was carried out by using a Zn-Al and a Zn-Al-Mg-Si molten alloys, and the optimum condition was investigated to make the galvanized

layer having high corrosion resistance.

(7) Pb-free solder.

Change in microstructure of a Pb-free solder due to composition and cooling rate during solidification was investigated. Effect of heat treatment on elastic modulus, microstructure and hardness of the solder was studied.

(8) TLP Bonding.

Dissolution and isothermal solidification behavior during transient liquid phase bonding process of Ni and Ni base alloys was investigated based on both experiment and computer simulation.

(9) Prediction of solidification structure of casting.

A method to simulate the macro structure of a casting was investigated by combining thermodynamics analysis, heat transfer calculation and Monte-Calro Method

(10) Simulation of microstructure development in solidifying alloy by Phase-field model.

The dendrite growth in the solidification process of an alloy was investigated by using a Phase-field Model. Change in dendrite morphology due to thermal, solutal and fluid flow conditions was examined.

Other activities

In April, Dr Yoshioka joined the laboratory as a post-doctoral researcher. In October, Mr. Segawa from Nihon Tokusyu Tohgyou Ltd. joined the laboratory as a visiting researcher. In October, Mr. Fukumoto quitted the graduate school and became a Research Associate at the Akita University. In October, Mr. Han Xue entered the graduate school of Hokkaido University. In December, Prof. Yu Zhiming returned to China and Dr. Zane Zhenyu Liu joined the laboratory as a visiting researcher.

Prof. Narita attended International Conference on The 4th Surface Science and Engineering, Chennai, India, February $19\sim25$, 2001. In March $3\sim20$, Prof.

Current Activities and Presentations

Narita visited to Prof. Nichools in Cranfield University, England, Prof. Schutze in DESHEMA, Germany, Prof. Montgomery in University of Denmark, Denmark and attended International Conference on NACE, Houston, USA. In April 14~18, Prof. Narita visited to Dr. Deevi in Chrysalis Technologies, Richmond, USA. In July 14~28, Prof. Narita visited to Prof. Gleeson in Iowa State University, USA, Dr.Graham in NRC Ottawa, Canada and attended Gordon Research Conference on High Temperature Corrosion along with Mr.Hayashi, Mr.Takahashi and Mr.Fukumoto. In October 8~18, Prof.Narita visited to Prof. Kim in Chungnam national University, Korea, Prof. Yun in Changwom University, Korea and attended The 12th Asian-Pacific Corrosion Control Congress, Seoul, Korea.

Presentations

Anti-Oxidation Property of Re Coated Nb-Mo-W Alloy; M.Fukumoto, S.Hayashi, K.Ohsasa, T.Narita, K.Sakamoto, A.Kasama and R.Tanaka: The Winter Joint Meeting of The Hokkaido Secs. of Jpn. Inst. Metals and Iron and Steel Inst. Jpn., Muroran, Jan., 2001.

Surface Modification of TiAl Alloy by Cr, Al Cementation Method; T.Izumi, T.Nishimoto, and T.Narita: ibid.

Annealing of the Cu Plate Immersed in Pb Free Solder; S.Saitoh, T.Yamamoto, T.Takashima, J.Tanaka and T.Narita: ibid.

Change in the Melting Depth of Substrate during Reactive Welding of NiAl; K.Matsuura, K.Ohsasa, M.Kudoh etc.: ibid.

Effect of Cr Contents for the High Temperature Corrosion of Ni-high Cr Alloys in the Atmospheres Containing 0.1%HCl, S.Najima, S.Hayashi, T.Narita, M.Noguchi, H.Yakuwa, and S.Kawamura; The 128th Annual Meeting of Jpn. Inst. Metals; Narashino, Mar., 2001.

Effect of Oxygen Content of Alloy Surface on Oxidation Resistance of Sulfidation Processed TiAl Alloys; T.Izumi, and T.Narita: ibid.

Inhabitation of High Temperature Oxidation of Fe-5mass%Al Alloy by the Oxygen in the Atmospheres Containing Water Vapor; S.Hayashi and T.Narita: ibid.

Surface Modification of TiAl Alloy by Cr,Al Pack Cementation Method; T.Nishimoto, T.Izumi and T.Narita: ibid.

Effect of Re Concentration on Oxidation of Re Coated Nb-Mo-W Alloy; M.Fukumoto, S.Hayashi, T.Narita, K.Sakamoto, T.Yi, A.Kasama and R.Tanaka: ibid.

Analysis of Dendrite Growth of Fe-C binary Alloy under Fluid Flow by Phase-field Method; Y.Natsume, K.Ohsasa and T.Narita: The 141th Annual Meeting of Iron and Steel Inst. Jpn., Narashino, Mar., 2001.

Melting Reaction at the Interface between Carbon Steel and Zn-Al melt; K.Ono, J.Tanaka and T.Narita: ibid.

The Evaluation of Nucleation Frequency of Al base alloys for the Prediction of Casting Structure; H.Shirosawa, K.Ohsasa and T.Narita: The 138th Annual Meeting of Jpn. Foundry Engineering Soc., Narashino, May, 2001.

The Evaluation of Heterogeneous Nucleation Frequency in Casting Alloys; H. Shirosawa, K. Ohsasa and T. Narita: Annual Meeting of Hokkaido Sec. of Jpn. Foundry Engineering Soc., Muroran, Jun., 2001.

Oxidation Resistance of TiAl Alloy Improved by Cr,Al Pack Cementation Method; T.Nishimoto,T.Izumi and T.Narita: The Summer Joint Meeting of The Hokkaido Secs. of Jpn. Inst. Metals and Iron and Steel Inst. Jpn., Muroran, July, 2001

Oxidation Behavior of Ni-low Al Alloys at 1073K; S.Tominaga, S.Hayashi and T.Narita: ibid.

Interdiffusion in the Re-Ni, Re-Cr Systems; S.Narita, T.Narita, and S.Hayashi: ibid.

Reaction between Pb Free Solder and Cu Plate(1); S.Saitoh, T.Yamamoto, T.Takashima, J.Tanaka and T.Narita: ibid.

Reaction between Pb Free Solder and Cu Plate(2); S.Saitoh, T.Yamamoto, T.Takashima, J.Tanaka and T.Narita: ibid.

Effect of Water Vapor on the Oxidation Properties of Sintered Fe-3mass%SiO₂ in Air at 1273K; M.Fukumoto, S.Hayashi, S.Maeda and T. Narita: Gordon Research Conference, New Hampshire, U.S.A., July, 2001

Formation of the Oxidation-resistance Coating Layer on the TiAl Alloy by Ni Plating Process; T.Izumi, T.Nishimoto, and T.Narita: The 48th Japan Conference on Materials and Environments: Sapporo, Sept., 2001

Effect of α -Cr Precipitates for the High Temperature Corrosion of Ni-high Cr Alloys in the Atmospheres Containing HCl; S. Najima, M. Noguchi, H. Yakuwa, M. Miyasaka, S. Hayashi, and T. Narita: ibid.

Processing of Re-diffusion Barrier Layers on a Nickel- based Alloys and its Property at High Temperature; D.Yoshida, S.Hayashi, T.Narita, M.Noguchi, H.Yakuwa, and M.Miyasaka: ibid.

Effect of Ni Concentration and Water Vapor on the Oxidation Properties of Fe-Ni Alloy; M.Fukumoto, S.Hayashi, S.Maeda and T. Narita: ibid.

Relationship Between Kinetics and Scale Structure of Fe-5mass%Al Alloy Oxidized in the Atmospheres containing both oxygen and water vapor; S. Hayashi and T. Narita: ibid.

Oxidation behavior of Fe-24Al foils; F. Lang, Z.Yu, S.Gedevanishvili, S.C.Deevi and T.Narita: ibid.

Analysis of the Effect of Solidification on the Liquid Diffusion Experiment of Ag/Ag-Au; K.Ohsasa, A.Hirata, M.Uchida and T.Itami: The 129th Annual Meeting of Jpn. Inst. Metals; Fukuoka, Sept., Mar., 2001.

Equilibrium partition Coefficient of Ni-Co base Super Alloy; M.Kudoh, M.Koizumi and K.Ohsasa: ibid.

Current Activities and Presentations

Melting and Reaction Behavior of Cu Plate due to Pb Free Solder; S.Saitoh, T.Takashima, J.Tanaka and T.Narita: ibid.

Corrosion Behavior of Zn Plated Power Supply Steel Tower; K.Ono, J.Tanaka and T.Narita: The 143th Annual Meeting of Iron and Steel Inst. Jpn., Fukuoka, Oct., 2001.

Formation Behavior of Rust in Zn Plated Steel; K.Ono, J.Tanaka and T.Narita: The 104th Annual meeting of Surf. Finish. Soc. Jpn., Fukuoka, Oct., 2001.

Reaction at the Interface between Steels and Zn-Al melt; K.Ono, J.Tanaka and T.Narita: North Forum of the Hokkaido Sec. of Iron and Steel Inst. Jpn., Sapporo, Oct., 2001.

Difference in Corrosion of Power Supply Steel Tower due to Different Environment; J. Tanaka, K. Ono and T. Narita: ibid.

Application of Thermodynamics Analysis to the Heat Transfer Simulation for Multi-Component Alloy Casting; K.Ohsasa: The Seventh Asian Foundry Congress, Taipei, Taiwan, Oct., 2001.

Formation of oxidation resistance coating on TiAl alloy by Cr,Al pack cementation Method; T.Nishimoto,T.Izumi and T.Narita: Annual Meeting of 123 Committee of Jpn. Soc. Promotion of Science, Tokyo, Nov., 2001.

INTERFACE MICRO-STRUCTURE ANALYSIS LABORATORY

Prof. Dr. H. Takahashi

Tel +81-11-706-7110, Fax +81-11-706-7881

E-mail: takahasi@elechem1-mc.eng.hokudai.ac.jp

Assoc. Prof. Dr. K. Kurokawa

Tel +81-11-706-7111, Fax +81-11-706-7881

E-mail: kazu@elechem1-mc.eng.hokudai.ac.jp

Res. Assoc. Dr. M. Sakairi

Tel +81-11-706-7112, Fax +81-11-706-7881

E-mail: msakairi@elechem1-mc.eng.hokudai.ac.jp

Researchers

Dr. A. Mozalev, Dr. S. Moon

Students

K. Watanabe, Y. Arai, T. Kikuchi, K. Yamauchi, Z. Kato, A. Shibayama, H. Hara, K. Itabashi, E. Sakata, S. Matsushita, Y. Okuyama, T. Miyamoto, S. Nishizawa and M. Yamada

Equipments

Atomic Force Microscope

Conforcal Scanning Laser Microscope

Pulsed Nd - YAG Laser patterning system

Oxidation Test Equipment with Thermobalance and Ultra-High Temperature Furnace

Optical Microscope with High Temperature Furnace

Research work at "Interface Micro-Structure Analysis Laboratory (IMSAL)" directs toward 1)the examination of structure and dielectric properties of anodic oxide films on aluminum and valve metals, 2) micro- and nano-patterning of aluminum using laser irradiation and AFM probe processing, 3) high temperature oxidation of metals and intermetallics, 4) interface reactions between metals and silicides, 5) sintering and synthesis of composites, and 6) localized corrosion of coated steels.

The topics of investigation are in the following:

(1) Formation of Si-Al composite oxide films with ultra high voltage sustainability by sol-gel coating / anodizing.

Aluminum specimen was coated with SiO_2 film by sol-gel dipping method, and then anodized galvanostatically in 0.5M boric acid solutions at 333K. Anodic oxide films grew with a high current efficiency for film formation up to 1,200 V during anodizing. The anodic oxide films were composed of an outer Al-Si composite oxide layer and an inner Al_2O_3 layer, and had no imperfections throughout both layers.

(2) Nano-patterning of aluminum surface by scratching with a probe of AFM.

Aluminum specimens covered with thin barrier type anodic oxide films were scratched with Si-probe of atomic force microscope in CuSO₄ solutions to remove the oxide film locally. After scratching, the specimen was cathodically polarized, using the Si-probe as a counter electrode. Copper was deposited only at the film-removed area during the cathodic polarization.

(3) Micro-patterning of aluminum surface by laser irradiation and metal deposition.

Local metal deposition by anodizing / laser irradiation / electroplating was still continued to make the pattern finer and more precise. A beam expander and doublet lens were set in the conventional optical system. It was found that the

oxide film is removed by laser irradiation at an area with 3 μ m line width, and that a Ni pattern with 5 μ m line width is fabricated after Ni-electroplating.

(4) Conforcal scanning laser microscopy (CSLM) of anodic oxide films formed on aluminum alloys.

Formation of porous-type anodic oxide films on 5052 aluminum alloy was studied by CSLM. The CSLM contrast images showed a number of dark spots in the anodic oxide film whose number and size increased with anodizing time. The CSLM height image revealed irregular morphology of dark spots. The scattering of incident and reflected laser beam by the irregular morphology can explain the reduced brightness of dark spots. Two different types of defects in the anodic oxide film were observed on the CSLM contrast images: dark spots and bright spots. The dark and bright spots were attributed to the irregular pore structure or holes in the oxide film left after the preferential dissolution of magnesium and iron-rich region in the oxide film, respectively.

(5) Formation and dielectric properties of niobium anodic oxide films.

Anode potential increased linearly with time during galvanostatic anodizing of niobium in H_3PO_4 solution, and subsequent potentiostatic anodizing allowed the anodic current to decrease exponentially. The reciprocal capacitance, Cp^{-1} increased linearly with film formation potential, E_f . Amorphous oxide films grew uniformly at $E_f < 100$ V, while crystalline oxides were formed locally to make craters at $E_f = 100$ V. By heat treatment, the capacitance of anodic oxide films increased and showed a bias-voltage dependency. This may be due to the growth of crystalline oxide during heating.

(6) Fabrication of Proto-type of Aluminum Electrolytic Capacitor with a Solid Organic Electrolyte.

Barrier type of anodic oxide films were formed on an electropolished aluminum plate or on aluminum covered with SiO₂ thin films by sol gel coatings. Both

anodized specimens were attached to poly-ethylenedioxy-thiophene and aluminum counter electrode to examine the dielectric properties of the metal / oxide / solid electrolyte / metal systems. The electric capacity of the systems was 20-50% smaller than that of metal / oxide / liquid electrolyte / metal systems. The film breakdown voltage of the system with solid electrolyte was much lower than the film formation potential.

(7) Formation of nano-structured Ta - Al oxide films and their application to electrolytic and thin-film capacitors.

Nano-structured Ta-Al oxide films were formed by anodic oxidation of Ta-Al double layers, which were coated on Si wafer by sputter-deposition, and examined for their application to dielectrics in thin-film capacitors.

(8) Localized corrosion of Zn-55Al and Al coated steel in anion-containing solutions with photon rapture method.

Zn-55Al and Al coated steels were anodized in a borate solution to form a compact anodic oxide film with a constant current up to 100 V. The anodized specimens were irradiated with a pulsed Nd-YAG laser in Cl and SO₄²⁻ ion containing solutions under potentiostatic conditions to remove the anodic oxide film locally. Reformation of oxide film at the laser-irradiated area occurred at a low potential region in all the solutions, while localized corrosion occurred in Cl ion containing solutions at a high potential region. The threshold potential for localized corrosion became more negative with increasing Cl concentration.

(9) Fabrication of new type plastic injection mold by anodizing, laser irradiation and Ni-P electroless plating.

A novel method involving a combination of pulsed YAG laser irradiation and local Ni-P deposition by electroless plating was attempted for fabrication of a new type plastic injection mold.

(10) Formation of Al-Ta composite oxide films by MOCVD / anodizing.

Aluminum specimens were covered with Ta₂O₅ films by metal organic chemical vapor deposition, and then anodized in a neutral borate solution. The electric capacitance of the anodic oxide film formed by the successive processes was twice as high as that formed on aluminum without MOCVD coatings.

(11) Thermal expansion behavior of SiO₂-based oxides.

The thermal expansion of SiO_2 -based oxides (SiO_2 -Al $_2O_3$, SiO_2 -Y $_2O_3$, SiO_2 -B $_2O_3$) are being measured. The aim is to clarify an optimum oxide scale for metal disilicides. The results demonstrated that dissolution of B $_2O_3$ to SiO_2 was most effective to improve the complex thermal expansion behavior of SiO_2 .

(12) Oxidation behavior of metal disilicides.

In order to clarify the oxidation process of metal disilicides, high-temperature oxidation tests are being done. In particular, the requisite vapor pressure of metal oxide for the formation of a SiO₂ scale was clarified from the observation of the oxide scales formed on Mo, V, Re and W disilicides.

(13) High temperature oxidation in H₂O-atmospheres.

In order to clarify the effect of H_2O vapor on oxidation behavior of steels and stainless steels in a hot rolling process, oxidation tests at 1473 K in $(N_2-3\%O_2)-XH_2O$ atmospheres are being done. The relationship between carbon content in steels and scale spallation was clarified. In addition, mechanism of degradation of a Cr_2O_3 scale was proposed.

Dr. A. Mozalev joined IMSAL in May, 2001 from Belarus by a young professorship project of JSPS, and Dr. S. Moon left at the end of October, 2001 after finishing two year post-doctoral fellowship of JSPS.

Prof. Takahashi stayed in Dijon, France, for one month between the end of March and end of April, to collaborate with Prof.R. Oltra, Universite de Bourgogne on the topics of "the influence of pulsed laser irradiation on the integrity of anodized aluminum". At the end of the term, he visited Prof. H. Terryn at Vrije Universiteit

Brussel, and Dr. Takenouti at Paris Univ to discuss passive films on metals and alloys.

Prof. Takahashi attended the joint meeting of ESC and ISE at San Francisco, U. S. A. with Dr. S. Moon, Mr. K. Watanabe, and T. Kikuchi in September, and they presented the papers entitled "Effect of Laser Irradiation Condition on the Fabrication of Microstructure on Aluminum via Anodizing, Laser Irradiation, and Electroplating (T. K)", "Scanning Confocal Laser Microscopy of the Surface of Anodized Al5052 Alloy (S. M)", "Effect of Mechanical, Chemical, and Thermal Treatments on the Repairing of Voids in the Re-Anodizing of Composite Oxide Films on Aluminum (H. T)", and "Anodizing of Aluminum Covered with SiO₂ by Sol-Gel Coating - Formation Mechanism of Composite Oxide Films with High Potential Sustainability (K. W)".

Prof. Takahashi was invited as a guest speaker in the fall meeting of Korean Electrochem. Soc. in October, and presented a paper entitled "Micro- and Nano-Technology on Aluminum Surface Using Anodizing". During his stay in Korea, he visited Prof. K. Kim at Yonsei Univ. in Seoul and discussed with him about super capacitors. Frontiers of Surface Engineering 2001 was held in Nagoya in October, and Prof. Takahashi, Mr. T. Kikuchi, and Z. Kato attended the symposium to present papers entitled "Fabrication of Nickel Micro-Pattern on Insulating Board by Anodizing / Laser Irradiation / Electro-deposition (T. K)" and "Nano-Patterning on Aluminum surfaces with AFM Probe (Z. K)".

In July, Assoc. Prof. Kurokawa attended the Third International Symposium on Applied Plasma Science (ISAPS'01) in Alaska, U.S.A., and presented a paper entitled "Synthesis and Oxidation Resistance of a Re Silicide". He also attended the International Symposium on Spark Plasma Sintering 2001 (ISSPS-2001) in Singapore in September, and presented a paper entitled "Interfacial Reaction and Bonding between Nb and MoSi₂".

In August, Dr. Sakairi visited department of metallurgy, electrochemistry and materials science Vrije Universiteit Brussel, Brussel Belgium, VUB, division of corrosion science Royal Institute of Technology, KTH, Stockholm Sweden,

department of materials technology and electrochemistry, Norwegian University of Science and Technology, NTNU, and SINTEF material technology applied physics, Trondheim Norway, institut für phsikalische vhemie und electrockemis Technishe Unversität Dresden, T.V.D., Dresden Germany, and department of materials science and technology faculty of applied sciences Delft University of Technology, TU-Delft, Delft the Netherlands. In VUB, he discussed with Prof. H. Terryn and J. Vereecken on ellipsometry results of Sol-Gel coated / anodized aluminum samples. At KTH, he discussed with Prof. G. Hultquist, Prof. C. Leygraf and Dr. J. Pan on high temperature oxidation, pulsed YAG laser spectroscopy for atmospheric corrosion, EIS in solution and in high temperature and educational situation in there. At NTNU, he discussed with Prof. K. Nisancioglu and some of the SINTEF members, Dr. J. Walmsley, Dr. A. J. Bjorgum, and Mr. O. Lundre, on his group's recent aluminum work and their recent results: electrochemical behavior and surface treatment on light metals. He discussed with Prof. Plieth, Dr. H. Dietz and some other members on surface enhanced Raman spectroscopy electrochemical results at TUD. At TU-Delfty, he discussed with Prof J. H. W. de Wit and Mrs. Canoestrini, who is PhD. cource students, with there resent research work.

He attended Asia-Pacific Corrosion Control Conference 2001,APCCC 12, Seoul Korea, held in Seoul Korea on October, and presented a paper, "Repairing of Anodic Oxide Films on Al - Zn Alloy Coated Steel After Removal with Photon Rupture in Solutions". After the conference, he visited Department of Material Science and Engineering, Korea Advanced Institute of Science and Technology, KAIST, and Korea Atomic Energy Research Institute Taejon Korea, KAERI. At KAIST, he presented the recent his groups research work "Micro-Surface Modification on Anodized Aluminum by Photon Rupture Technique" and discuss with Prof. Su-Il Pyun. And also visited Department of Industrial Chemical Engineering Chungbuk National University, CBNU, Cheongju Korea. At CBNU, he presented "Surface Modification on Aluminum by Photon Rupture Technique and Electrochemistry" and met and discussed with dean of College of Engineering

Current Activities and Presentations

Graduate School of Industry, Prof. Kim Kyoung Ho and Prof. Su-gil Park.

The foreign scientists visited to IMSAL in 2001 are Prof. H. Terryn, Vrije Universiteit Brussel, Belgium, in July, Prof. S. Park, Chungbuk Univ., Korea, in July, Prof. M. Lohrengel, Heinrich Heine Univ., Germany in October, Dr. Hassel, Max Plank Inst., Germany in October.

Presentations

Problem-based Subject and Admission Office Entrance Examination at Material Engineering and Applied Chemistry Course, Fac. of Engr., Hokkaido Univ., H. Takahashi: Symposium on New Education at High School, Sapporo, Jan. 2001.

Electroless Ni-P Deposition on the Anodic Oxide Film-covered Aluminum, S.Moon, M. Sakairi, H. Takahashi, and K. Shimamura: The joint Meeting of The Hokkaido Secs. of Elechtrochem. Soc. Jpn., Surf. Finish. Soc. Jpn., and Jpn. Soc. Corros. Eng., Sappro, Jan., 2001.

Micro Patterning on Aluminum Surface with Electrochemical AFM, Z. Kato, M. Sakairi and H. Takahashi: ibid.

The Effect of Fe³⁺ ions on Corrosion of Stainless Steel in HNO₃ Solutions, Y. Arai, S. Honda and H. Takahashi: ibid.

Study on Void Structure of Composite Oxide Films on Aluminum - Its Changes by Thermal, Chemical, Mechanical Treatment -, Y. Tamaru, M. Sakairi, H. Takahashi and H. Uchi: ibid.

Preparation and Oxidation Behavior of Re Silicides, H. Hara, K. Kurokawa, H. Takahashi: The Winter Joint Meeting of The Hokkaido Secs. of Jpn. Inst. Metals and Iron and Steel Inst. Jpn., Muroran, Jan., 2001.

Degradation of Chromia Scale in H₂O-Containing Atmospheres, A. Yamauchi, K. Kurokawa, H. Takahashi: ibid.

Formation of Composite Oxide Films by Sol-Gel Coating and Anodizing, H. Takahashi, Seminar on Capacitor Technology, Osaka, Jan., 2001

Formation of the Composite Oxide Film with High Potential Sustainability by Sol-Gel Coating/Anodizing, K. Watanabe, M. Sakairi, H. Takahashi, and S. Hirai:

Current Activities and Presentations

The Hokkaido Secs. of Chem. Soc. Jpn. And Jpn. Soc. Anal. Chem., Sappro. Feb., 2001.

Effect of Laser Irradiation Condition on LASER Fabrication and Fine Pattering on Aluminum, T. Kikuchi, M. Sakairi, H. Takahashi, Y. Abe and N. Katayama: ibid.

Structure of Anodic Oxide Film Formed on Al and Al Alloy in Solutions., M. Sakairi, P. Skeldon, G.E. Thompson, G.C. Wood, and K. Stevens: ibid.

High Temperature Oxidation Behavior of Re Silicide, H. Hara, K. Kurokawa, and H. Takahashi: The 128th Annual Meeting of Jpn. Inst. Metals, Narashino, Mar., 2001.

Degradation of Chromia Scale Formed in Early Stage of Oxidation in H₂O-Containing Atmospheres, A. Yamauchi, K. Kurokawa, H. Takahashi: ibid.

Model of New Type Plastic Injection Mold: Anodizing / Laser Irradiation / Ni-P Electroless Plating Process. H. Takahashi, M. Sakairi, S. Moon, K. Shimamura, Y. Abe: Society for the study Electroforming and Mold, Tokyo, Mar. 2001.

Scanning Laser Microscopy of Al 5052 Alloy Anodized in Sulfuric Acid, S. Moon, M. Sakairi, and H. Takahashi: The 103th Annual Meeting of Surf. Finish. Soc. Jpn., Miyashiro, Mar. 2001.

Patterning of Aluminum Surface by Anodizing and Laser Irradiation — Influence of Thickness of Oxide Film on Fabrication of Micropattern - . T. Kikuchi, M. Sakairi, H. Takahashi, Y. Abe, and N. Katayama ibid.

Preparation and Oxidation Resistance of a Re Silicide, K. Kurokawa, H. Hara, and H. Takahashi: The 8th Annual Meeting of Applied Plasma Science, Himeji, Mar., 2001.

Anodizing of Aluminum Coated with SiO₂ by Sol-Gel Coating -Formation of Anodic Oxide Films with High Potential Sustainability- coating, K. Watanabe, M.

Sakairi, H. Takahashi, and S. Hirai, The 68th Annual Meeting of the Electrochem. Soc. of Jpn., Kobe April 2001.

Anodizing Behaviour of Aluminum Alloy in Solutions., M. Sakairi, P. Skeldon, G.E. Thompson, G.C. Wood, and K. Stevens: ibid.

Effect of Probe Damage on AFM Processing., Z. Kato, M. Sakairi and H. Takahashi, ibid

Micro- and Nano-Patterning on the Surface of Aluminum with Laser Irradiation and AFM Probe Processing, H. Takahashi: Seminar at Bulgoniur University, Dijon, France April, 2001.

Void Structure in Composite Oxide Films on Aluminum and Its Repairing, Y. Tamura, M. Sakairi, H. Takahashi and H. Uchi: 2001 Annual Meeting of Jpn. Soc. Corro. Eng. Tsukuba, May 2001.

Micro Technology on Aluminum Surface, H. Takahashi: The 8th Surface Engineering Seminar, sponsored by Committee of Development of Industry Collaboration, Sapporo, Jun, 2001.

Surface Morphological Change of Al 5052 Alloy during Anodizing in Sulfuric Acid, S. Moon, M. Sakairi and H. Takahashi, Lilac Seminar, Otaki, Jun, 2001.

Application of Photon Rapture Technique on Localized Corrosion, M. Sakairi: The 3rd North Forum, Sapporo, July, 2001.

Repairing of Oxide Film on Al-Zn Alloy with Laser Irradiation.K. Itabashi, M. Sakairi and H. Takahashi: The Summer Joint Meeting The Hokkaido Secs. of Chem. Soc. Jpn. And Jpn. Soc. Anal. Chem. of Muroran, July, 2000.

Problem-Based Subject at Fac. of Engr., Hokkaido Univ., H. Takahashi: Symposium on Chemistry Education in Hokkaido, sponsored by Hokkaido branches of Jpn. Chem. Soc. and Anal. Chem. Soc. Jpn., Sapporo, July, 2001

Current Activities and Presentations

Evaporation Behavior of WO₃ in Oxidation of WSi₂, A. Shibayama, K. Kurokawa, and H. Takahashi: The Summer Joint Meeting of The Hokkaido Secs. of Jpn. Inst. Metals and Iron and Steel Inst. Jpn., Muroran, July., 2001.

Development of Silicide Having Outstanding Oxidation Resistance, K. Kurokawa: Symposium of Japan Institute Metals, Tokyo, July, 2001.

Synthesis and Oxidation Resistance of a Re Silicide, K. Kurokawa, H. Hara, and H. Takahashi, Intern. Sympo. on Applied Plasma Science, Fairbanks, July, 2001

Aluminum Surface Micro- and Nano-Technology, H. Takahashi:Two Day Univerwsity Life, Sapporo, Aug., 2001

Formation of Al-(Si, Zr, Nb, BaTiO₃) Composite Oxide Film by Sol-Gel Coating / Anodizing, K. Watanabe, M. Sakairi, H. Takahashi, Material for Charge Device Study Summit, Tokyo, Aug., 2001.

Effect of Laser Irradiation Condition on the Fabrication of Microstructure on Aluminum via Anodizing, Laser Irradiation, and Electroplating., T.Kikuchi, M.Sakairi, H.Takahashi, Y.Abe, and N.Katayama: Joint International Meeting of the Electrochemical Society (200th) and International Society of Electrochemistry (52nd), SanFrancisco, Sep. 2001.

Scanning Confocal Laser Microscopy of the Surface of Anodized Al5052 Alloys. M. Moon, M. Sakairi, and H. Takahashi, ibid.

Effect of Mechanical, Chemical, and Thermal Treatments on the Repairing of Voids in the Re-Anodizing of Composite Oxide Films on Aluminum, H. Takahahsi, Y. Tamura, M. Sakairi, and H. Uchi, ibid.

Anodizing of Aluminum Covered with SiO₂ by Sol-Gel Coating - Formation Mechanism of composite Oxide Films with High Potential Sustainability-,K. Watanabe, M. Sakairi, H. Takahashi, S. Hirai, and S. Nagata, ibid.

Micro-Structure Fabrication on Aluminum by Anodizing and Laser Irradiation – Usage of Doublet Lens - . T. Kikuchi, M. Sakairi, H. Takahashi, Y. Abe, and N. Katayama.: The Autumn Meeting of Electrochm. Soc. of Jpn., Tokyo, Sep., 2001.

Anodizing of Aluminum Coated with Si-oxide by Sol-Gel Coating — For the Preparation of Anodic Oxide Film with High Potantial Sustainability — , K. Watanabe, M. Sakairi, H. Takahashi, and S. Hirai, ibid.

Anodizing of Aluminum Coated with Nb-oxide by Sol-Gel Coating, K. Watanabe, M. Sakairi, H. Takahashi, and S. Hirai, ibid.

Nano-Technology Using Anodiziing of Aluminum, H. Takahashi, ibid.

Relationship between Evaporation Rate of WO₃ and Formation of SiO₂ Scale in Oxidation of WSi₂, A. Shibayama, K. Kurokawa, and H. Takahashi: The 129th Annual Meeting of Jpn. Inst. Metals, Fukuoka, Sep. 2001.

Effect of Addition of B₂O₃ on Structure of SiO₂ Scale Formed on Re Silicide, H. Hara, K. Kurokawa, and H. Takahashi: ibid.

Degradation of Cr₂O₃ Scale in H₂0-Containing Atmospheres, A. Yamauchi, K. Kurokawa, and H. Takahashi, ibid.

Formation of Al-Si Composite Oxide Films with High Potential Sustainability by Sol-Gel method / Anodizing, K. Watanabe, M. Sakairi, H. Takahashi, and S. Hirai, The 48th Discussion Meeting of J. Soc. Corr. Eng., Sappro, Sep. 2001

Reformation of Al-Zn Alloy Anodic Oxide Film with Photon Rapture Method., K. Itabashi, M. Sakairi and H. Takahashi, ibid.

Fine Surface Modification on Aluminum by AFM Diamond Probe, Z. Kato, M. Sakairi and H. Takahashi, ibid.

Current Activities and Presentations

Degradation Mechanism of Cr₂O₃ scale in H₂O-Containing Atmospheres, A. Yamauchi, K. Kurokawa, and H. Takahashi: ibid.

Interfacial Reaction and Bonding between Nb and MoSi₂, K. Kurokawa, G. Ochiai, H. Takahashi, and H. Takahashi: Intern. Sympo. on Spark Plasma Sintering, Singapore, Sep., 2001.

Spark Plasma Sintering Behavior of Cr₂O₃ and SiO₂, A. Yamauchi, K. Kurokawa, and H. Takahashi: The 6th Meeting of Spark Plasma Sintering, Okinawa, Oct., 2001.

Fabrication of Nickel Micro-pattern on Insulating Board by Anodizing / Laser Irradiation / Electrodeposition., T.Kikuchi, M.Sakairi, H.Takahashi, Y.Abe, and N.Katayama, Frontiers of Surface Engineering 2001, Nagoya, Oct. 2001.

Nano-patterning on Aluminum Surfaces with AFN Probe, Z. Kato, M. Sakairi, and H. Takahashi ibid.

Micro- and Nano-Technology on Aluminum Surface Using Anodizing, H. Takahashi: Fall Annual Meeting of Korea Electrochem. Soc., Seoul Oct., 2001.

Repairing of Anodic Oxide Films on Al-Zn Alloy Coated Steel After Removal with Photon Rupture in Solutions, M.Sakairi, K. Itabashi and H.Takahashi, APCCC 12th, Seoul, Oct., 2001.

Micro-Surface Modification on Anodized Aluminum by Photon Rupture Technique, M. Sakairi: KAIST Annual Lectrure, Taejon, Koria, Oct. 2001.

Surface Modification on Aluminum by Photon Rupture Technique and Electochemistry. M. Sakairi: Koria Ind. Chem. Chungbuk Branch Annual Lecture, Cheongju, Koria, Oct. 2001.

Estimation of Corrosion of Zn-Al Coated Steel by Laser Irradiation Method, K. Itabashi, M. Sakairi, H. Takahashi: Seminar on Corrosion of Galvanized Steel and Prediction of Service Life, Tokyo, Oct. 2001

High Temperature Oxidation and Protection of New Heat Resistant Materials, K. Kurokawa: Seminar of Japan Inst. Metals, Tokyo, Oct., 2001.

Formation of Al-(Si, Zr, Nb, BaTiO₃) Composite Oxide Filmby Sol-Gel Coating / Anodizing", H. Takahashi, M. Sakairi, and K. Watanabe, The 18th ARS (Anodizing Research Society, SFJ) Conference, Rokkou, Nov. 2001.

Applications of Anodically Oxidized Double Layer of Valve Metal Combinations in Microelectronics Microelectronics, A. Mozalev, M. Sakairi, and H. Takahashi, ibid.

Observation of Anodic Oxide Film Formed on Aluminum with Conforcal Scanning Laser Microscope., M. Sakair, S. Moon and H. Takahashi, ibid.

Structure of Oxide Scales Formed on Silicides, K. Kurokawa: Commission on Self-Healing Technology, Nagoya, Nov., 2001.

DENTAL MATERIALS AND ENGINEERING LABORATORY

Prof. Dr. F. Watari
Tel&Fax:+81-11-706-4251 E-mail:watari@den.hokudai.ac.jp
Assoc. Prof. Dr. M.Uo
Tel&Fax:+81-11-706-4251 E-mail:uo@den.hokudai.ac.jp
Res. Assoc. Dr. S.Ohkawa
Tel&Fax:+81-11-706-4251 E-mail:ohkawa@den.hokudai.ac.jp
Technician Mr.T.Sugawara
Tel&Fax:+81-11-706-4251 E-mail:stoshi@den.hokudai.ac.jp

Students

Y.Tamura, Y.Tanimura, T.Tsuchiya, J.Konishi, M.K.Yamada, S.Tanaka, Y.Iwasaki, K.Tani, K.Tamura, K.Kondo, N.Kamishima

The research activities cover (1)the development, evaluation and application of dental and biomaterials, (2)the development of methods and equipments for fabrication of materials and prostheses and (3)the measurement of properties. These are concerned with mechanical, thermal properties, corrosion, surface treatment, biocompatibility, bioreactivity, estheticity and various methods of imaging and microanalysis. Many researches are related to dental, biological and engineering fields and performed in collaboration with clinical departments Removable Prosthetic Dentistry(Prof.Takao KAWASAKI), including Orthodontics(Prof.Junnichiro IIDA), Operative Dentistry (Prof.Hidehiko SANO), Oral and Maxillofacial Surgery(Prof.Yasunori TOTSUKA), Crown and Bridge Prosthodontics(Prof.Noboru OHATA) and Protective Dentistry(Prof.Manabu MORITA).

Equipments

XSAM: HORIBA XGT-2000V, Scanning X-ray analytical microscope for elemental mapping analysis

AFM: TopoMetrix TMX2000 Explorer, AFM for dry and wet specimens NSOM: TopoMetrix Aurora, Near field Scanning Optical Microscope

Laser Raman Spectrometer: Dilor Labram, Laser Raman Spectrometer with mapping analysis

ICP: HITACHI P-4010, ICP emission spectrometer for analysis of elements in aquaous solution

FT/IR: Jasco FT/IR-300E, FT/IR spectrometer with microscopic IR measurement Universal Testing Machine: INSTRON MODEL 4204, Testing for mechanical properties of materials

Laser Welder: ATJ TLL7000, Nd-YAG pulse laser welder with computer controlled x-y stage

Cold Isostatic Press: Hikari Koatsu Kiki (10000atm type and 20000atm type)

Kobelco, Large volume isostatic press (4000atm)

Vickers Hardness Tester: Shimadzu

Acoustic Emission: Physical Acoustic Corporation

Thermal Gravitometry and Differential Thermal Analysis(TG/DTA): Rigaku

Denki

Diamond Cutter: Buehler and Struers diamond cutter

Current topics on research are as follows;

(1) Development of functionally graded dental implant.

The dental implant with the structure of functionally graded materials (FGM) has been fabricated to satisfy different properties. The typical example is such that the composition changes from the biocompatible metal, Ti, at one end, increasing the content of ceramics, hydroxyapatite (HAP), principal component of bone and teeth, toward 100% HAP at the other end. This can control the functions of mechanical properties and biocompatibility, optimize them, depending on the necessity of each part of implant, without the abrupt change by the formation of discrete boundary. The effect of FGM structure Ti/HAP, Ti/Co on tissue response is investigated by the animal implantation test into rats and rabbits. The tissue reaction and new bone formation around the implant to the gradient composition is evaluated by both the conventional method using an optical microscope with stained specimens and by elemental mapping and other imaging methods using electron microprobe analysis(EPMA) and X-ray scanning analytical microscope(XSAM) with unstained specimens.

(2) Development of FRP esthetic orthodontic wire.

To realize the esthetic, transparent orthodontic wire the FRP wires of the diameter 0.5mm with the multiple fiber structure has been fabricated by either drawing of fiber-polymer complex at 250C or photopolymerization method. Biocompatible CaO-P₂O₅-SiO₂-Al₂O₃ (CPSA) glass fibers of 8-20 μ m in diameter are oriented unidimensionally to the longitudinal direction in polymer matrix of PMMA, UDMA or bis-GMA. The improvement has been done to obtain the adequate flexural strength and higher torque. FRP wire shows the sufficient flexural strength and a very good elastic recovery. The dependence of Young's modulus and flexural stress on fiber fraction obeys very well the rule of mixture. This FRP wire can cover the range of the strength corresponding to the conventional metal orthodontic wires from Ni-Ti used in the initial stage of orthodontic treatments to Co-Cr used in the last stage by changing the volume ratio of glass fibers with the same external diameter. FRP wire can satisfy both mechanical properties and estheticity, which is not possible for the conventional metal wire.

(3) Cytotoxicity due to ions and fine particles of Ti and other metals in vivo and in vitro.

The removal of Ti plates for fixing jaw bone in 6 months after operation often reveals the slightly dark colored tissue in the circumferential soft tissue. The observation and analysis by optical microscopy, electron microscopy and XSAM revealed that the colored tissue contains the abraded fine particles of Ti, probably produced during plate fixation in operation.

The animal experiments to implant various sizes of Ti particles of 1-100 μ m and macroscopic cylindrical Ti implant in μ m order for 3 days to 8 months showed that the macroscopic size of Ti was encircled with fibrous connective tissue layer from early stage and there was no inflammation. As the size of particle becomes smaller, many phagocytic cells appear with fibrous connective tissue layer inside the particle inserted region and tissue showed inflammation. It takes more time to encircle the particle-contained tissue region and heal inflammation. For 1-3 μ m the inserted region is never encircled with fibrous connective tissue layer and inflammation continues.

The in vitro cell functional tests on cell survial rate, LDH(Lactate Hydrogenase

CII) protein released at the breakdown of cell membrane and superoxided anion(O^2) sing human neutrophils showed that Ni solution has he cell disruption effect. The deformed and disrupted morphology of neutrophils was confirmed by SEM observation. Whilst Ti and V solution showed the increase of superoxide anion and negligible change in the others, which suggests the cell stimulation effect. SEM observation confirmed that neutrophis are inflated with more complicated polyacicular morphology. One of the marking cytokines released at phagocytization, TNF- α , was not detected in any solution of Ni, V, Ti, the simulated body fluid(Hank's solution) mixed with 10mm paricles of Ti and with submicron size Ni particles. TNF- α was found only in the 1-3 μ m Ti particle mixed Hank's solution, which suggests that particles were phagocytized. SEM observation and EDS elemental analysis confirmed the phagocytosis of Ti particles by neutrophils.

The difference of cell reaction to 1-3 μ m and 10 μ m Ti particles suggests that the particles(1-3 μ m) smaller than cell size(about 5 μ m in neutrophils) induces cytotoxicity as a result of phagocytosis, while for particles larger than cell size(10 μ m) phagocytosis is not possible, resulting in the less clear cytotoxicity effect.

The study shows the cytotoxicity originating from physical size effect of particles other than biochemical toxicity effect, which is significant for the cases where the fine particles are produced during abrasion by long term usage of moving parts in the artificial bone joint.

(4) In situ observation of etching process of human teeth in acid agent by atomic force microscopy.

Composite resin with fillers of ceramic powders in polymer matrix has estheticity similar to natural teeth color and is widely used for treatments of caries in incisal teeth. Physical-mechanical anchoring effect plays an important part in binding force between teeth and composite resin. The pretreatment to make etching of teeth is generally done using acid agents for enhancement of binding. SEM is usually used for the evaluation of etching effect. It can observe, however, only the result after a certain etching time. To observe the sequence of etching process it is necessary to prepare the series of specimens treated with different etching time. Atomic force microscope is applied for the in-situ observation of etching process of human enamel and dentin in acid agents. The chronological

change of surface morphology can be successively observed and quantitative analysis is done for different etching conditions.

(5) Fabrication of composite resin prostheses by laser lithography.

Laser lithography, one of the CAD/CAM systems to fabricate the polymer models by piling up the thin slices, which are photo-polymerized by scanning laser beam originally on the shallow depth of liquid epoxy monomer, was applied for the fabrication of dental prosthoses of photo-curing composite resin composed of silica fillers in the matrix of high strength UDMA resin. The full dental crown could be fabricated using the shape data pre-designed by computer with high accuracy due to the smaller polymmerization shrinkage than by conventional methods. Then the functionally graded dental core and post with gradually changing filler content from 70 to 0% from the head of core abutment toward the apex of post was successfully fabricated. The stress concentration at the pulp root inserted with the conventional dental post has often caused the fracture in the surrounding dentin by impact force on the tooth crown. The stress relaxation effect by application of the functionally graded dental post was confirmed by simulation using the photoelastic method and finite element method(FEM).

(6) Radiation effects on polymer resin.

Radiation effects by C⁺ion, γ -ray from Co⁶⁰ and electrons on one of the main matrix polymer UDMA(urethane dimethacrylate) for dental composite resin were investigated with various mechanical tests and spectroscopies. C⁺ion radiation induced the large change in the structure sensitive properties of mechanical properties, Vickers hardness, flexural strength, abrasion resistance and little change in the non-structure sensitive properties of spectroscopies, FT-IR, Raman scattering, Fluorescence, NMR and thermal expansion coefficient. The results suggest that the mechanism of radiation effect is mostly due to the physical structure change such as lattice defects of vacancies, interstitials, depleted zone rather than the chemical effect of cross-linking by further progress of polymmerization of residual monomers.

(7) Evaluation of biocompatibility of refractory metals and their application.

Refractory metals of IVA group(Ti, Zr, Hf), VA group(V, Nb, Ta) and VIIA group(Re) are investigated in their biocompatibility and other bioreactivities. Animal implantation tests show that the fraction of direct contact of newly formed bone to implant material without intervening of fibrous connective tissue at the interface and the amount of new bone vary depending on materials. The composites of these refractory metals are also made and the comparison and the composite effect is investigated.

(8) Surface treatment of dental and biomedical materials with sol-gel method.

Biocompatibility and adhesivity to tissue is important for dental materials. Various dental metals were coated by amorphous silica gels with sol-gel method. In some cases, biocompatibility were improved.

(9) Tissues and dental materials observation by XSAM.

The scanning X-ray analytical microscope (XSAM) was applied for the analysis of the soft tissue of rat in which various metals including Fe, Cu, SUS, V, Co, Ni were implanted. The dissolution of implanted metals and inflammation of tissues were observed by elemental mapping image obtained by XSAM.

(10) Bonding property and cytotoxicity of dental zirconia ceramics (YPSZ).

Yttria partially stabilized zirconia (YPSZ) ceramic is suitable for dental and medical use because of it's high fracture toughness and chemical durability. The bonding properties of dental zirconia with various luting cements and surface treatments are investigating. The cytotoxicity dental zirconia ceramics compared to other dental ceramics was also evaluated.

(11) Dental Applications of Acoustic Emission Technique.

Fracture toughness of dental materials including more detailed discussions using an acoustic emission technique. Acoustic emission (AE) is employed to evaluate the microscopic and macroscopic aspects of mechanical behavior of metal-, ceramics-and polymers- based materials and their composite materials.

(12)Grafting of Methyl Methacrylate onto Collagen Using Ferric Chloride-N-Phenylglycine.

Graft polymerization of vinyl monomer onto human hard tissues has not been studied extensively, without tri-n-buthylborane initiated MMA-based materials. The purpose of this study was to grafting of MMA onto collagen using various ferric ions-N-phenylglycine as a redox initiator.

(13) Development of halide fluxes for titanium soldering.

The reactivity of KHF2-LiF-NaCl-KCl fluxes with titanium were examined. The reactivity of the fluxes were promoted in the order of (NaCl+KCl)<(56KHF2-14LiF-30(NaCl+KCl))<(50KHF2-50LiF)<(70KHF2-30LiF)<(KHF2)<LiF.The reactivity of the fluxes was not alway consistent with the increasing in the spreading areas of solder.

(14) Abrasion-resistant implant made of refractory metal nitrides and carbides.

Surface-nitrided titanium(Ti(-N)) showed high corrosion resistance and nearly equivalent biocompatibility with Ti in soft and hard tissue in animal implantation test. Surface durability was evaluated by three static and dynamic mechanical tests; Vickers hardness test, Martens scratch test and for more practical viewpoint newly developed abrasion test using ultrasonic dental scaler which is used to remove calculus on teeth in dental clinics. Vickers hardness of Ti(-N) was 1300, ten times larger than Ti. Martens scratch test showed that the bonding of nitrided layer with 2μ m thickness is coherent to matrix Ti and enough strong. Abraded volume by ultrasonic scaler was increased with the load in Ti, while no trace was formed in Ti-(N), instead stainless tip of scaler was abraded. The test showed that abrasion would be negligibly small under the practical conditions of the load 50g in clinics. Ti-(N) with biocompatibility and surface abrasion resistance would be suitable as abrasion-resistant implant materials for the application to the artificial joint of implant and abuttment part of dental implant.

(15) Development of visible-light responsible photocatalysis and its application.

The current photocatalysis of anatase TiO₂ mostly works only by ultraviolet light. To make applicable for medical use it is necessary to develop the visible-light reactive photocatalysis. Visible light sesitization was obtained by surface

modification with caions of Au, Ag, Cu, Pt, Pd. Depigmentation with visible light around 470nm which is used for photopolymerization of composite resin restoration in dental clinics could be done with the Ag activated TiO₂ in contrast to very little effect in an untreated TiO₂. Antibacterial effect was also confirmed to streptococcus mutans, one of the most popular bacteria for caries. The application to bleaching of pigmented teeth was developed.

(16) Development of discrimination method of resin-restored teeth.

In the health checkup in school mass of patients must be checked in the limited time. Due to the recent development of estheticity of composite resin it is now very difficult to recognize the resin-restored teeth and discern resin part from natural teeth. Total reflection spectroscopy and fluorescence spectroscopy were measured and images were taken with reflected light and fluorescence light using the filters to select the appropriate wave length. In the long wave length region for more than 600nm the reflectivity of teeth is higher than that of composite resin. The image formed with filtered light, however, did not show the contrast enough to discern the resin part from tooth. For less than 400nm both teeth and resin showed the fluorescence emission with high and comparable intensity. For the light of 430-450nm teeth emitted higher fluorescence and the relative difference is larger. The images formed with fluorescence light for more than 500nm emitted by 430-450nm light excitation showed the easily recognized contrast to discriminate resin from tooth.

Other activities

The international collaborations are continued with Institute of Dental Materials Science, Umea University, SWEDEN (Emerita Prof. Maud BERGMAN) on application of Ti, ZrO₂, amalgum for dentistry, and research on side effects, with Department of Dental Materials, Chonbuk National University, KOREA (Prof.Tae-Sung BAE) on evaluation of mechanical properties of laser-welded Ti, dental porcelain, and with Institute for Materials Science, Dresden Institute of Technology, GERMANY (Prof.W.POMPE) on the biocompatibility evaluation and application of collagen-hydroxyapatite composites.

Prof.I.DEMETRESCU of University Polytechnica Bucharest, Bucharest, Romania visited on June 19 and started the continual exchange of informations and collaborations on the development of biomaterials.

Prof.Tae-Sung BAE of Department of Dental Materials, Cho]nbuk National University (KOREA) and his colleagues of Chonbuk University Dental School visited on Sep.28-29.

Prof.WATARI attended and made presentation in the second China-Japan Joint Seminar/ Designning, Fabrication and application of Functionally Graded Materials held at Tsingua University, Beijing, China, on Oct. 10-12.

The collaboration with Laboratory for Advanced Materials, Institute for Materials Research, Tohoku University (Dr.Mamoru OMORI) is also undergoing on the fabrication of new biomaterials including composite materials and functionally graded materials by applying a spark plasma system(SPS) as a method to enhance sintering. The research on the surface treatment of Ti by sol-gel method and evaluation of cytotoxicity is developed in cooperation with Department of Materials Science and Engineering, Muroran Institute of Technology (Prof.Kazuyoshi SHIMAKAGE, Assoc.Prof.Shinji HIRAI). The development of FRP esthetic orthodontic wire has continuously been done with Department of Industrial Chemistry, Chiba Institute of Technology(Associate Prof.Masahiro KOBAYASHI).

Presentations

Fabrication of functionally graded materials for bio-medical and dental application: F.Watari, M.Omori, T.Hirai, A.Yokoyama, R.Miyao, T.Kawasaki, S.Matsuo, N.Ohata, The second China-Japan Joint Seminar/ Designning, Fabrication and application of Functionally Graded Materials, Abstracts, Ed.Pan Wei, Tsingua University, Beijing, Oct., 2001

Bonding properties of dental zirconia ceramics(Denzir) with various cements: M.Uo, G.Sjögren, A.Sundh, F.Watari, M.Bergman, 79th IADR(Int.Assoc.for Dent Res.), Chiba, June, 2001

Effect of surface property on bonding property of dental zirconia ceramics; M.Uo, T.Sugawara, S.Ohkawa, F.Watari: Japanese Society of Dental Materials and Devices, Fukuoka, Oct., 2001

Observation of dissolution behavior of soft tissue implanted metallic specimens using X-ray scanning analytical microscope; M.Uo, F.Watari: 48th Japan Conference on Materials and Environments, Sapporo, Sept., 2001.

Sintering of slip cast titanium crowns in the investment mold: S.Ohkawa, K.Ishii, S.Kondo, M.Uo, T.Sugawara, F.Watari, 79th IADR(Int.Assoc.for Dent Res.), Chiba, June, 2001

Biocompatibility of Titanium/Hydroxyapatite functionally graded implant fabricated by SPS: R.Miyao, A.Yokoyama, H.Matsuno, F.Watari, M.Uo, T.Kawasaki, M.Omori, T.Hirai: 79th IADR(Int.Assoc.for Dent Res.), Chiba, June, 2001

Evaluation of material properties of titanium nitride as biological implants; Y.Tamura, A.Yokoyama, H.Matsuno, R.Miyao, T.Kawasaki, S.Ohkawa, M.Uo, F.Watari, S.Hirai, K.Hoshino: Joint Meeting of the Iron and Steel Society and the Japan Institute of Metals, Hokkaido Division, Muroran, Jan., 2001.

Current Activities and Presentations

Evaluation of material properties and biocompatibility of surface nitrided titanium; Y.Tamura, A.Yokoyama, H.Matsuno, R.Miyao, T.Kawasaki, S.Ohkawa, M.Uo, F.Watari, S.Hirai, K.Hoshino: Japanese Society of Dental Materials and Devices, Tokyo, Apr., 2001.

Evaluation of basic properties of surface nitrided titanium as an implant material; Y.Tamura, A.Yokoyama, H.Matsuno, R.Miyao, T.Kawasaki, S.Ohkawa, M.Uo, F.Watari, S.Hirai, K.Hoshino: Japanese Society of Dental Materials and Devices, Fukuoka, Oct., 2001

Influence of titanium on cellular function of human leukocyte: R.Kumazawa, N.Takashi, Y.Tanimura, T.Tsuchiya, Y.Totsuka, M.Uo, S.Ohkawa, T.Sugawara, S.Kondo, F.Watari, 5th Int.Symp.on Titanium in Dentistry, Chiba, June, 2001

Influence of Titanium on Cellular Function of Human Leukocyte; R.Kumazawa, N.Takashi, Y.Tanimura, T.Tsuchiya, Y.Totshuka, M.Uo, S.Ohkawa, T.Sugawara, S.Kon dou and F.Watari: 5th International symposium in titanium in dentistry, Tokyo, July 2001

The influences of titanium ion and particles against vital reaction; R.Kumazawa, F.Watari, N.Takashi, M.Uo, Y.Tanimura, T.Tsuchiya, Y.: 48th Japan conference on Materials and environments, Sapporo Sept., 2001.

Evaluation of photocatalytic ability of ion-decorated titanium dioxide for dental application; Y.Tanimura, R.Kumazawa, Y.Totsuka, M.Uo, S.Ohkawa, T.Sugawara, F.Watari: The Japanese Society of Dental Materials and Devices, Fukuoka, Oct., 2001.

Suspension type friction test of FRP aesthetic orthodontic wires on brackets; N.Suwa, S.Yamagata, K.Nagayama, H.Toyoizumi, M.Uga, J.Iida, F.Watari: The Japanese Orthodontic Society, Tokyo, Oct., 2001

Dependence of time on the flexural action of orthodontic wire; S.Tanaka, S.Yamagata, M.Uga, N.Suwa, J.Iida, M.Uo, S.Ohkawa, T.Sugawara, F.Watari: The

Japanese Society of Dental Materials and Devices, Fukuoka, Oct., 2001.

Bracket designed for the use of esthetic orthodontic wires; M.Uga, F.Watari, M.Kobayashi, S. Yamagata, N. Suwa and J. Iida: IADR 79th General Session & Exhibition, Chiba, Jun., 2001

Mechanical properties and contraction of experimental porcelain inlays processed by CIP method; J.Konishi, C.Kawamoto, H.Sano, F.Watari: 115th Meeting of the Japanese society of Conservative Dentistry, Tokyo, Nov., 2001

Fabrication of functionally gradient resin composite posts by laser lithography; S.Matuo, N.Sato, Y.Ueda, N.Ohata, M.Uo, S.Ohkawa, T.Sugawara, S.Kondo, F.Watari; The Japanese Society for Dental Materials and Devices, Tokyo, Apr. 2001.

Radiation effect on physical properties of UDMA resin: S.Haque, S.Takinami, F.Watari, 79th IADR(Int.Assoc.for Dent Res.), Chiba, June, 2001

Grafting of MMA monomer onto collagen by ceric ion: S.Kondo, S.Ohkawa, M.Uo, T.Sugawara, F.Watari, 79th IADR(Int.Assoc.for Dent Res.), Chiba, June, 2001

LABORATORY OF ADVANCED MATERIALS CHEMISTRY

Prof. Dr. Hidetaka Konno
Tel.&Fax:+81-11-706-7114
E-mail:ko@eng.hokudai.ac.jp
Assoc. Prof. Dr. Hiroki Habazaki
Tel.&Fax:+81-11-706-6575
E-mail:habazaki@eng.hokudai.ac.jp
Instructor Mr. Akira Shimizu
Tel.:+81-11-706-6577
akira@eng.hokudai.ac.jp

Students

Y. Aoki, Y. Hayashi, A. Yoneda, M. Endo, M. Uozumi, K. Yokoyama, T. Kinomura, S. Sato, A. Sudo, T. Matsuo, H. Tachibana

Equipments

DC magnetron sputtering : Shimadzu SP-2C X-ray diffractometer: Rigaku Geigerflex

Laser Raman Spectrometer: Jasco TRS-401 and Jobin Yvon T64000

FT-IR spectrometer: Jasco FT-IR350 Uv-vis spectrometer: Jasco V-550

EPMA: JEOL JSM-5410 equipped with Oxford WDX-400

TG/DTA: Seiko TG/DTA32

TOC analyzer: Shimadzu TOC-5000A

Capillary Electrophoresis analyzer: Ohtsuka Electronics CAPI-3100

The research activities of the laboratory are directed toward (1) formation and characterization of carbon-based composites, carbides, and double oxides with unusual valence state ions (2) formation of dielectric layers by anodizing of valve metal alloys and (3) electrochemical and biochemical water treatments.

Current research topics are in the following:

(1) Formation and characterization of composite materials of carbon, ceramics and metals.

Various carbon composites were formed by carbonization of 1) polyimide films containing metal complexes, 2) powder mixtures of organic polymer and ceramics and 3) chelate resins complexed with metal ions. Basic researches on the structure, composition, electric and magnetic properties of the composites are in progress by using XRD, TEM, SEM, Raman spectroscopy, SQUID, EIS and others.

(2) Development of a new formation process of B/C composites and B₄C carbide.

New precursors were found for production of title materials. They were prepared by chemical processes using the combinations of (a) sugars, polyhydric alcohols or the compounds containing N-glucamine functional groups and (b) boric acid or organoboranes. Carbonization of these precursors provided the B/C composites with high boron concentration and B₄C. Preliminary characterization revealed that the composites show good oxidation resistance in a pure oxygen atmosphere.

(3) Synthesis and characterization of rare earth-chromium(V) compounds.

Unusual chemical state compounds, RECrO₄ (RE=rare earth elements) were synthesized and their structures including atomic positions, composition, vibrational structures, electric properties, electron configurations were investigated

in detail. Reversible structural transformation of these compounds, caused by reaction with methanol and oxidation in air, has been demonstrated.

(4) Anodic oxidation of aluminum in solutions containing metal-complex anions.

Aluminum was anodized in the solutions containing complex anions of metals (Fe, Ti, etc.). Some of the solutions provided oxide films having interesting properties. Further investigation of these processes is in progress.

(5) Electrochemical wastewater treatment using oxide anodes.

Various oxide anodes have been prepared by thermal decomposition of precursor salts on titanium substrate and anodic deposition. Using these anodes electrochemical decomposition of organic pollutants such as phenol, which are not easily decomposed by other methods, in wastewater has been examined to clarify the suitable electrochemical conditions and to develop effective anodes for their anodic decomposition.

(6) Formation of barrier-type amorphous anodic films on titanium and niobium alloys.

Alloying of titanium with other valve metals is found to result in the formation of uniform amorphous anodic films to relatively high voltages in neutral and acid electrolytes, in contrast to an amorphous-to-crystalline transition of anodic films on titanium at low voltages. Such anodic films formed on the titanium alloys are possible candidates of new dielectric materials for electrolytic capacitors. The positive effects of nitrogen addition to niobium on the dielectric properties and thermal stability of its anodic film for capacitor applications has been found recently.

(7) Tailoring of novel oxidation- and sulfidation-resistant materials at high temperatures.

Since niobium has exceptionally high sulfidation resistance and aluminum and chromium are most effective elements in enhancing the oxidation resistance of metals, Nb-Al-Cr ternary alloys have been prepared by sputter deposition, and their sulfidation and oxidation behavior has been examined. These alloys are found to possess high oxidation resistance comparable to typical chromia formers as well as high sulfidation resistance.

Other activities

Professor Konno attended International Conference on Carbon in 2001 (CARBON 2001) held at Lexington, U.S.A. in July and presented two papers entitled "Formation of oxidation-resistant carbon composites from exfoliated graphite and silicone" and "Formation of graphite at 1100-1200 °C from hard-carbon precursors". He also attended International Symposium on Nanocarbon 2001 held at Nagano, Japan, in November and presented a paper entitled "Synthesis of C/B₄C composites from sugar-boric acid mixed solutions".

Associate Professor Habazaki attended ECS/ISE Joint International Symposium held at San Francisco in September and presented a paper entitled "Corrosion Behavior of Copper-Mold Cast and Sheath-Rolled Ni-Cr-Nb-P-B Bulk Amorphous Alloys in HCl Solutions". He also attended 12th Asian-Pacific Corrosion Control Conference held at Seoul in October and presented a paper entitled "The sulfidation and oxidation behavior of sputter-deposited Nb-Al-Cr alloys at high temperatures". Associate Professor Habazaki and Mr. Uozumi attended International Symposium on Frontier of Surface Engineering (FSE2001) held at Nagoya in October and presented two papers entitled "Formation of black anodic films on aluminum in acidic electrolytes containing titanium complex anion" and "Formation of barrier-type amorphous anodic films on Ti-Mo alloys".

Presentations

Formation of Amorphous, Barrier-type Anodic Oxide Films on Ti-Mo Alloys; M. Uozumi and H. Habazaki: The joint Meeting of Hokkaido Secs. of ECSJ, SFSJ and JSCE, Sapporo, Jan, 2001.

Formation of Anodic Oxide Films on Aluminium in Metal-complex solutions; T. Takenaka, H. Konno and H. Habazaki: The joint Meeting of Hokkaido Secs. of ECSJ, SFSJ and JSCE, Sapporo, Jan, 2001.

Corrosion Protection of Steels of Al/Mo Oxyhydroxide films; K. Narumi and H. Konno: The joint Meeting of Hokkaido Secs. of ECSJ, SFSJ and JSCE, Sapporo, Jan, 2001.

Preparation of Carbon Composites Using Chelate Resins and Their Properties; R. Matsuura, H. Konno: The Winter Joint Meeting of Hokkaido Secs. of Chem. Soc. Jpn. And Jpn. Soc. Anal. Chem., Sapporo, Feb., 2001.

Low Temperature Graphitation of Polymers Using Metal Catalysts; K. Fujita, H. Habazaki and H. Konno: The Winter Joint Meeting of Hokkaido Secs. of Chem. Soc. Jpn. And Jpn. Soc. Anal. Chem., Sapporo, Feb., 2001.

Synthesis of B/C Composites by Thermal Decomposition of Suger-Organoboran Complexes; N. Inoue, T. Erata, Y. Aoki, H. Konno: The Winter Joint Meeting of Hokkaido Secs. of Chem. Soc. Jpn. And Jpn. Soc. Anal. Chem., Sapporo, Feb., 2001.

Synthesis of C/Si/O Composites and β -SiC from Exfoliated Graphite and Silicone; H. Konno, H. Kinomura: 257th Meeting of JSPS 117 Committee, Tokyo, April, 2001.

Formation of Oxidation-resistant Carbon Composites from Exfoliated Graphite and Silicone; H. Konno, H. Kinomura: CARBON'01, Lexington, July 2001.

Formation of Graphite at 1100-1200°C from Hard-carbon Precursors; H. Konno, K. Fujita, M. Inagaki: CARBON'01, Lexington, July 2001.

Preparation of C/Si/O Composites from Exfoliated Graphite and Silicone and Their Properties, T. Kinomura, H. Konno: The Summer Joint Meeting of Hokkaido Secs. of Chem. Soc. Jpn. And Jpn. Soc. Anal. Chem., Muroran, July., 2001.

Effect of Carbon Fibers on Water Purification Using Manganese-Oxidizing Bacteria; M. Endo, K. Sasaki and K. Konno: The Summer Joint Meeting of Hokkaido Secs. of Chem. Soc. Jpn. And Jpn. Soc. Anal. Chem., Muroran, July., 2001.

Electrochemical Decomposition of Phenol Using Oxide Anodes; Y. Hayashi, H. Habazaki and H. Konno: The Summer Joint Meeting of Hokkaido Secs. of Chem. Soc. Jpn. And Jpn. Soc. Anal. Chem., Muroran, July., 2001.

Formation of Amorphous Anodic Films on Ti Alloys; M. Uozumi, H. Habazaki and H. Konno: 48th Conference on Materials and Environments, Sapporo, September, 2001.

Electronic Conductivity of Carbon Films Obtained from Kapton-Type Polyimide Films; H. Konno, A. Yoneda and H. Habazaki: 259th Meeting of JSPS 117 Committee, Tokyo, September, 2001.

Formation of Black Anodic Films on Aluminum in Acidic Electrolytes Containing Titanium Complex Anion; T. Takenaka, H. Habazaki and H. Konno: FSE 2001, Nagoya, October, 2001.

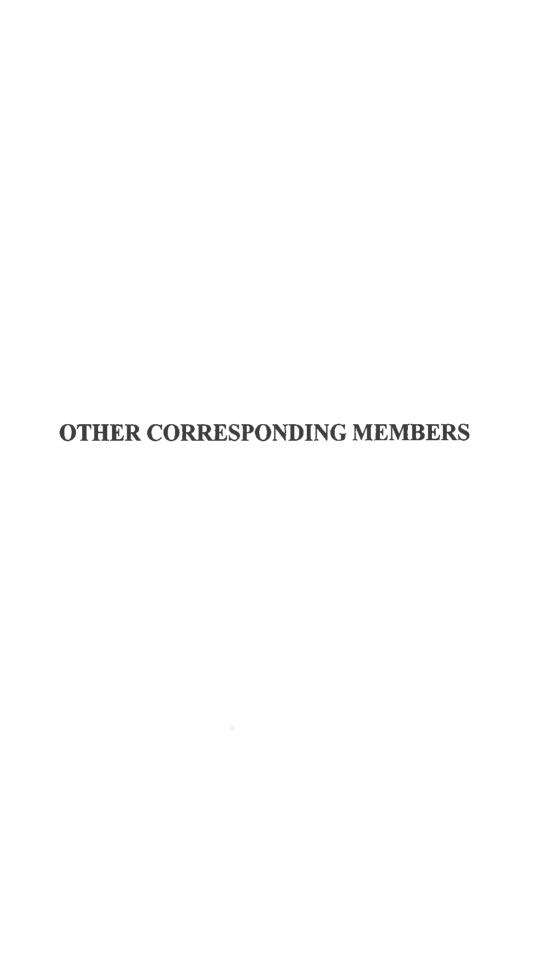
Formation of Barrier-type Amorphous Anodic Films on Ti-Mo Alloys; M. Uozumi, H. Habazaki, H. Konno, S. Nagata and K. Shimizu: FSE 2001, Nagoya, October, 2001.

Current Activities and Presentations

Synthesis of C/B₄C Composites from Sugar-Boric Acid Mixed Solutions; H. Konno, A. Sudoh, Y. Aoki, and H. Habazaki: ISNC 2001, Nagano, November, 2001.

Thermal Decomposition Behavior of Kapton-Type Polyimide Films Containing small amounts of Metal Ions; A. Yoneda, H. Konno, H. Habazaki: 28th Meeting of the Carbon Society of Japan, Kiryu, December, 2001.

Oxidation Resistance of C/Si/O Composites Prepared from Exfoliated Graphite and Silicone; T. Kinomura, H. Konno: 28th Meeting of the Carbon Society of Japan, Kiryu, December, 2001.



ē				

NS ELECTROCHEMICAL LABORATORY

Prof. Emeritus Dr. Norio Sato
Office address: Hanakawa Kita 1-3-30, Ishikari, Hokkaido, Japan 061-3211
Tel & Fax: +81-133-74-6969
E-mail: norios@hucc.hokudai.ac.jp

On February 12-15, 2001 Emeritus Professor Sato attended TMS 2001 Annual Meeting held in New Orleans and presented a talk entitled "Corrosion of metals by contact with metal oxides" at the symposium "Chemistry and electrochemistry of corrosion and stress corrosion cracking" honoring the contributions of R. W. Staehle. After the meeting he paid a visit to Professor A. T. Fromhold at the Department of Physics, School of Arts and Science, Auburn University, Alabama, who had once worked with Professor Sato for several months at Hokkaido University.

On July 19-20 2001 Professor Sato was invited to an International Workshop on Long-term Extrapolation of Passive Behavior held at Arington, Virginia, USA by the United States Nuclear Waste Technical Review Board and presented there a talk on the corrosion-accelerated and -decelerated effects of surface oxides on the passive behavior of corrosion-resistive alloys.

On September 2-7, 2001 Professor Sato attended the 2001 ECS and ISE Joint International Meeting held in San Francisco. During the meeting Professor Sato was conferred the 2001 ECS Olin Palladium Award on October 3 and he delivered the award lecture entitled "Surface oxides in metallic corrosion" on October 4. His lecture was later remarked by the Electrochemical Society Interface's Editor and Managing Editor as most impressive in terms of its clarity and even a non-specialist could come away from it with at least a basic knowledge of the importance of electron and ion transfer phenomena in corrosion processes.

On October 8-12, 2001 Professor Sato attended the 12th Asian-Pacific Corrosion Control Conference 2001 held in Seoul, Korea and presented an invited lecture

Current Activities and Presentations

entitled "Surface oxide films affecting metallic corrosion" on October 9. After the conference he paid a visit to Professor Su-II Pyun at the Department of Materials Science and Engineering, KAIST, Taejon, Korea and delivered on October 15-16 four invited lectures on corrosion and electrochemistry.

On October 29-November 3 Professor Sato attended the 2nd International Conference on Environment Sensitive Cracking and Corrosion Damage and presented an invited talk entitled "The stability and breakdown of passive films on metals".

Assoc. Prof. Dr. Hiroki Tamura

Tel.: +81-11-706-6741, Fax.: +81-11-706-6740 E-mail: h-tamura@eng.hokudai.ac.jp

Presentations

Adsorption of Alkali Metal Ions on Titanic Acid with Layer Structure; K. Nakamura, H. Tamura, and S. Kikkawa: The 2001 Winter Joint Meeting of the Hokkaido Secs. of Jpn. Soc. for Anal. Chem. and Chem. Soc. Jpn., Sapporo, Feb., 2001.

Ion Exchange Properties for Nano-interlayes of Titanic Acid: H. Tamura, K. Nakamura, and S. Kikkawa: The 49th Spring Annual Meeting of Chem. Soc. Jpn., Osaka, Mar., 2001.

Characterization of Active Cluster Water (ACWA) (1) A Simple Method for Evaluating the Lifetime of ACWA; T. Yokono, T. Erata, H. Tamura, and S. Shimokawa, The 2001 Summer Joint Meeting of the Hokkaido Secs. of Chem. Soc. Jpn. and Jpn. Soc. for Anal. Chem., Muroran, Hokkaido, Jul., 2001.

Amount of Hydroxyl Groups and Zero Point of Charge on Zinc Oxide as a Model Corrosion Product; H. Tamura: Forum for the Corrosion Protection of Zinc Plated Steels by Rust Layers, Tokyo, Oct., 2001.



Synergistic Effect of Three Corrosion-Resistant Elements on Corrosion Resistance in Concentrated Hydrochloric Acid

H. Katagiri, S. Meguro, M. Yamasaki, H. Habazaki, T. Sato, A. Kawashima, K. Asami and K. Hashimoto

Corros. Sci., 43, 171-182 (2001).

The best combination of small additions of corrosion-resistant elements in enhancing the corrosion resistance in 6 M HCl open to air at 303 K is examined for amorphous Ni-16P-4B alloys by adding chromium, tantalum and molybdenum The highest corrosion resistance is obtained by the additions of all three corrosion-resistant elements. The Ni-5Cr-5Ta-5Mo-16P-4B alloy is immune to corrosion. The most protective passive film on the Ni-5Cr-5Ta-(3-5)Mo-16P-4B alloys consists of outer double oxyhydroxide of Ta⁵⁺ and Cr³⁺ and inner Mo⁴⁺ oxide.

An Attempt at Preparation of Corrosion-Resistant Bulk Amorphous Ni-Cr-Ta-P-B Alloys

H. Katagiri, S. Meguro, M. Yamasaki, H. Habazaki, T. Sato, A. Kawashima, K. Asami and K. Hashimoto

Corros. Sci., 43, 183-191 (2001).

Preparation of cylindrical amorphous alloys with low contents of three corrosion-resistant elements, chromium, tantalum and molybdenum, were attempted by copper-mold casting. Ni-5Cr-5Ta-3Mo-16P-4B alloy of 1 mm diameter is identified as a single amorphous phase alloy and spontaneously passive in 6 and 12 M HCl, similar to the melt-spun amorphous counterpart, although high resolution TEM observation reveals the presence of nanocrystalline precipitates of about 2 nm diameter. Ni-5Cr-5Ta-5Mo-16P-4B alloy is also amorphous as shown by X-ray diffraction studies but contains nanocrystallites of about 5 nm diameter, the anodic current in 6 M HCl being more than one order of magnitude higher than that of the melt-spun amorphous counterpart. All other copper-mold cast Ni-16P-4B alloys with chromium, tantalum and molybdenum are composed of crystalline precipitates in the amorphous matrix.

Preparation of Corrosion-Resistant Amorphous Ni-Cr-P-B Bulk Alloys Containing Molybdenum and Tantalum

H. Habazaki, T. Sato, A. Kawashima, K. Asami and K. Hashimoto

Mater. Sci. Eng. A, 304-306, 696-700 (2001).

Cylindrical amorphous Ni-15Cr-10Mo-16P-4B and Ni-(10 and 5Ta-16P-4B alloys of 1 and 2 mm in diameter have been obtained by a copper mold casting method. These amorphous alloys are spontaneously passive in 6 M HCl at 303 K, and the corrosion resistance of the bulk alloys of 1 nm diameter in 6M HCl at 303 K is as high as that of the rapidly quenched alloy ribbons with the same composition. However potentiodynamic polarization reveals that the corrosion rate of the Ni-10Cr-5Ta-16P-4B alloy of 2 mm diameter is about three times higher than that of the alloy of I mm diameter though both sizes of the specimens are identified to be amorphous from X-ray diffraction patterns. The further detailed structural analysis using high resolution transmission electron microscopy indicates the presence of fcc nickel precipitates, 2-3 nm size, in the amorphous matrix only for the specimen of 2 mm diameter. Ni-15Cr-10Mo-16P-4B alloy of 2 mm diameter contains larger precipitates, about 20 nm size, of fcc nickel, showing about two orders of magnitude higher anodic current density than the amorphous single phase alloy of 1 mm diameter. Thus, the precipitation of a nanocrystalline nickel phase, which actively dissolves in 6M HCl, is detrimental to the corrosion resistance of the amorphous Ni-Cr-(Mo or Ta)-P-B alloys, although the smaller size of the precipitates is less detrimental.

Highly Corrosion-Resistant Ni-Based Bulk Amorphous Alloys

A. Kawashima, H. Habazaki and K. Hashimoto

Mater. Sci. Eng. A, 304-306, 753-575 (2001).

Bulk amorphous Ni-Nb-Ta-P alloys were successfully prepared by copper mold casting method. The addition of tantalum is effective in decreasing the corrosion rate. The corrosion rates of the alloys containing certain amounts of tantalum are more than four orders of magnitude lower than that of nickel metal and are almost equivalent to that of tantalum even in aggressive 12M HCl open to air at 30 °C. They are spontaneously passive and are characterized by immune to pitting by anodic polarization. The corrosion behavior of the bulk amorphous alloys is almost the same as corresponding melt-spun amorphous alloy ribbons.

Effects of Nanoscale Heterogeneity on the Corrosion Behavior of Non-Equilibrium Alloys

K. Asami, B.-P. Zhang, M. Mehmood, H. Habazaki and K. Hashimoto

Scripta. Mater., 44, 1655-1658 (2001).

Existence of nanocrystalline phases in amorphous alloys some times gives large effects to corrosion resistance of the alloy. The effects are detrimental or favorable depending on the size, composition and stability of the nanocrystalline phases. In general, precipitates less than 20 nm in diameter do not give large effect as far as the matrix contains enough amount of elements such as Cr which is responsible to the corrosion resistance.

Corrosion Behavior of Amorphous Ni-Cr-Nb-P-B Bulk Alloys in 6M HCl Solution

H. Habazaki, H. Ukai, K. Izumiya and K. Hashimoto

Mater. Sci. Eng. A318, 77-86 (2001).

Amorphous Ni-Cr-Nb-16P-4B bulk alloys highly corrosion-resistant in a 6 M HCl solution have been obtained by copper mould casting. The as-cast Ni-Cr-Nb-16P-4B alloys (Cr, Nb = 5 or 10 at.%) of 1 mm diameter are composed of an amorphous single phase, and they are spontaneously passive in the 6 M HCl solution at 303 K. Their polarization curves are almost the same as those of the rapidly quenched amorphous alloy ribbons. corresponding Ni-10Cr-5Nb-16P-4B bulk specimen of about 20 x 20 x 2 mm in size has been also prepared by consolidation of gas-atomized amorphous alloy powders by sheath rolling at 708 K, at which the alloy is in the super-cooled liquid state. Although X-ray diffraction pattern of the specimen revealed a halo, typical of amorphous structure, its corrosion resistance in the 6 M HCl is not as high as that of the as-cast one. After immersion of the sheath-rolled specimen in the 6 M HCl solution, spherical pit-like attacks have been observed on the surface, suggesting the presence of nanocrystalline precipitates locally. Thus, for the Ni-Cr-Nb-P-B alloys the formation of single amorphous phase appears to be necessary to have high corrosion resistance in aggressive environments.

Extremely Corrosion-Resistant Bulk Amorphous Alloys

K. Hashimoto, H. Habazaki, M. Yamasaki, A. Kawashima, K. Izumiya, H. Ukai, K. Asami and S. Meguro

Mater. Sci. Forum, 377, 1-8 (2001).

The addition of chromium, tantalum and molybdenum was the best combination of small additions in enhancing the corrosion resistance of amorphous Ni-16P-4B alloys in concentrated hydrochloric acid. Preparation of rod-shaped amorphous alloys with small contents of these three corrosion-resistant elements were attempted by copper-mold casting. Ni-5Cr-5Ta-3Mo-16P-4B alloy of 1 mm diameter is identified as a single amorphous phase alloy and spontaneously passive in 6 and 12 M HCl, similarly to melt-spun amorphous counterpart, although high resolution TEM observation reveals the presence of nanocrystalline precipitates of about 2 nm in diameter. Ni-5Cr-5Ta-5Mo-16P-4B alloy is also amorphous by X-ray diffraction but contains nanocrystallites of about 5 nm in diameter, the anodic current in 6 M HCl being more than one order of magnitude higher than that of the melt-spun amorphous counterpart. All other copper-mold cast Ni-Cr-Ta-Mo-16P-4B alloys are composed of crystalline precipitates in the amorphous matrix. Sheath-rolling consolidation of gas-atomized amorphous alloy powders to form the amorphous alloy sheet of about 2 mm was attempted for the Ni-10Cr-5Nb-16B-4B alloy which has a particularly wide temperature interval of the supercooled liquid of 64K. Because of inclusions of very minor crystalline powders in the major amorphous alloy powders before consolidation, crystalline powder inclusions in the consolidated amorphous matrix was preferentially dissolved by an immersion test in 6 M HCl. In a waste incinerator, the sheath-rolled Ni-10Cr-5Nb-16P-4B alloy showed no detectable weight loss at 393 and 433K for 20 days, maintaining metallic luster.

Corrosion of Metals by Contact with Metal Oxides

N. Sato

"Chemistry and Electrochemistry of Corrosion and Stress Corrosion Cracking: A Symposium Honoring the Contributions of R. W. Staehle", Edited by Russell H. Jones, pp. 289-300, The Mineral & Materials Society, (2001).

The electrode potential of oxide-covered metals and the mixed electrode potential of corrodible metals in contact with metal oxides were discussed in view of ionic and electronic transfer processes across the electrode introduces. The oxide-covered metal electrode stands either at the electrode potential of metal oxide formation or at the flat band potential of metal oxide. The mixed electrode potential of a corrodible metal and a metal oxide shifts its metal potential toward the flat band potential of the metal oxide in the cathodic direction if the oxide is n-type, or in the anodic direction if the oxide is p-type. Photoexcitation of contacting oxides enables the anodic oxygen evolution to occur on p-type oxides and the cathodic hydrogen evolution to occur on p-type oxides. Consequently, n-type oxides tend to reduce and p-type oxides tend to increase the metallic corrosion. (English)

Surface Oxides Affecting Metallic Corrosion

N. Sato

Corrosion Reviews, 19,153-272(2001).

Depending on their ionic and electronic properties, surface oxides influence metallic corrosion in aqueous solutions. The ion-selective property controls the transport of ions through the surface oxide, and the electronic property of the oxide influences the electrode potential of corroding metals. Anion-selective surface oxides accumulate corrosive anions accelerating the metallic corrosion, whereas cation-selective oxides inhibit the corrosion by removing corrosive hydrogen ions from the metal surface. The presence of n-type surface oxides lowers the electrode potential to decrease the metallic corrosion, while p-type surface oxides raise the potential accelerating the corrosion. Photoexcitation enhances these electronic effects of semiconducting surface oxides on the corrosion. (English)

Potential-Dimension Diagram of Localized Corrosion

N. Sato

"Marine Corrosion of Stainless Steels --Testing, Selection, Experience, Protection and Monitoring" Edited by D. Feron, pp. 185-201, The European Federation of Corrosion, IDM Communication Ltd., London, (2001).

Chloride-pitting in stainless steels proceeds at noble potentials in the polishing mode of metal dissolution, provided that the pit solution is enriched with chlorides beyond a critical concentration. It ceases to progress by pit repassivation if the pit is small, but it transforms into the active mode of pitting if the pit grows greater than a critical size. The boundary potential between the polishing mode and the active mode of pitting corresponds to the passivation-depassivation potential in the pit solution of the critical chloride concentration. Crevice corrosion is characterized by the crevice protection potential, at which the occluded crevice solution maintains the passivation-depassivation pH of the crevice metal. The crevice corrodes in the active mode at potentials more noble than the protection potential, where the crevice solution is more acidic than the pH. The stability of localized corrosion is represented in a diagram comprised of the electrode potential and the size of the localized corrosion. (English)

Measurement of Surface Thin Films on Electrodes by Ellipsometry

T. Ohtsuka

Electrochemistry, 60, 357-361 (2001)

The principles and equipments of ellipsometry were reviewed. The following recent applications to electrochemistry were introduced. (1) The growth of anodic oxide film on titanium depending on the potential sweep rate, (2) Chang of the anodic oxide film on titanium by uv light irradiation, (3) Electrodeposit layer of zinc-nickel alloy deposition, (4) Redox change of self-organized monolayers, and (4) Application of spectroscopic ellipsotry to the porous oxide film on aluminum. (Japanese)

Luminescence with Band-Gap Energy by UV-Light Excitation to Anodic Oxide Films on Titanium

M. Ueda and T. Ohtsuka,

Proc. the 2nd Intern. Conf. on Environment Sensitive Cracking and Corrosion Damage, 43-45 (2001)

Luminescence light from the anodic thin oxide films on titanium was measured by photo-excitation of ultra-violet light irradiation with 3.82 eV energy. The luminescence light is observed with a peak of about 3eV energy that corresponds to the band–gap energy of the n-type semiconductive TiO₂ oxide. It can therefore be presumed that the luminescence is induced by deexcitation or recombination between electrons in the conduction band and holes in the valence band. The peak wavelength of the luminescence light changes with the formation potential of the oxide film from 409 nm at 1 V to 425 nm at 6 V. The difference of the peak may reflect an amorphous-crystalline transition with increase of potential.

Nano-Mechano-Electrochemical Aspect of Passive Metal Surfaces

M. Seo, M. Chiba and Y. Kurata

Proceedings of "Corrosion and Corrosion Protection", ed. by J. D. Sinclair, R. P. Frankenthal, E. Kalman, W. Plieth, Electrochemical Society PV 2001-22, p. 217, Electrochemical Society. Inc., Pennington, NJ, USA(2001).

The nano-mechano-electrochemical properties of the single crystal iron (100) and (100) surfaces passivated at 0.25 V (SHE) for 1 h in pH 8.4 borate solution without and after the dichromate treatment (immersion in 5 x 10⁻² M K₂Cr₂O₇ solution for 24 h) and of the titanium surfaces anodically oxidized at - 0.5 V and 4.5 V(SHE) for 1 h in pH 8.4 borate solution were evaluated from the load-depth curves measured with in-situ and ex-situ nanoindentation tests. The dichromate treatment increased both the hardness, H, and the ratio of elastic work to total work, W_e/W_t, during the indentation for the iron (100) and (110) surfaces. It is inferred that during the loading, the film rupture and repair are repeated at the very edge of the contact surface. The increases in H and W_e/W_t were ascribed to the high repassivation rate at the ruptured sites of the chromium-enriched film formed by the dichromate treatment. Moreover, the hardness values, H, measured under the potential control in solution for the titanium surfaces anodically oxidized at - 0.5 V and 4.5 V were three or four times as high as those measured in air after the anodic oxidation. The high hardness values obtained with in-situ measurement were also ascribed to the high repassivation rate under the potential control in solution. (English)

Stress Generation During Anodic and Cathodic Polarization of a Titanium Thin Film Electrode in pH 8.4 Borate Buffer Solution

J.-D. Kim, S.-I. Pyun and M. Seo

Proceedings of "Corrosion and Corrosion Protection", ed. by J. D. Sinclair, R. P. Frankenthal, E. Kalman, W. Plieth, Electrochemical Society PV 2001-22, p. 154, Electrochemical Society. Inc., Pennington, NJ, USA(2001).

The stresses of anodic oxide film on titanium thin film / glass electrode in pH 8.4 borate solution with various potential scanning and steps were investigated by the modified bending beam method. The compressive stresses were always observed in the anodic potential range. The increases in compressive stress with cathodic potential sweep and steps were attributed to the volume expansion of the film due to the compositional change from TiO₂ to TiOOH. The differences in stress between before absorption and after desorption of hydrogen were due to the changes of interface from Ti /TiO₂ to TiH_x / TiO₂. The transients in current density and stress produced by various potential steps demonstrated well the relation between the changes in stress and the amount of hydrogen in the oxide film. (English)

Transport of Alkaline Cation and Neutral Species through the α -Ni(OH)₂ / γ -NiOOH Film Electrode

J.-W. Lee, J.-N. Han, M. Seo and S.-I. Pyun

J. Solid State Electrochem., 5, 459 – 465 (2001)

The transport of alkaline cation and neutral species through the α -Ni(OH)₂/ γ -NiOOH film electrode has been investigated during the hydrogen extraction from and injection into the film electrode in 0.1 M LiOH, KOH and CsOH solutions by using electrochemical quartz crystal microbalance (EQCM) technique combined with potentiostatic current transient technique and cyclic voltammetry. From the ohmic relationship between initial current density and applied potential step, it is suggested that the hydrogen transport through the film electrode is exclusively governed by 'cell-impedance'. Based upon the 'cell-impedance controlled' hydrogen transport, the mass change measured indicates that during the hydrogen extraction, the alkaline cation is slowly inserted into the film electrode before the finish of current plateau. After the period of current plateau is finished, it is drastically inserted in an exponential rate. By contrast, during the hydrogen injection, the desertion of alkaline cation is nearly completed before the finish of current plateau. Most of the neutral species are incorporated into the film electrode during the proceeding immersion stage prior to the hydrogen extraction. The minority is not incorporated until the finish of current plateau during the succeeding hydrogen injection. (English)

Nano-mechano-electrochemistry of Passive Metal Surfaces

M. Seo and M. Chiba

Electrochim. Acta, 47 (1-2), 319-325 (2001).

In-situ nanoindentation tests were performed to evaluate the mechanical properties of the iron (100) and (110) surfaces passivated potentiostatically for 1 h in pH 8.4 borate solution after or without immersion in 5 x 10^{-2} M $K_2Cr_2O_7$ solution for 24 h. It was found from the measured load-depth curves at a maximum load of 400 μ N that the hardness (3.2 - 3.3 GPa) of the passivated iron (110) surfaces was larger by 10 % than that (2.9 - 3.1 GPa) of the passivated iron (100) surfaces. Moreover, the hardness of the passivated iron (100) and (110) surfaces increased slightly with increasing formation potential of passive film, which was ascribed to the presence of passive film. The dichromate treatment increased the hardness of the iron (100) and (110) surfaces to some extent. The loading discontinuity appeared frequently at a load of about 90 μ N in the load-depth curves for the passivated iron (110) surfaces as compared with the passivated iron (100) surfaces. The loading discontinuity in the load-depth curves for the iron (110) surface, however, disappeared completely due to the dichromate treatment. (English)

Susceptibility of Local Breakdown of Passive Film Formed on Iron

K. Fushimi and M. Seo.

Proceedings of "Corrosion and Corrosion Protection", ed. by J. D. Sinclair, R. P. Frankenthal, E. Kalman, W. Plieth, Electrochemical Society PV 2001-22, p. 325, Electrochemical Society. Inc., Pennington, NJ, USA(2001).

A small amount of Cl ions could be locally generated from a liquid-phase ion gun (LPIG), which consists of a silver microelectrode covered with silver chloride, by cathodic polarization. The LPIG was employed to induce the local breakdown of passive films formed on iron in deaerated borate solutions. The time period, t_{BD}, was required for induction of the local breakdown. The longer induction period was needed for local breakdown of the thicker passive film with the lower electric field. The structural changes of passive films due to Cl ions before initiation of the local breakdown were discussed. Moreover, the induction period depended on the substrate grain-orientation, which was explained in terms of difference in thickness or defective structure of passive film on the substrate grains. (English)

Initiation of a Local Breakdown of Passive Film on Iron due to Chloride Ions Generated by a Liquid-Phase Ion Gun

K. Fushimi and M. Seo

J. Electrochem. Soc., 148 (11), B450-B456 (2001).

A small amount of Cl⁻ could be locally generated from a liquid-phase ion gun (LPIG), which consists of a silver microelectrode covered with silver chloride, by cathodic polarization. The LPIG was employed to induce the local breakdown of the passive films formed on iron in deaerated borate solutions. The concentration of Cl⁻ generated locally on the passivated iron surface was estimated to be about 1 mol dm⁻³ from the measurement of the potential difference between the narrow space enriched with Cl⁻ and bulk solution. The induction period, t_{BD}, was required for initiation of local breakdown. The longer induction period was needed for initiation of local breakdown of the thicker passive film with the lower electric field. The structural changes of passive films due to Cl⁻ before initiation of local breakdown were discussed. Moreover, the induction period depended on the substrate grain-orientation, which was explained in terms of difference in thickness or defective structure of passive films on substrate grains. (English)

Double Zincate Pretreatment of Sputter Deposited Al Films

K. Azumi, T. Yugiri, M. Seo and S. Fujimoto

J. Electrochem. Soc., **148** (6), C433-438 (2001)

The characteristics of double zincate pretreatment of thin Al films deposited on glass plates using magnetron sputtering and ion-beam sputtering were investigated. Traces of Zn deposition and immersion potential as well as surface observations using SEM and AFM showed that continuous dissolution of an Al film during the double zincate pretreatment occurred in the case of a magnetron sputter deposited film, resulting in Al film failure from the substrate. On the other hand, the substitution reaction of Al dissolution and Zn deposition occurring on the ion-beam sputter deposited film ceased during the first and the second zincate treatment processes. The difference between the behaviors of the double zincate treatments for the two kinds of sputter deposited films is related to the film structure. A magnetron sputter deposited film has a columnar structure, resulting in higher susceptibility to the dissolution reaction in a concentrated alkaline zincate solution. On the other hand, an ion-beam sputter deposited film has a fine micro-crystalline structure with a low density of defects, resulting in lower susceptibility to the dissolution reaction. (English)

Changes in Electrochemical Properties of the Anodic Oxide Film Formed on Titanium During Potential Sweep

K. Azumi and M. Seo

Corrosion Science, 43, 533-546 (2001).

Changes in electronic properties of the anodic oxide films formed on titanium in weakly-alkaline borate solution were investigated by using impedance measurements. Analysis of the cyclic voltammogram and capacitance during the cyclic potential sweep suggested that the outer part of the anodic oxide film was converted from an n-type semiconductor to a dielectric above 3 V, and converted to an n-type semiconductor again below 0.5 V. This phenomenon seems to be related to the dissociation of bound water in the film due to very high electric field applied to the oxide film. Formation of OH in the film may compensate the positive charge of the donor states and form Ti peroxide such as TiO₃. These compounds are reduced below 0.5 V to show a characteristic cathode current peak. (English)

Effect of Anodic Oxide Film Structure on The Prevention of Electroless Ni-P Deposition on Al 5052 Alloy

S.-M. Moon, M. Sakairi, H. Takahashi, and K. Shimamura,

Electrochem. Soc. Proc. Vol., 2000-25, 383-392, (2001).

This work is concerned with the effects of anodic oxide film structure, including defects and pores in the film and thickness of the film, on electroless Ni-P deposition on Al5052 alloy. The unsealed anodic oxide film of Al5052 alloy showed easier nucleation of Ni-P deposits and higher density of Ni-P nucleation site than that of pure aluminum, revealing the presence of defects in the film on Al5052 alloy. The defects seem to be mainly voids generated by the dissolution of second-phase particles. Sealing treatment of anodic oxide films on Al5052 alloy and pure aluminum, markedly reduced the number of Ni-P deposits. The number of Ni-P deposits was also reduced by the formation of thicker anodic oxide film on Al5052 alloy. These results suggest that small size defects in anodic oxide films become readily inactive by sealing treatment and large size defects can be inactive by the formation of thicker anodic oxide film and sealing treatment.

Repairing of Anodic Oxide Films on AI – Zn Alloy Coated Steel After Removal with Photon Rupture in Solutions

M. Sakairi, K. Itabashi and H. Takahashi

Proc. of APCCC12, 542-551 (2001)

Analysis of abrupt destroyed of passive oxide films on Al - Zn alloy layer coated on steel and its repair is important to understand the localized corrosion of steels. In the present investigation, anodic oxide films formed on Al - Zn coated steel specimens were removed by photon rupture method (one pulse of focused pulsed Nd - YAG laser beam irradiation) at a constant potential in sodium borate solutions, pH = 9.2, with / without chloride ions to monitor the current transient. Irradiation with a pulsed laser in solutions causes abrupt removal of the anodic oxide film on the specimen at the laser-irradiated area. Without chloride ions, oxide films were reformed in the sodium borate solution at - 0.5 to 1 V after removal of the anodic oxide film. However, in chloride ions containing solutions, pitting corrosion of Zn - 55 mass % Al coated layers occurs at high potentials, while film reformation occurs at low potentials. It was also found that chloride ions enhance dissolution of aluminum and zinc at the very initial period after laser irradiation.

Morphology and Composition of Layered Anodic Films on InP

F. Echeverria, P. Skeldon, G.E. Thompson, H. Habazaki, K. Shimizu

J. Mater. Sci., 36, 1253-1260 (2001).

The composition and morphology of the double-layered anodic film formed at 5 mA cm⁻² on InP in aqueous sodium tungstate electrolyte is examined by transmission electron microscopy (TEM), atomic force microscopy (AFM), Rutherford backscattering spectroscopy and nuclear reaction analysis. The outer layer is composed mainly of In₂O₃ of relatively low atomic density, about 50% that of crystalline In₂O₃. The low density is probably due partly to the presence of numerous cavities in the layer, revealed by TEM and AFM. The inner layer is enriched in phosphorus relative to the composition of the substrate, with a P: In atomic ratio of about 2.17. From the measured ratio of phosphorus to indium, the composition of the inner layer can be expressed as either In₂O₃·2.17P₂O₅ or $In(PO_3)_{2.17}$. The average nm V⁻¹ ratio is 1.99 ± 0.07. However, there are wide variations of the local film thickness, associated with roughness at the substrate/film and film/electrolyte interfaces and local variability in the ionic current density due to cavities in the film. The film forms with a small loss of indium species to the electrolyte. The outer layer represents about 32% of the total thickness of a film formed at 100% efficiency.

Enrichment of Alloying Elements Beneath Anodic Oxides: Investigation of Ta-1.5 at.% Cu Alloy

S. Mato, G.E. Thompson, P. Skeldon, K. Shimizu, H. Habazaki and D. Masheder

Corros. Sci., 43, 993-1002 (2001).

In order to elucidate the factors controlling enrichment of alloying elements during anodic oxidation of alloys, and anodic oxidation behaviour of alloys generally, the influence of anodic film growth on a Ta-1.5 at.% Cu alloy has been examined by transmission electron microscopy, Rutherford backscattering spectroscopy and glow discharge optical emission spectroscopy. Contrasting with the behaviour of Al-Cu alloys, film growth proceeds without significant enrichment of copper in the tantalum alloy substrate, although a thermodynamic driving force for enrichment exists. Factors controlling the development of enriched alloy lavers are considered, including influences of distributions of alloying element in the substrate, film structure and ionic transport in the anodic film. Comparisons of alloy systems suggest kinetic factors may be important, in particular the influence of film formation at the alloy/oxide interface on concentrations of vacancies and diffusion rates in the alloy layer immediately beneath the growing oxide film.

Behaviour of Bismuth During Simulated Processing of Model Aluminium Capacitor Foils

Z. Ashitaka, G.E. Thompson, P. Skeldon, H. Habazaki and K. Shimizu

J. Mater. Sci., 36, 2237-2244 (2001).

The production of high specification, aluminium-based, electrolytic capacitors requires optimization of material composition and heat and surface treatments in order to maximize the area available for formation of the dielectric, anodic film. Commercial foils contain low additions of copper and lead in order to achieve this goal. The present study examines the effects of heat and surface treatments on aluminium foil containing either 50 or 1000 ppm bismuth, as a replacement for lead, by a combination of Rutherford backscattering spectroscopy and scanning electron microscopy. Heat treatment at 823 K results in segregation of bismuth to the surface regions of the foils, with enrichments in the range 4-8 x 10¹⁴ Bi atoms cm⁻², localized mainly just beneath the thermal oxide, for the selected treatment conditions. The enrichment reduces following alkaline etching, to the range 1-4 x 10¹⁴ Bi atoms cm⁻². This level of enrichment is maintained during subsequent anodizing, with the enrichment partitioned between the metal and the outermost layers of the anodic films. The enrichment of the metal is about 4 x 10¹³ Bi atoms cm⁻². Electropolishing in perchloric acid solution eliminates the enrichment developed during the heat treatment, probably due to activation during the polishing process. The enrichment remains very low or negligible during subsequent anodizing. The general behaviours of bismuth and lead are similar in aluminium foils subject to the selected heat and surface treatments. However, additional studies are needed of tunnel etching to determine the feasibility of substitution of lead by bismuth in commercial foils.

History Effects in Anodic Oxidation of Al-W Alloys

L. Iglesias-Rubianes, P. Skeldon, G.E. Thompson, H. Habazaki and K. Shimizu

Phil. Mag. A, 81, 1579-1595 (2001).

Stepped-current experiments are applied to the study of barrier film formation on an Al-6.5 at.% W alloy prepared by magnetron sputtering. These reveal transient changes in the composition and/or the density in local regions of the anodic film immediately following changes in the current density between 0.1 and 10 mA cm⁻². Specifically, following an increase and a decrease in the current, bands of film material approximately 6 nm thick are generated at, or near, the alloy-film interface, which are, firstly, respectively enriched and depleted in tungsten species and/or, secondly, of enhanced and reduced density respectively. There is also evidence that similar bands are generated simultaneously at, or near, the film-electrolyte interface. Further, either the density or the composition of film material formed at the alloy-film interface, or a combination of these factors, depends upon the current, with material retaining to some extent its original property as the film develops at the new current. Possible reasons for the occurrence of these features are considered.

Role of Oxygen Bubble Generation in Anodic Film Growth on InP

P. F. Echeverria, P. Skeldon, G.E. Thompson, J.W. Fraser, J.P. Mccaffrey, S. Moisa, M.J. Graham, H. Habazaki and K. Shimizu

Corros. Sci., 43, 2173-2184 (2001).

The morphologies of barrier-type anodic films grown on InP have been investigated using atomic force microscopy, scanning electron microscopy and transmission electron microscopy in order to gain further understanding of the non-linear voltage-time behaviour and the development of blisters in the films. The films. which are two layered, with an outer layer of In₂O₃ and an inner phosphorus-rich layer, containing also indium species, were formed at 50 A m⁻² in aqueous 0.1 M sodium tungstate electrolyte at 298 K. During the early stages of anodizing, i.e. within the initial region of linear voltage-time response, a relatively compact and uniform film forms, with a comparatively featureless surface. However, as the voltage increases, cavities develop within the film., and in places the anodic film material detaches partially from the substrate. The film surface then discloses fine-textured roughness and coarse protuberances associated with cavity formation and detachment respectively. Such transformation of the film morphology correlates with a decrease in slope of the voltage-time response, which commences at a formation voltage of approximately 17 V, with a film thickness of about 25 nm. The behaviour is explained by generation of oxygen within the anodic film material, which forms high pressure bubbles of gas. Such gas formation is related to the presence of an In₂O₃ outer layer of the film and the presence of units of In₂O₃ in the inner layer of the film, which facilitate oxidation of O²- ions of the film material.

Influence of Current Density in Anodizing of an Al-W Alloy

L. Iglesias-Rubianes, P. Skeldon, G.E. Thompson, K. Shimizu and H. Habazaki

Corros. Sci., 43, 2217-2228 (2001).

The influences of current density in development of amorphous, barrier anodic films on a metastable, solid solution, Al-6.5at.%W alloy is examined, with focus on enrichments in the alloy, oxidation processes at the alloy/film interface and migration of species in the film. The films were formed at current densities between 0.01-100 mA cm⁻² in sodium tungstate electrolyte and examined by transmission electron microscopy and Rutherford backscattering spectroscopy. Enrichments of tungsten in the alloy develop at each of the selected current densities, with enrichments in the range 2-4 x 10¹⁵ W atoms cm⁻². Incorporation of tungsten species into the films at the alloy/film interface proceeds non-uniformly, with cycles of local enrichment of the alloy, oxidation of the enriched tungsten and subsequent depletion of the alloy. The tungsten species migrate more slowly than Al³⁺ ions, leading to layering of the film composition. The cyclic incorporation of tungsten species into the film and the migration of tungsten species within the film are similar for the selected current densities, at the resolution of the experiments.

Influence of Surface Treatment on Detachment of Anodic Films from Al-Mg Alloys

Y. Liu, P. Skeldon, G.E. Thompson, X. Zhou, H. Habazaki and K. Shimizu

Corros. Sci., **43**, 2349 – 2358 (2001).

Previous work of the authors has revealed detachment of anodic films during anodizing of elect to polished, solid-solution Al-3 at.%Mg alloy at constant current density, with the possibility of the electropolishing pre-treatment having a significant influence on the loss of the film material. Here, anodic films were formed on a similar alloy, with pre-treatment by electropolishing, alkaline etching or mechanical polishing. The results disclose the detachment of the anodic film for all pre-treatments, thus demonstrating that prior electro polishing is not essential for initiation of detachment. However, the occurrence of detachment was sensitive to the current density, with lower current densities promoting detachment at earlier stages of growth of the anodic film for a particular pre-treatment.

Influence of Interfacial Depth on Depth Resolution During GDOES Depth Profiling Analysis of Thin Alumina Films

K. Shimizu, H. Habazaki, P. Skeldon, G.E. Thompson, R.K. Marcus

Surf. Interface Anal., 31, 869-873 (2001).

Factors controlling the depth resolution in radio frequency glow discharge optical emission spectroscopy (rf-GDOES) depth profiling analysis of thin films have been investigated using anodic alumina films of varying thicknesses with delta function marker layers of similar to 2 nm width located at various depths from the oxide surface. In rf-GDOES depth profiling analysis, where a relatively large area of similar to 4 mm in diameter is analysed, it was found that the depth resolution is determined mainly by the large-scale variation of sputtering rate across the crater. Despite the relatively large area analysed, the uniformity of sputtering rate across the crater was constant to within 1% under the optimum Ar pressure except for near-edge regions of similar to 0.4 mm width, where the sputtering rate was similar to 6% higher than in the central crater region. Owing to this relatively minor non-uniformity of sputtering rate, the depth resolution degrades approximately linearly with depth. A depth resolution of similar to 1.3 nm was realized to depths of similar to 25 nm, where the degradation of depth resolution due to the non-uniformity in sputtering rate is insignificant. The depth resolution is close to the ultimate depth resolution in sputter depth profiling, claimed to be 0.7-1.0 run, and arises from the minimal atomic mixing associated with film sputtering with Ar ions of very low energy, similar to 50 eV, in rf-GDOES analysis.

Migration of Oxalate Ions in Anodic Alumina

K. Shimizu, H. Habazaki, P. Skeldon, G.E. Thompson, G. C. Wood

Electrochim. Acta., 46, 4379-4382 (2001).

The migration rate of oxalate ions, (COO)₂ in anodic alumina has been determined by analysis of a barrier film, containing an immobile boron marker and thin oxalate-doped layer, by SIMS depth profiling. From the relative distributions of the boron marker and the carbon species in the depth-profiled film, it is shown that oxalate ions migrate inward at a rate of about 0.57 relative to that of oxygen ions.

Reproducibility in r.f.-GDOES Depth Profiling Analysis of Thin Films

K. Shimizu, H. Habazaki, P. Skeldon and G.E. Thompson

Surf. Interface Anal., 31, 1085-1086 (2001).

The reproducibility in radiofrequency glow discharge optical emission spectroscopy (r.f.-GDOES) depth profiling has been examined using a 360 nm thick anodic alumina film with a chromium-containing delta-function layer. The time required to sputter through the film was constant, to within 1%, whereas the signal intensities of film species agreed to within 3%. This level of reproducibility together with high depth resolution makes the technique ideal for on-site quality control of various surface-enhanced industrial products, embracing electronics and protective surface treatments.

The Stability and Breakdown of Passive Oxide Films on Metal Anodes

N. Sato

J. Indian Chem. Soc., 78, October-December, 517-524 (2001).

The passive oxide film on metals in aqueous solutions is stable as long as the Fermi level at the Film/ solution interface remains within the electronic energy band gap of the film (in the state of electronic band level pinning). Transpassivation that leads to a potential-dependent dissolution of the passive film occurs in the range of electrode potential in which the Fermi level is pinned in the electronic valence band level at the film/solution interface. Chloride adsorption introduces the surface state of electronic acceptor levels of the passive oxide films. When the Fermi level of passive metal anodes is pinned at the chloride-induced surface state, the localized transpassive dissolution of the passive film proceeds at the chloride adsorption sites to cause a local film breakdown. The critical potential for the local film breakdown appears less anodic (more negative) than the general transpassivation potential. (English)

Ion Selective Lust Layers and Passivation of Metals

N. Sato

" Passivity of Metals and Semiconductors: Proceedings of the Eighth International Symposium", Edited M. B. Ives, J. L. Luo and J. R. Rodda, pp. 289-300, Proceedings Volume 99-42, The Electrochemical Society, Inc., Pennington, USA, (2001).

Anodic metal dissolution produces hydrated metal salts concentrated at the anode interface and modifies the ion transport in the interfacial diffusion layer to be either anion-selective or cation-selective. The anion-selective diffusion layer formed with monovalent chloride or hydroxide contributes to the formation of a chloride film, giving rise to either the chloride-film-induced passivation if the chloride is insoluble (e.g. Ag/AgCl) or the transition from the active mode to the polishing mode of dissolution if the chloride is soluble (e.g. Fe/FeCl₂). The cation-selective diffusion layer formed with multivalent phosphate or sulfate ions gives rise to the formation of an oxide, and thereby to the oxide-film-induced passivation of metal anodes (e.g. Fe/Fe₂O₃). Generally, rust layers are anion-selective in acidic solutions and cation-selective in basic solutions. Adsorption of multivalent oxyanions often changes the lust layers from the anion-selective to the cation selective. The anion-selective lust layer accelerates the localized corrosion of metals; whereas, the cation-selective rust layer inhibits the localized corrosion. The ion-selective bipolar rust layer suppresses the anodic metal dissolution and leads to metal passivation. (English)

Surface Oxide Films Affecting Metallic Corrosion

N. Sato

Proceedings of the 12th Asian-Pacific Corrosion Control Conference Vol. 1, pp. 45-58, Corrosion Science Society of Korea, (2001).

Discussion is made on the comprehensive effects of the ionic and electronic properties of surface oxide films upon metallic corrosion in aqueous solutions. The ionic property controls the transport of ions in the corrosion processes, and the electronic property influences the electrode potential of corroding metals. Anion-selective oxide films accumulate corrosive hydrated anions on the metal surface and thus accelerate metallic corrosion, whereas cation-selective oxide films inhibit metallic corrosion by removing corrosive hydrogen ions from the metal surface. The presence of n-type oxides on the metal surface shifts the corrosion potential in the cathodic direction thus reducing the corrosion probability. On the contrary, p-type oxides shift the corrosion potential in the cathodic direction accelerating the corrosion. Photoexcitation of n-type and p-type oxides increases these potential shifts further in the cathodic and the anodic direction (photopotential), respectively; hence, photoexcitation enhances the electronic effect of surface oxides on metallic corrosion. (English)

The Stability and Breakdown of Passive Oxide Films on Metals

N. Sato

Proceedings of the 2nd International Conference on Environment Sensitive Cracking and Corrosion Damage (ESCCD), Edited by M. Matsumura, H. Nagano, K. Nakasa and Y. Isomoto, Hiroshima University, pp. 49-54, (2001).

A study is made on how the electronic energy levels affect the stability of passive oxide films on metals in aqueous solutions. The passive oxide film is stable and corrosion-resistive to the extent that the Fermi level at the film/solution interface remains within the electronic energy band gap of the film, i.e. in what is called the electronic band edge pinning. Transpassivation that leads to a potential-dependent dissolution of the passive film occurs in the range of electrode potential in which the Fermi level is pinned at the electronic valence band edge on the film/aqueous solution interface. Chloride adsorption introduces the surface state of electronic acceptor levels on the passive oxide film. When the Fermi level of passive metal anodes is pinned at the chloride-induced surface state, the localized transpassive dissolution of the passive film proceeds at the chloride adsorption sites to produce a local film breakdown. The critical potential for the local film breakdown is thus less anodic (more negative) than the general transpassivation potential. The film-breakdown site either grows into a pitting corrosion if the film breakdown potential is more anodic than the pit initiation potential or repassivate itself if the former potential is more cathodic than the latter potential. (English)

On Long-Term Extrapolation of Passive Behavior

N. Sato

Proceedings from an International Workshop on Long-Term Extrapolation of Passive Behavior, July 19-20, 2001, Arlington, Virginia, USA, Edited by A. A. Sagues and C. A. W. DiBella, United States Nuclear Waste Technical Review Board, (2001).

Under radiation conditions semiconducting p-type oxides, if formed on Alloy 22, will shift the open circuit potential of the alloy in the anodic direction and cause passivity breakdown leading to a localized mode of corrosion in the alloy. Semiconducting n-type oxides will shift the alloy potential in the cathodic direction and prevent the passivity breakdown, though increasing the probability of hydrogen damage in the alloy. In order to prevent the passivity breakdown due to p-type oxides application of the coating of n-type oxide layers such as TiO₂ on the Alloy 22 will be effective. (English)

The Behaviour of Iron During Anodic Oxidation of Sputtering-Deposited Al-Fe Alloys

H. Habazaki, K. Shimizu, P. Skeldon, G.E. Thompson, G.C. Wood

Corros. Sci., 43, 1393-1402 (2001).

Interfacial enrichment of iron atoms and iron ions has been observed at the alloy/film and film/electrolyte interfaces respectively during anodizing of sputtering-deposited, non-equilibrium Al-7.5 at.% Fe alloys. The formation of the anodic oxide involves initial oxidation of aluminium and enrichment of iron in a layer of alloy, about 2 nm thick, immediately beneath the oxide film. When the level of enrichment reaches about 3.8 x 10¹⁹ Fe atoms m⁻², corresponding to an average composition of the enriched alloy layer of approximately Al-25 at.% Fe, both aluminium and iron species are incorporated into the film in the presence of the enriched layer. The incorporated iron species, namely Fe3+ ions, migrate outward in the growing anodic film, about 2.0 times faster than Al3+ ions. Consequently, the iron species eventually reach the film/electrolyte interface forming a thin, amorphous layer probably composed of Fe₂O₃. Oxygen is generated at, or near, the alloy/film interface subsequent to incorporation of iron species into the film. The general anodizing behaviour is similar to that reported previously for an Al-4 at.% Fe alloy, although in that case significant oxygen generation and void formation, which limits thickening of uniform films, is postponed to higher voltages, while the outer, iron-rich layer is composed mainly of crystalline FeOOH.

Water Layer in Course of Corrosion of Copper in Humid Air Containing SO₂

T. Sasaki, J. Ito, and T. Ohtsuka

Proc. the 12th Asian-Pacific Corrosion Control Conf. 2001, 1395-1400 (2001)

The technique for in situ simultaneous measurements of IR-RAS and QCM, which has been developed for investigation of corrosion in gaseous environments, was employed to study the effects of an extremely thin water layer on the corrosion rate. An evaporated copper film on a OCM element was exposed to air containing water vapor and SO₂, and time-resolved IR-RAS spectra were measured and mass gains were simultaneously followed with OCM. The tested ranges of relative humidity (RH) and concentration of SO₂ were 60% - 90% and 1 - 20 ppm, respectively. On the basis of 2D-IR analysis, the corrosion products were determined to be Chevreul's salt (CuSO₃Cu₂SO₃·2H₂O) and CuSO₄·5H₂O. By constructing curves of the relations between band intensities of IR spectra and mass gains of QCM for the corrosion products, the time variations in each product were determined from spectral experiments on copper plates. The thickness of physically adsorbed water layers in course of the corrosion process were also determined from water The results showed that the thickness of the physically adsorbed band intensities. water layer increased with increase in RH, and it also increased with increase in accumulation of corrosion products. The latter is probably due to the capillary effect of the corrosion products.

Durable Al-Zn Coating on Steels by Two-step Hot Dipping

J. Tanaka and T. Narita

Surface Science and Engineering, India (2001)

A two-step hot dipping was developed to from Al-Zn coating on steels, which was highly durable against various corrosion atmospheres, and it is low cost and has advantages, such as relatively low bath temperature with easy handling, controlled structures of the coating, and diversity of conventional facilities for Zn baths.

Steels were first dipped to a conventional Zn bath to from Fe-Zn coating, which has a columnar structure, consisted mainly of ζ phase containing η phase, and then they were immersed into the Zn-7mass%Al bath, in which the Zn-Al melt penetrated through boundaries of columnar grains and Al replaced Zn to form Al-Fe-Zn coating. At bath temperatures lower than about 700K the coating has an acicular Fe₄Al₁₃-Zn₂ with small amounts of the Zn-Al, whereas at higher temperatures the Al-Fe-Zn was plate-like Fe₂Al₅-Zn_x in an inner layer and fine precipitates of Fe₄Al₁₃-Zn_x in an outer layer. Changes in structure and composition of the coating from Zn-Fe to Al-Fe-Zn were discussed, basing on a ternary Al-Fe-Zn phase diagram. A salt splaying test was carried out at room temperature fore the Fe-Al-Zn coating and for a conventional Fe-Zn coating for comparison purpose. The Fe-Al-Zn coating has little rust after 3000 hrs and tended to rust after 10000 hrs in contrast to the results that a red-rust appeared for the Fe-Zn coating after 240 hrs and became so much for prolonged corrosion. The high durability of the Al-Fe-Zn coating is due to its fine structure, reducing preferential corrosion paths. (English)

Anodizing of Aluminum Coated with Silicon Oxide by a Sol-Gel Coating

K. Watanabe, M. Sakairi, H. Takahashi, K. Takahiro, S. Nagata, S. Hirai

J. Electrochem. Soc, 148, B473-B481 (2001)

Aluminum specimens were covered with SiO₂ film by a sol-gel coating and then anodized galvanostatically in a neutral borate solution. Time variations in the anode potential during anodizing were monitored, and the structure and dielectric properties of anodic oxide films were examined by transmission electron microscopy, Rutherford back scattering spectroscopy, and electrochemical impedance measurements.

It was found that anodizing of aluminum coated with SiO₂ films leads to the formation of anodic oxide films, which consist of an outer Al-Si composite oxide layer and an inner Al₂O₃ layer, at the interface between the SiO₂ film and the metal substrate. The capacitance of anodic oxide films formed on specimens with SiO₂-coating was about 20% larger than without SiO₂-coating.

In the film formation mechanism, the conversion of Al₂O₃ to Al-Si composite oxide at the interface between the inner and outer layers is discussed in terms of inward transport of Si-bearing anions across the outer layer.

Anodizing of Aluminum Covered with SiO₂ by Sol-Gel Coating – Formation Mechanism of Composite Oxide Films with High Potential Sustainability –

K. Watanabe, M. Sakairi, H. Takahashi, S. Hirai and S. Nagata

Electrochem. Soc. Proc. Vol. 2000-25, 146-153 (2001)

Aluminum specimens were covered with SiO₂ film by a sol-gel coating and then anodized galvanostatically in diluted borate solution. Time-variations in the anode potential during anodizing were monitored, and the structure and dielectric properties of anodic oxide films were examined by TEM-EDX, RBS, and electrochemical impedance measurements.

It was found that anodizing of aluminum coated with SiO₂ films leads to the formation of anodic oxide films, which consist of an outer Al-Si composite oxide layer and an inner Al₂O₃ layer, at the interface between the SiO₂ film and the metal substrate. The breakdown potential of anodic oxide films formed on specimens with SiO₂-coating was about 100V larger than without SiO₂-coating. In the film formation mechanism, the conversion of Al₂O₃ to Al-Si composite oxide at the interface between the inner and outer layers is discussed in terms of inward transport of Si-bearing anions across the outer layer.

Formation of Nickel Dispersed Carbon Spheres from Chelate Resin and Their Magnetic Properties

F. Goutfer-Wurmser, H. Konno, Y. Kaburagi, K. Oshida, M. Inagaki

Synth. Met., 118, 33-38 (2001)

Carbon spheres with well-dispersed nickel particles were formed by the carbonization of chelate resin complexed with Ni(II) ions at 600 and 1000°C, When the amounts of nickel after carbonization were less than 1 mass%, more than 90% of Ni species were paramagnetic or superparamagnetic, irrespective of carbonization temperature, indicating that they were dispersed as small clusters. For samples with 2.2-3.4 mass% Ni and formed at 600°C, most of Ni species were ferromagnetic and their coercive force was less than 10 Oe at 280 K. The Ni metal particles in these samples were around 10 nm in size and well dispersed, but the number density of particles was not uniform in the samples of <1 mass% Ni. For samples with 3.4 mass% Ni and formed at 1000°C, more than 80% of Ni species were ferromagnetic and the coercive force slightly increased to about 20 Oe. The results of XRD measurement and TEM observation showed that the Ni metal particles were around 10-30 nm and well dispersed in agreement with the magnetic properties. The results showed that the present method is promising to form the carbon materials containing well dispersed fine metal particles.

Synthesis and Structure of Novel Cr^V-Cr^{VI} Mixed Valence Compounds, Nd_{1-x}Ca_xCrO₄ (x=0.02-0.20)

Y. Aoki and H. Konno

J. Solid State Chem., 156, 370-378 (2001)

Single phase $Nd_{1x}Ca_xCrO_4$ (x = 0-0.20) oxides were synthesized by the pyrolysis of precursors prepared from Nd^{III}-Ca^{II}-Cr^{VI} mixed solutions. Nd_{1-x}Ca_xCrO₄ having x greater than or equal to 0.25 was not obtained as a single phase. All Nd_{1.x}Ca_xCrO₄ were zircon type (tetragonal, I4(1)/amd), and the composition was almost stoichiometric without any essential defects, which was determined by chemical analyses. The lattice constants and atomic positions was refined by the X-ray Rietveld method. The calculated densities of Nd_{1-x}Ca_xCrO₄ (x = 0-0.20) were in good agreement with the ones measured by the picnometry. XPS and Raman spectra indicated that $Nd_{1-x}Ca_xCrO_4$ (x = 0.02-0.20) are mixed valence oxides containing two types of tetrahedra, (CrO₄³)-O-V and (CrO₄²-)-O-VI) having D-2d symmetry in the structure, and this compensates the decrease of positive charges introduced by Call ions. Though two types of tetrahedra were not distinguishable by XRD, lattice constants a and c decreased almost linearly with x. The values for x = 0.02-0.20, however, were not on the line expected by Vegard's law between NdCrO₄ and CaCrO₄ but larger. The calculated O-Cr-O bond angles, however, did not change monotonously as lattice constants and other crystallographic parameters such as Cr-O bond length did, indicating that CrO₄ tetrahedra in Nd_{1-x}Ca_xCrO₄ (x = 0.02-0.20) are more elongated than in NdCrO₄ and CaCrO₄. It was deduced that the limit of x (about 0.25) may be determined by the difference in geometry between (CrO₄²-)-O-IV and (CrO₄³-)-O-V tetrahedral.

Characterization of Rust Layers of Weathering Steels Exposed to the Atmosphere for 17 Years

M. Yamashita, K. Asami, T. Ishikawa, T. Otsuka, H. Tamura, and T. Misawa

Kankyo-to-Zairyo, 50 [11], 521-530 (2001)

Structures and properties of protective rust layers on weathering steels systematically exposed to the atmosphere underneath the 5 bridges in the mainland of Japan for 17 years were investigated using various analytical methods. The weathering steels formed protective rust layers containing alloying elements such as Cr and Cu. It was shown that the rust layers on the weathering steels were mainly composed of goethite-type materials. The protective properties of the rust layers are likely to be due to the suppression of ion transport in the densely packed structure that was observed by nitrogen adsorption analysis. The influence of air-borne salt on the rust structure was explained in the following way: the content of β -FeOOH and the rust particles size increase with increasing amount of air-borne salt, leading to less dense rust structures, which would reduce the protective properties of rust layers on weathering steels. (Japanese)

Mechanism of Hydroxylation of Metal Oxide Surfaces

H. Tamura, K. Mita, A. Tanaka, and M. Ito

J. Colloid Interface Sci., **243** [1], 202-207 (2001)

Surface hydroxyl groups on metal oxides are sites for adsorption of cations or anions from water, which in turn release protons or hydroxide ions to solution resulting in ion exchange reactions. It is important to know the mechanism of the formation of surface hydroxyl groups to understand the ion-exchange capacities and properties of metal oxides. The hydroxyl groups are formed by dissociative chemisorption of water molecules, and it is generally considered that hydration and hydroxylation occur at exposed lattice metal ion sites on the surface as the lattice metal ions are strong Lewis acids. With this mechanism the surface hydroxyl site density would be different for different oxide samples as the number of metal ions exposed is different depending on the metal ion valency and the lattice planes exposed. In the study here, the Grignard reagent method was applied to determine the surface hydroxyl site densities of a variety of metal oxide samples. The measured surface hydroxyl site densities were similar for different oxides with ditri-, and tetravalent metals. Considering this, a different mechanism of hydroxylation is proposed: Lattice oxide ions (rather than lattice metal ions) are exposed to aqueous solutions due to their large size and low polarizing power, and the surface oxide ions which are strong Lewis bases due to insufficient coordination to the lattice metal ions take up protons from water to form acid and base type hydroxyl groups. The maximum possible surface hydroxyl site density was calculated from the hydroxide ion size with the assumption that metal oxides have the structure of the closest packing of oxide ions. The measured values could be explained with the calculated value. (English)

A Kinetic Model of the Dissolution of Copper(II) Oxide in EDTA Solutions Considering the Coupling of Metal and Oxide Ion Transfer

H. Tamura, N. Ito, M. Kitano, and S. Takasaki

Corrosion Sci., 43, 1675-1691 (2001)

The dissolution of metal oxides in solutions is related to the durability of protective oxide films on metals and the removal of corrosion scales on steels, and is important in corrosion science and corrosion protection engineering. In the study here, copper(II) oxide was sintered in a disk shape to maintain a constant surface area throughout dissolution, and the concentration of Cu(II) dissolved in EDTA solutions was measured as a function of time for different pH and EDTA concentrations at 80°C. Generally, only initial dissolution rates have been the object of study, but here the dissolution rate throughout the run could be examined. Without EDTA CuO did not dissolve, but with EDTA the dissolved Cu(II) concentration increased with time linearly at pH≤7 and in a parabolic manner at $pH \ge 8.5$. The dissolution rate increased with increasing pH at $pH \le 7$, but it decreased with pH at pH≥8. As a result, the concentration of dissolved Cu(II) at a specific time showed a peak at pH 7~8. Assessment and prediction of the extent of dissolution for given times, pH, EDTA concentrations, etc. with a model would be valuable for engineering purposes. A kinetic model is proposed by assuming the following successive elementary steps: (1) the transfer of Cu(II) ions as EDTA chelates CuY² to the solution leaving reactive and unstable "lone oxide ions" -O² on CuO with a backward reaction, and this is coupled with (2) the reaction of the "lone oxide ions" with protons to form water. The derived rate equation reproduced the linear and parabolic time changes in the dissolved Cu(II) concentration and the dissolution rate peak at pH 7~8. The deviation from linearity in the alkaline range is due to the increasing backward reaction in step (1). From the pH dependence of the model parameters, the H₂Y² and HY³ were estimated to be the dissolving EDTA species in solution. (English)

Modeling of the Kinetics of Metal Oxide Dissolution with Chelating agents

H. Tamura, M. Kitano, N. Ito, S. Takasaki, and R. Furuichi,

Studies in Surface Science and Catalysis, 132, 715-718 (2001)

The kinetics of the dissolution of metal oxides with chelating agents were modeled, and the model rate equations were able to explain and reproduce the time changes in dissolved metal concentrations and the pH peak dissolution rates. (English)

Glow Discharge Optical Emission Spectroscopy - a Powerful Tool for the Study of Compositional Non-Uniformity in Electrodeposited Films

K. Shimizu, G.M. Brown, H. Habazaki, K. Kobayashi, P. Skeldon, G.E. Thompson and G.C. Wood

Corros. Sci., 43, 199-205 (2001).

The potential of glow discharge optical emission spectroscopy for the analysis of thin films on metals is examined using the example of electrodeposited Ni-P, about 0.53 µm thick. The glow discharge optical emission spectroscopy depth profiles reveal layering of the deposited material with a good correlation between the sequence of layers in the composition profile and that observed by transmission electron microscopy.

Electron Transfer of Mangnese Hologenayed Tetraphynilporphyrin Derivatives Assembled on a Gold Electrode

T. Yamada, T. Hashimoto, S. Kikushima, T. Ohtsuka and M. Nango

Langmuir, 17, 4634-4640 (2001)

Didulfide-linked manganese halgenated tetraphenylporphyrin derivatives spacer methylene-chanin groups (Cn) (MnPFPP-Cn-S)2, (MnDCPP-Cn-S)₂ and (MnTPP-Cn-S)₂ [n= 2, 6, 12], were synthesized. The formation and redox response of self-assembled monolayers of these derivatives on a gold electrode were examined by electrochemistry combined with optical techniques in aqueous solutions as well as dimethyl sulfoxide (DMSO) solution. The self-assembly depended on the spacer methylene-chain length and the halogen species bound to the porphyrin. The fluorinated porphyryn with long methylene-chain length exhibited the largest surface concentration on the electrode. Electron transfer of the monolayers on the electrode was assumed to occur between Mn(III) and Mn(II) occluded in the porphyrin ring from results of cyclic voltammetry. (CV) and potential modulation reflectance, that is, electroreflectance (ER) in DMSO and aqueous solution. The ER could detect the electron transfer at higher sensetivities than CV especially in aqueous solution. The porphyrin with the lomger methylene chain induced the larger positive shift of the formal potential in addition to the larger surface concentration of the prophyrins in the monolayer. The shift in the formal potential also depended on the halogen species in the order of MnTTP-Cn-S monolayer > MnDCPP-Cn-S monolayer > MnPfPP-Cn-S monolayer. Rate constants of the electron transfer from the monolayer to the electrode in DMSO and aqueous solutions, which can be calculated from the ER versus modulation frequency relation, invreases with decreasing chain length and changed with halogen species bound to porphyrin in the order MnDCPP-Cn-S monolayer > MnTPP-Cn-S monolayer > MnPFPP-Cn-S monolayer. The effect of the halogen species may be explained by steric hindrance against aggregation among the porphyrin units in the monolayers especially in aqueous splution.

A Bipolar Electrode Cell for Aluminum Electrorefining

M. Ueda, T. Ohmura, S. Konda, T. Sasaki, T. Ohtsuka and T. Ishikawa

J. Applied Electrochem., 31, 871-875 (2001)

Electrorefining of aluminum was carried out at 750°C using bipolar electrode cells with center holes 2, 10, or 20 mm in diameter. Through the center holes liquid electrorefined aluminum rises to the electrolyte surface. The bipolar electrode cell consists of graphite cathodes, Al-Cu-Fe-Mn or Al-Cu-Fe-Zn alloy anodes and a BaCl₂-NaCl-AlF₃-NaF electrolytic melt. The center hole size of more 20 mm in diameter is required to continuously float up the aluminum electrodeposited onto the electrolyte surface, while the current efficiency of the cell decreases with increase of the center hole size, from 97 % at 2 mm diameter to 92 % at 20 mm diameter. Aluminum of 99.97 % purity precipitates at the cathode. Iron, manganese and zinc included in the alloy as impurities are hardly deposited and the concentration of these elements in the deposit are 100. 80 and 170 ppm, respectively. In this process aluminum can be produced with an energy consumption of about 4.9×10³ kWh (t-Al)⁻¹, which is one-third smaller than that of the Gadeau process.

Cathodic Decomposition and Changes in Surface Morphology of InP in HCI

M. Seo, M. Aihara and A. W. Hassel

Proceedings of Pits and Pores II: Formation, Properties, and Significance Advanced Materials", ed. by P. Schmuki, D. J. Rockwood, Y. H. Ogata, H. S. Isaacs, Electrochemical Society PV 2000-25, p. 576, Electrochemical Society. Inc., Pennington, NJ, USA(2001).

The cathodic decomposition of n-InP (100) plane and followed by anodic dissolution of deposited indium were investigated in relation to surface roughening. The cathodic decomposition proceeded in parallel with hydrogen evolution when n-InP (100) plane was cathodically polarized in 1.0 M HCl at potentials lower than 0.6 V (SHE). The metallic indium was deposited as a result of the cathodic decomposition, and anodically dissolved at potentials higher than 0.5 V (SHE) in anodic potential sweep after the cathodic decomposition. The reaction fraction of cathodic decomposition could be determined from the ratio of anodic charge for anodic dissolution of deposited indium to total cathodic charge for cathodic decomposition and hydrogen evolution, and took a maximum value of x = 0.5 for cathodic polarization at - 0.75 V (SHE) for 50 s. The changes in surface morphology of InP were observed with an atomic force microscope (AFM). The surface roughness of the InP surface increased with repeating the cathodic decomposition and anodic dissolution of deposited indium. When the cyclic potential steps between 0.75 V (SHE) for 30 s and 0.3 V(SHE) for 30 s were performed, the mean value of surface roughness, R₂, increased with increasing cycle number up to 150 cycles and then attained to a steady state of $R_a = 25$ nm. (English)

Cathodic Decomposition and Anodic Dissolution and Changes in Surface Morphology of n-Type InP in HCI

M. Seo, M. Aihara and A. W. Hassel

J. Electrochem. Soc., 148 (10), B400-B404 (2001).

The cathodic decomposition of n-InP (100) plane and followed by anodic dissolution of deposited indium were investigated in relation to surface roughening. The cathodic decomposition proceeded in parallel with hydrogen evolution when n-InP (100) plane was cathodically polarized in 1.0 M HCl at potentials lower than 0.6 V (SHE). The metallic indium was deposited as a result of the cathodic decomposition, and anodically dissolved at potentials higher than 0.5 V (SHE) in anodic potential sweep after the cathodic decomposition. The reaction fraction of cathodic decomposition could be determined from the ratio of the anodic charge for anodic dissolution of deposited indium to the total cathodic charge for cathodic decomposition and hydrogen evolution, and took a maximum value of x = 0.5 for cathodic polarization at 0.75 V (SHE) for 50 s. The changes in surface morphology of InP were observed with an atomic force microscope (AFM). The surface roughness of the InP surface increased with repeating the cathodic decomposition and anodic dissolution of deposited indium. When the cyclic potential steps between 0.75 V (SHE) for 30 s and 0.3 V(SHE) for 30 s were performed, the mean value of surface roughness, Ra, increased with increasing cycle number up to 150 cycles and then attained to a steady state of $R_a = 25$ nm. (English)

Analysis of Anodic Current Transient and Beam Deflection Transient Simultaneously Measured from Pd Foil Electrode Pre-charged with Hydrogen

J.-N. Han, M. Seo, and S.-I. Pyun

J. Electroanal. Chem., 499, 152-160 (2001).

Anodic current and beam deflection transients were measured simultaneously on a Pd foil electrode pre-charged with hydrogen at -0.02 and 0.09 V(RHE) in 0.1 M NaOH solution as a function of the hydrogen discharging potential. From the analysis of the anodic current transient measured, it is recognized that when the preceding potential jump is small enough to be below the transition discharging potential and this is followed by subjecting the electrode surface to a constant discharging potential, the hydrogen concentration corresponding to the discharging potential is not fixed at the electrode surface, but the change in surface concentration with time is then determined by the Butler-Volmer equation. From the hydrogen concentration profile transient simulated under the two constraints at the electrode surface depending on the discharging potential, we calculated numerically the transient of the deflection in the tensile direction caused by a smaller molar volume of α -PdH_d near the surface region than that in the inner region of the electrode during the hydrogen extraction. By comparison of the measured transient with that calculated, the movement of the maximum deflection in tensile and compressive directions was discussed in terms of the positive gradient of the molar volume towards the inner direction and the negative gradient due to the formation of α PdOH phase on the electrode surface, respectively. (English)

Analysis of Stresses Generated during Hydrogen Transport through a Pd Foil Electrode under Potential Sweep Conditions

J.-N. Han, J.-W. Lee, M. Seo and S.-I. Pyun

J. Electroanal. Chem., 506, 1-10 (2001).

In the present work, the stresses generated during cyclic voltammetric measurement on a Pd foil electrode in 0.1 M NaOH solution have been analyzed by using a laser beam deflection technique combined with cyclic voltammetry. From the linear relationship between the anodic peak current density and the scan rate on a logarithmic scale, it is recognized that the hydrogen concentration at the electrode surface is determined by the applied potential above the transition scan rate, whereas the change in the hydrogen concentration at the electrode surface with time is specified by the Butler-Volmer equation below the transition scan rate. The deflection transient measured simultaneously with the cyclic voltammogram shows that in the high scan rate range, the compressive deflection increases to a maximum value and then is completely relaxed. In the low scan rate range, however, the deflection transient is characterized by the occurrence of a maximum compressive deflection, a transition of compressive to tensile deflection, a maximum tensile deflection and finally a complete decay of the tensile deflection in sequence. From the hydrogen concentration profile transient simulated under the two constraints at the electrode surface, we simulated the deflection transients as a function of the scan rate. From the coincidence of the calculated deflection transient with that measured, the movement of the deflection in the compressive and tensile directions can be accounted for in terms of the difference in the molar volume of α -PdH_d across the whole electrode, developed during hydrogen diffusion. (English)

Characterization of Pd Electrode Surface Modified by Phase Transformation-induced Plastic Deformation using Fractal Geometry

J.-N. Han, M. Seo and S.-I. Pyun

J. Electroanal. Chem., 514, 118 – 122 (2001)

The surface change of α Pd electrode developed by plastic deformation due to the phase transformation of α -PdH to β -PdH has been characterized by fractal geometry. The β -PdH phase formed in the matrix electrode of α -PdH phase causes the plastic deformation of the electrode and hence increases the surface roughness as well as the surface area. The fractal dimension of the Pd electrode surface modified by the plastic deformation was determined from the diffusion-limited peak current density during linear sweep voltammetric measurements. The surface fractal dimension obtained is increased from 1.97 to 2.09 with increasing fraction of β -PdH phase in the matrix electrode from zero to unity. (English)

An SECM Observation of Dissolution Distribution of Ferrous or Ferric Ion from a Polycrystalline Iron Electrode

K. Fushimi and M. Seo

Electrochim. Acta, 47 (1-2), 121-127 (2001).

The dissolution of iron as ferrous or ferric ion from a polycrystalline iron electrode during anodic polarization in pH 2.3 sulfate solution was evaluated by using scanning electrochemical microscopy (SECM). A graphite reinforcement carbon (GRC) microelectrode was employed as a probe electrode of SECM to detect ferrous or ferric ion dissolved from the iron electrode in the active-dissolution, passive or trans-passive region. The probe current above the iron electrode surface subjected to active-dissolution showed the dissolution distribution of ferrous ion, depending on the substrate grains. It was found that the active-dissolution rate of iron as ferrous ions from the grain on which the thicker film was formed in the passive region, was lower than that from the grain on which the thinner film was formed in the passive region. (English)

In-situ Glow Discharge Spectroscopy of Stainless Steel in Electrolyte

K. Azumi, M. Kawaguchi and M. Seo

Hyomen Gijutsu, 52, 155-156 (2001).

Light emission is observed from SUS304 stainless steel electrodes immersed in electrolyte solutions under the cathodic polarization at the cell voltage larger than -100 V. Because the plasma temperature is very high as several thousands K, charged particles in the plasma phase sputter the electrode surface causing a gradual change in light spectra dependent on the depth profile of atomic composition of the electrode surface. In this paper change in intensities of light emitted from Fe and Ni atoms emitted from the electrode surface was measured as a function of polarization period. Depth profiles of relative light intensities, I(Cr) / I(Fe) and I(Fe) / I(OH) before and after potential cycling to enrich Cr on the surface confirmed that Cr concentration increased after this treatment. This result showed that the glow discharge spectroscopy can be potentially used for an in-situ analytical method for electrodes immersed in the solution. However, intrinsic problems of this technique, such as instability of plasma phase mainly contributed by gas evolution and vaporization of electrolyte on electrode, should be overcome to achieve better accuracy and thus wider application. (English)

Application of Resistmetry to the Corrosion Study of Metals

K. Azumi, T. Ueno, K. Iokibe and M. Seo

Proceedings of "Corrosion and Corrosion Protection", ed. by J. D. Sinclair, R. P. Frankenthal, E. Kalman, W. Plieth, Electrochemical Society PV 2001-22, p. 1074, Electrochemical Society. Inc., Pennington, NJ, USA(2001).

Applicability of resistmetry to various corrosion-related phenomena of metal electrodes such as anodic dissolution loss of Fe, growth of anodic oxide films on Fe, Ti and Al, changes in thickness of the space charge layer formed in a n-type semiconductor oxide films on Ti and Fe, hydride growth in Ti and cathodic dissolution of Al were examined. Using an AC technique and thin wire electrodes with small cross sectional area to obtain large resistance response, high sensitivity was achieved enough for use as an in-situ measurement method. (English)

Effect of Water Vapor on the Oxidation Properties of Sintered Fe-3mass%SiO₂ in air at 1273K

M. Fukumoto, S. Hayashi, S. Maeda, and T. Narita

J. Japan Inst. Metals, 65, 115-121 (2001)

Oxidation properties of sintered Fe-3mass%SiO₂(Fe-3SiO₂) as well as Fe-1.5mass%Si alloy(Fe-1.5Si) and Fe, for comparison, were investigated at 1273K for up to 7.2ks in air and air containing 10.5vol%H₂O(air-10.5H₂O). In air-10.5H₂O, the Fe-3 SiO₂ was oxidized faster than in air and also than the Fe-1.5Si in air-10.5H₂O. The scale was composed of a duplex structure, an inner FeO+Fe2SiO4 and an outer Fe-oxides layers, where many voids existed in both layers. The similar scale structure containing voids was observed for the Fe-3SiO₂ in air. Marker experiment with a small Pt wire was carried out for the Fe-3SiO₂ oxidized in air-10.5vol%H₂O and the Pt-marker located between the inner and outer layers, suggesting that the inner layer grows due to inward migration of oxygen and the outer layer due to outward iron diffusion. In both air and air-10.5H₂O Fe showed a parabolic oxidation, forming exclusively an outer Fe-oxides scale. It was suggested that SiO₂, which changed to FeO+Fe₂SiO₄, acts as an obstacle for the outer layer recession, leading a formation of voids in the inner layer. Oxygen used to form the inner FeO+Fe₂SiO₄ layer was supplied by the dissociation of outer Fe-oxides, leaving voids, probably by a perforating dissociation mechanism. Both oxygen and water molecules could be diffusing species through the void. (Japanese)

Effect of Water Vapor on the Oxidation Behavior of Fe-1.5mass%Si Alloy in Air at 1073 and 1273K

M. Fukumoto, S. Hayashi, S. Maeda, and T. Narita

Oxidation of Metals, 55, 401-422 (2001)

The oxidation behavior of an Fe-1.5mass%Si alloy was investigated at 1073 and 1273K in air, air-H₂O, Ar-H₂O, O₂-H₂O, and O₂ atmospheres. Corrosion amounts in atmospheres containing H₂O increased rapidly after an incubation period with slow oxidation, and the incubation period became shorter in the order, O₂-H₂O, air-H₂O, and Ar-H₂O. With increasing H₂O contents in air-H₂O the incubation time decreased. During the incubation period oxidation was slow due to the formation of an inner Si-rich oxide layer, and a Pt-marker was located between the external Fe₂O₃ (Fe₃O₄ included) and an inner Si-rich oxide layer. During the rapid oxidation the inner FeO+Fe₂SiO₄ layer thickened and a Pt-maker became located at the interface between an external Fe-oxide and an inner FeO+Fe₂SiO₄ layer. Observation on scale cross-sections indicated that voids made channels along the boundary of columnar FeO crystals, suggesting transport of water molecules. The Si-rich oxide layer changed into a FeO+Fe₂SiO₄ mixture due to penetration of water molecules. A combined process of perforating dissociation and transport of water molecules was suggested to be the cause of the rapid growth of the inner FeO+Fe₂SiO₄ layer. (English)

Oxidation Behavior of Sulfidation Processed TiAl-2at%X (X=V, Fe, Co, Cu, Nb, Mo, Ag, and W) Alloys at 1173K in air

T.Izumi, T.Yoshioka, S.Hayashi, and T.Narita

Intermetallics, 547-558 (2001),

The oxidation behavior of sulfidation processed TiAl-2at%X (X=V, Fe, Co, Cu, Nb, Mo, Ag, and W) alloys was investigated at 1173K in air for up to 630ks under a heat-cycle condition between 1173K and room temperature. Oxidation behavior was classified into two groups: group A with alloys containing W, Mo, Fe, and Nb, and group B containing V, Co, Cu, and Ag. The TiAl binary alloy belonged to group B. During the sulfidation processing the alloying elements in group A formed aluminides on the TiAl₃ layer, while the group B alloys formed a TiAl₃ (TiAl2 included) layer including a small amount of the third element. The cross-sectional microstructures for group A show the sequence; oxide scale/TiAlX/TiAl2/alloy substrate, and for group B oxide scale/Ti3Al/alloy substrate. The alloys in group A (except Nb containing alloy) showed some scale exfoliation at the initial stage of oxidation, but only very little exfoliation after long oxidation times, whereas alloys in group B showed little exfoliation at the first several cycles, and then tended to exfoliate significantly, resulting in very rapid oxidation. The TiAIX/TiAl₂ layers formed by the reaction between the X-aluminide and TiAl, improve the oxidation properties of the group A alloys. (English)

Competitive effect of water vapor and oxygen on oxidation of Fe-5mass%Al alloy at 1073K

S. Hayashi and T. Narita

Oxidation of metals, 56, 249-268, (2001)

The effect of oxygen on the oxidation of Fe-5wt%Al alloy was investigated at 1073K in N₂-12.2vol%H₂O, O₂-12.2vol%H₂O, and N₂-O₂-12.2vol%H₂O with various oxygen amounts. The results showed S-shaped oxidation curves that consisted of three parts, a slow incubation stage, a rapid transition stage, and a relatively slow oxidation stage. The amount of oxidation increased with increasing oxygen contents up to 0.9vol%O₂ and then rapidly decreased. On the oxygen rich side a slow incubation oxidation stage was observed and its duration increased with increasing oxygen contents. The extent of oxidation decreased gradually with decreasing oxygen content from the critical value, and the incubation period disappeared. In the transient period Fe₂O₃ was formed on the lean oxygen content side, and elongated voids were formed in the outer Fe₃O₄ and FeO layer. It was suggested that the differences in the morphology of Fe₂O₃ formed on the surface affected the dissociation and gas transport process due to differences in oxygen partial pressure at the gas/scale interface. (English)

Effects of Temperature and Atmosphere for Dissolution of Cr Carbide Precipitate near the Surface on Fe-Cr-C allov

H.Takahashi, Y.Miyakoshi, S.Kamota, S.Hayashi, T.Narita, H.Jimbo, Y.Urakami, T.Oka, H.Yakuwa and M.Noguchi

Zairyo-to-Kankyo, 50, 472-476 (2001)

The dissolution behavior and mechanism of chromium carbide precipitation near the surface of Fe-Cr-C alloy were investigated by electron probe microanalysis. There was a 100 $\,\mu$ m of chromium carbide dissolution layer near the surface of SHC2 heat resistant steel exposed at 1273 K for 345.6 ks in air. The chromium carbide dissolution layer was also identified on the specimen exposed at 1473 K for 345.6 ks in air and at 1273 K for 14.4 ks in H_2 . The result of EPMA analysis showed that not only chromium but also carbon were depleted on chromium carbide dissolution layer. The chromium content that was detected at the chromium carbide dissolution layer/chromium carbide layer interface was higher than the critical chromium content to form chromium carbide on Fe-Cr-C phase diagram. The Fe-Cr-C phase diagram shows that critical chromium content to form the Cr carbide increases with the reduction of carbon. This shows that the chromium content that was detected at the chromium carbide dissolution layer/chromium carbide layer interface was increased by decarburization from the surface during the exposure.

It was concluded that the chromium carbide dissolution layer formed at 1273 K was formed both in air and H_2 by the same mechanism as that at higher temperature up to 1473 K.

Sulfidation Behavior of a Thermal Barrier Coating at 1173 K in H₂S-H₂ Gas Mixture with a 10^{-0.65} Pa Sulfur Partial Pressure

Z.Yu, H.Taumi and T.Narita

Zairyo-to-Kankyo, 50, 376-379 (2001)

Sulfidation behavior of a thermal barrier coating consisted of CoNiCrAIY and YSZ (ZrO₂-8mol%Y₂O₃) cating, prepared by low pressure and air plasma sprayings, respectively, on a nickel based heat resistant alloy was investigated in a H₂S-H₂ atmosphere with a 10^{-0.65} Pa sulfur partial pressure at 1173 K for 43.2 ks. The corrosion product with a network structure was identified by X-ray diffraction and electron probe microanalyses to be Zr₃Y₄S_{3.5}O_{9.4}, which was formed from the Zr₃Y₄O₁₂ by replacement of oxygen by sulfur, having the elongated c-axis and the shrunken a-axis in contrast to those of the Zr₃Y₄O₁₂. Sulfur and/or hydrogen sulfide gases were assumed to diffuse throgh flaws such as cracks and voids across the YSZ coating and reacted with Cr to form Cr-sulfide surrounding the aluminum-rich oxide layer at the YSZ/CoNiCrAlY interface.

Application of Rhenium Coating as Diffusion Barrier to Improve the High Temperature Oxidation Resistance of Nickel-Based Superalloy

M.Shoji, Y.Hisamatu, D.Yoshida, M.Fukumoto, T.Narita and S.Hayashi

CORROSION 2001 Paper 01157/1-01157/11

A nickel-based single crystal superalloy with or without a Re/Al coating was Al-diffusion treated and then oxidized in air at 1373 K for up to 2.54 Ms under thermal cycling and isothermal conditions. The Al-diffusion treatment, carried out at 1273 K for 57.6 ks in a mixture of FeAl and Al₂O₃ powder, resulted in a triplex layer structure in the sequence β -NiAl / Re-rich layer / Al-diffusion zone on the alloy. The Re-rich layer contained 25Ni, 19Al and 16Cr (at.%). When oxidized at 1373 K for 460 ks in air under thermal cycling, a very protective α -Al₂O₃ scale formed, while the β -NiAl layer changed to Ni-aluminide (presumably γ '-Ni₃Al) containing 21at.%Al and the Re-rich layer to a Re-based alloy containing 31Cr, 21Ni, 12Co, 6W and 3Al (at.%) plus Re, which corresponded to σ -phase in the Ni-Cr-Re phase diagram. The protective α -Al₂O₃ scale and the resulting triplex coating structure of γ '-Ni3Al / σ -phase (Cr-Re-Ni system) / alloy substrate were maintained with little change for up to 2.54 Ms under isothermal oxidation. The formation of the triplex structure was discussed by using the diffusion path on the ternary Ni-Cr-Re and binary Ni-Al phase diagrams. In the Al-diffusion and subsequent initial stage of oxidation the Al, Ni, Co and Cr diffused rapidly though the Re/Al coating and the Re-Ni-Al-Cr alloy layer. With further oxidation at 1373 K the Re-Cr-Ni (Co) (σ -phase) alloy layer formed between the alloy substrate and γ'-Ni₃Al layer and it was found to act as a very effective diffusion barrier to the alloying elements and Al.

Oxidation Behavior of Plasma Sprayed Co Ni Cr Al Y/YSZ Film at 1173 and 1273 K in Air

M.Narumi, Z.Yu, H.Taumi and T.Narita

Zairyo-to-Kankyo, 50, 466-471 (2001)

A CoNiCrAlY/YSZ (ZrO₂-8mol%Y₂O₃) film prepared by low-pressure and air plasma spraying was oxidized in air at 1173 and 1273 K for up to 3240 ks. Thicknass and concentration profiles across oxide scales and Al depleted zone with disappearing β-NiAl phase were measured for both the CoNiCrAlY/YSZ interface and the CoNiCrAlY surface by using an electron probe micro-analysis. The oxide layer at the interface was Al-rich oxide containing Co, Ni and Cr in addition to Y, while the oxide at the surface consisted of pure Al₂O₃, except for that it contains Y at the alloy side. The former grew three times thicker than the latter. A ratio of thickness between the Al depleted zone and the oxide layer ranged from 3 at 1173 K to 4 at 1273 K. Concentration profiles of each element measured across the Al depleted zone were almost flat, except for that at the interface oxidized at 1173 K, where Al and Ni concentrations decreased towards the Al-rich oxide layer, whereas Co and Cr concentrations increased.

Effect of Water Vapor on the Oxidation Behavior of Fe-0.5 and 5 mass% Ni Alloys in Air at 1273 K

M.Fukumoto, S.Hayashi, S.Maeda and T.Narita

J.Japan Inst.Metals, 66, 513-520 (2002)

Oxidation behavior of Fe-0.5 and 5 mass%Ni alloys (0.5Ni, 5Ni) as well as Fe for comparison, was investigated at 1273 K for up to 7.2 ks in air and air containing 10.5 vol%H₂O (air-10.5H₂O). In the air-10.5H₂O, the 0.5Ni and 5Ni were oxidized faster than in air. The scale was composed of a duplex structure, an outer Fe-oxides layer and an inner FeO+Ni layer containing voids. Marker experiments with a small Pt wire were carried out for the 5Ni oxidized in air and the Pt-marker was located between the inner and outer layers, suggesting that the inner layer grows due to inward migration of oxygen and the outer layer due to outward iron diffusion. A similar scale structure was observed for the 5Ni oxidized in air but the inner layer thickness of the 5Ni oxidized in air-10.5H₂O was thicker than in air. Oxygen in the inner FeO+Ni layer formed in air was supplied by the dissociation of outer Fe-oxides, leaving voids there, probably by the perforating dissociation mechanism. Both oxygen and water molecules could be diffusing species through the void in the atmosphere containing water vapor. Concentration profiles of each element indicated that concentration of Ni was increased at the scale/alloy interface. The Ni-concentration of the 0.5Ni oxidized in air was lower than that in air-10.5H₂O, but the Ni-concentration of the 5Ni oxidized in air was higher than that in air-10.5H₂O.

High-Temperature Corrosion Resistance of Al-Re and Re Coatings

Z. Yu and T. Narita

Oxidation of Metals, **56**, Nos.5/6 (2001)

The oxidation behavior in air at 1473 K, and sulfidation behavior in a H₂S-H₂ gas mixture with a sulfur partial pressure of 10⁻² Pa 973 K of Al-Re coated CMSX-4 were studied. Investigation on the sulfidation behavior of the Re-coated CMSX-4 was carried out in a H₂S-H₂ gas mixture with a sulfur partial pressure of 10⁻² Pa at 973 K. The experimental results show that a Re-rich alloy layer was formed between an α -Al₂O₃ layer and the inner concentration zone of Ta and Ti for the CMSX-4 single crystal alloy with an Al-Re coating after oxidation. The Re-rich alloy layer containing Cr, W, Ni, Co and Mo effectively inhibited the outward diffusion of alloying elements and the inward diffusion of Al. The Al/Re-coated CMSX-4 single crystal alloy had excellent sulfidation resistance; the Re-rich alloy layer, containing W,Ti,Ta and Mo, which formed during the sulfidation process and located between the alumina scale and the CMSX-4 base alloy, plays a role in inhibiting the outward diffusion of alloying elements. The sulfidation resistance of CMSX-4 single-crystal alloy is greatly improved by a Re coating on the CMSX-4 alloy surface; this is attributed to a Re-Cr-W alloy layer that retarded the outward diffusion of cations and the oxide layer containing Ta, Ti and Al, which inhibited the inward penetration of sulfur.

Synthesis and Oxidation Resistance of a Re Silicide

K. Kurokawa, H. Hara, and H. Takahashi

Advances in Applied Plasma Science, 3, 215-220, (2001)

Fabrication of a dense Re silicide (ReSi_{1.75}) was performed with a spark plasma sintering method. For the fabrication, the mixed powders of elemental Re and Si were employed as starting materials. The interface structure between Re and Si changed with temperature as follows: Re/ReSi_{1.75}/Si at 1223 K, Re/Re₅Si₃/ReSi_{1.75} at 1573 K, and Re/Re₅Si₃/ReSi/ReSi_{1.75} at 1723 K. On the basis of the results on the interfacial reaction, synthesis and sintering of ReSi_{1.75} were simultaneously performed, resulted in the fabrication of dense ReSi_{1.75}. In addition, oxidation tests of ReSi_{1.75} were carried out in air at temperature ranging from 773 to 1473 K. Although a silica scale formed on ReSi_{1.75} by the evaporation of Re₂O₇, a protective silica scale formed at temperatures of 1273 K and above.

Silicides as Coatings Having High Oxidation Resistance

K. Kurokawa

Applied Plasma Science, 9, 3-8, (2001)

Silicides are receiving much attention as high-temperature materials having extremely-high oxidation resistance based on the formation of a protective silica scale. However, they are limited in application because of their brittleness. Therefore, the use of them as coatings on refractory metals, which have poor oxidation resistance, is strongly desired. The mechanism of oxidation of silicides has not been clarified. In other words, it is not well-known that a protective silica scale is formed in what kind of silicides. This review focuses on the classification of oxidation behavior in silicides. In addition, chemical compatibility between a refractory metal (Nb) and a silicide (MoSi₂) is also described. (Japanese)

The Sulfidation and Oxidation Behavior of Sputter-Deposited Nb-Al-Cr Alloys at High Temperatures

H. Habazaki, K. Yokoyama and H. Konno

Proc. of 12th Asian-Pacific Corrosion Control Conference, Seoul, Korea, 785-794 (2001)

Sputter-deposited Nb-Al-Cr alloys, 3-5 µm thick, have been prepared on quartz substrates as oxidation- and sulfidation-resistant materials at high temperatures. The oxidation of the alloys in the Ar-O₂ atmosphere of an oxygen partial pressure of 20 kPa follows approximately the parabolic rate law, thus being diffusion controlled. Their oxidation rates are almost the same as or even lower than those of the typical chromia-forming alloys. The multi-layered oxide scales are formed on the ternary alloys. The outermost layer is composed of Cr₂O₃, which is mainly responsible for the high oxidation resistance of these alloys. In contrast to sputter-deposited Cr-Nb binary alloys reported previously, the inner layer is not porous. TEM observation as well as EDX analysis indicates that the innermost layer is a mixture of Al₂O₃ and niobium oxide. The dispersion of Al₂O₃ in niobium oxide may be attributable to the prevention of the formation of the porous oxide layer. The sulfidation rates of the present ternary alloys are higher than those of the sputter-deposited Nb-Al binary alloys, but still several orders of magnitude lower than those of conventional high temperature alloys. Two-layered sulfide scales are formed, consisting of an outer Al₂S₃ layer containing chromium and an inner layer composed of NbS2 and a small amount of Cr2S3. The presence of Cr₂S₃ in the inner protective NbS₂ layer may be attributed to the increase in the sulfidation rates.

Local Surface Modification of Aluminum by Laser Irradiation

T. Kikuchi, S.Z. Chu, S. Jonishi, M. Sakairi, H. Takahashi

Electrochimica Acta. 47, 225-234 (2001)

A novel method involving a combination of pulsed YAG laser irradiation and electrochemistry for chemical and physical modification of aluminum surface at a selected area is reviewed. Local metal deposition is carried out by successive steps of anodizing, laser irradiation, and electroplating (or electroless plating), and the fabrication of a prototype for printed circuit boards is attempted. Local organic film deposition with anodizing, laser irradiation, and electrophoretic deposition is introduced, and the formation of microtrenches and pores on aluminum surfaces with anodizing, laser irradiation, and electrochemical etching (or chemical etching) is also described. It is emphasized that the key technology in these procedures is to use aluminum as a target for the laser irradiation in solution, and that anodic oxide films on aluminum play an important role in the processes.

Formation of Composite Oxide Films on Aluminum by Sol-Gel Coating and Anodizing. -For the Development of High Performance Aluminum Electrolytic Capacitors-

K. Watanabe, M. Sakairi, H. Takahashi, K. Takahiro, S. Nagata and S. Hirai

Electrochemistry, 69, 407-413 (2001)

Aluminum coated with ZrO₂, SiO₂, and BaTiO₃ films by a sol-gel dip coating was anodized to examine the structure and dielectric properties of anodic oxide films. Anodizing leads to the formation of anodic oxide films, which consist of an outer Al- (Zr, Si, BaTiO₃) composite oxide layer and an inner Al₂O₃ layer, at the interface between the coated-oxide layer and Al substrate. The composite oxide converted into Al₂O₃ at the interface between the outer and inner layers during anodizing for the ZrO₂- and BaTiO₃-coated specimens, whereas Al₂O₃ converted into Al-Si composite oxide for the SiO₂-coated specimens. The capacitance of the anodic oxide films formed on ZrO₂- and SiO₂-coated specimens was about 20% larger than that of anodic oxide films on aluminum without coating, and the capacitance for BaTiO₃-coated specimens was almost identical to that without coating.

Film formation mechanisms are discussed in terms of inward transport of Si-bearing anions and outward transport of Zr- and Ti-bearing cations across the composite oxide layer.

Fabrication of Micropores and Grooves on Aluminum by Laser Irradiation and Electrochemical Technique

T. Kikuchi, M. Sakairi, H. Takahashi, Y. Abe, and N. Katayama.

J. Electrochem. Soc., 148, C740-C745(2001)

Micro-pores and micro-grooves were fabricated on aluminum specimens using anodizing, laser irradiation and electrochemical techniques. In the fabrication of the micro-pores, aluminum specimens covered with anodic oxide film were irradiated with a pulsed Nd-YAG laser a) on open circuit or b) under anodic polarization in NaCl solution. The laser irradiation caused the formation of cone-shaped pores, while the laser irradiation under anodic polarization caused the formation of hemispherical pores. In the fabrication of micro-grooves, successive procedures of anodizing, laser irradiation, re-anodizing at the laser-irradiated area, and stripping of oxide film were carried out. Micro-grooves with a 30 μ m line width and 20 μ m depth were obtained.

Fabrication of Grooves on Aluminum Surface with Atomic Force Microscope Probe Processing

Z. Kato, M. Sakairi, and H. Takahashi

J. Electrochem. Soc., 148, C790-C798 (2001)

Aluminum specimens covered with anodic oxide films were scratched with an atomic force microscope probe in air, pure water, CuSO₄ solutions, Cu-electroless plating solution, and diluted NaOH solutions to examine the effect of the probe load, scratch number, and processing environment on the rate of groove development. The rest potential of the aluminum was monitored during scratching in the solutions, and in-situ AFM observations were carried out after the scratching. Probe wear was also examined in pure water and NaOH solution.

The rate of groove development was in the order NaOH > $CuSO_4$ > air = pure water > Cu-electroless solution, and decreased with decreasing probe load and increasing scratch number. The rest potential remained steady in the solutions during scratching with loads below 12.5 μN , while it dropped rapidly above 25 μN . Copper was deposited in and around grooves during scratching in Cu- SO_4 and Cu-electroless plating solution at the high loads, and after the scratching copper deposits grew only during immersion in Cu-electroless plating solution. Probe-tip wear was greater in NaOH solution than in distilled water.

Fabrication of Grooves on Aluminum Surface with Atomic Force Microscope Processing

H. Takahashi, Z. Kato and M. Sakairi

Proc. of Electrochem. Soc., 2000-25, 212-226 (2001)

Aluminum specimen covered with anodic oxide films were scratched with an atomic force microscope probe in a) air, b) distilled water, c) copper sulfate solution, d) copper electroless plating solution, and e) NaOH solution to investigate the fabrication of grooves as functions of load of AFM probe and the number of scratching. Rest potential of aluminum was monitored during scratching in the solutions to examine how the oxide film is removed.

Depth of grooves increased linearly with the scratching number in all atmospheres, and the processing rate was in the order of NaOH > CuSO4 > distilled water = air > copper electroless plating solution. The rest potential dropped rapidly by loading a force above a threshold value, and recovered gradually with time after scratching in all solutions. Copper was deposited in and around grooves during immersion in copper electroless solution after scratching at the high load.

Fabrication of Fine Pattern Coils by Anodizing, Laser Irradiation, and Metal Deposition

T. Kikuchi, M. Sakairi, H. Takahashi, Y. Abe, and N. Katayama

Electrochem. Soc. Proc. 99-42, 923-929 (2001)

A novel method of fabrication of fine pattern coils on an insulating organic board has been proposed by anodizing, laser irradiation, and metal deposition. Aluminum specimens covered with porous anodic oxide films were irradiated by a pulsed Nd-YAG laser through a convex lens and quartz window in a solution containing Ni^{2^+} ions to remove the anodic oxide film. After laser irradiation, the specimen was cathodically polarized to deposit Ni metal layer at the laser irradiated area. The specimen was, then, pasted on an epoxy resin before dissolving the aluminum substrate. A fine pattern coil, which has a 15 μ m Ni line width and 25 μ m interval between lines, was made on the insulating board successfully.

Fabrication of Printed Circuit Board by Anodizing of Aluminum

H. Takahashi, M. Sakairi, and T. Kikuchi

J. Surf. Science Soc. Jpn. 22, 370-375 (2001)

Printed circuit boards are used in many electronics, and fabricated by photolithography, where copper attached to an organic board is etched locally to fabricate fine patterns.

Here, the authors introduce an innovative method for the fabrication of printed circuit boards, using anodizing, laser irradiation, and electro-plating or electroless-plating. Aluminum foil covered with anodic oxide films is immersed in solutions containing metal ions, and then irradiated with a pulsed Nd-YAG laser through a convex lens. Laser irradiation removes the oxide film locally and allows metal particles to be deposited by redox reactions between the metal ions and the aluminum substrate at the film removed-area. Electro-plating or electroless-plating after laser irradiation enables the deposition of metal layers only at the laser irradiated-area. An organic resin is attached to the aluminum deposited by the metal layer, and the metal substrate is removed by dissolving in alkaline solutions.

The procedure described above gives a pattern with 9 μm line width and 12 μm interval. (Japanese)

Fabrication of New Type Plastic Injection Mold by Anodizing, Laser Irradiation and Ni-P Electroless Plating

M. Sakairi, S. Moon, H. Takahashi and K. Shimamura

J. Surf. Fin. Soc. Jpn., 52, 553-556 (2001).

A novel method involving a combination of pulsed YAG laser irradiation and electrochemistry for fabrication of a new type plastic injection mold. Local metal deposition is carried out by successive steps of anodizing, laser irradiation and Ni - P electroless plating.

This work is also concerned with the effects of anodic oxide film structure, including defects in the film and thickness of the film, on electroless Ni-P deposition on Al5052 alloy. The unsealed anodic oxide film of Al5052 alloy showed easier nucleation of Ni-P deposits. Sealing treatment of anodic oxide films on Al5052 alloy, markedly reduced the number of Ni-P deposits. (Japanese)

Formation of B/C Composites Containing B₄C from Sugar-organoborane Complexes

H. Konno, T. Erata, K. Fujita, Y. Aoki, K. Shiba and N. Inoue

Carbon, 39, 779-782 (2001)

A simple method to form B/C composites containing B_4C was developed. It utilizes borate complexes with organic compounds as precursors, which were synthesized by the combinations of (A) sugars, polyhydric alcohols or the organic compounds having N-glucamine functional groups and (B) a boric acid or organoboranes. In the present paper, the results using sugar-organoborane complexes are reported. With these precursors, B_4C was formed at as low temperature as $1300^{\circ}C$.

Formation of Graphite Crystals at 1000-1200°C from Mixtures of Vinyl Polymers with Metal Oxides

M. Inagaki, M. Fujita. Y. Takeuchi, K. Oshida, H. Iwata, and H. Konno

Carbon, 39, 921-929 (2001)

The formation of graphite crystals from mixtures of different carbon precursors, poly(vinyl chloride) (PVC), poly(vinyl alcohol) (PVA) and poly(vinyl pyrrolidone) (PVP), with iron oxides Fe₃O₄ and Fe₂O₃, nickel oxide NiO, cobalt oxide Co₃O₄ and iron powder was studied at a temperature between 800 and 1200°C. The formation of flaky graphite crystals was confirmed from X-ray diffraction and transmission electron microscopy, and the reaction mechanism was studied by differential thermal analysis. From the powder mixtures of vinyl polymers, PVC, PVA and PVP, with Fe₂O₃, Fe₃O₄, Fe and Co₃O₄, graphite was obtained by the heat treatment at the temperature above 1000°C for 1 h, the higher temperature and the longer residence time giving the higher crystallinity of graphite. However, the mixture of NiO with PVA behaved a little different; well-developed turbostratic structure at 1000°C for 1 h and well-crystallized graphite at 1100°C for 24 h. The formation of graphite crystals was supposed to occur through the following steps: thermal decomposition and carbonization of vinyl polymers below 500 °C, reduction of metal oxides to metal by carbonaceous products and then catalytic action of metals to precipitate graphite. Since carbons were consumed for the reduction of metal oxides, the mixing ratio of PVA to metal oxides suitable for the formation of graphite crystals was found to be related to the oxidation state of metals

The Electronic and Magnetic Properties of LaCrO₄ and Nd₁₋,Ca,CrO₄ (x=0-0.2) and Their Conduction Mechanism

Y. Aoki, H. Konno and H. Tachikawa

J. Mater. Chem., 11, 1214-1221 (2001)

The electric conductivity of monazite-type LaCrO₄ and zircon-type $Nd_{1-x}Ca_xCrO_4$ (x = 0-0.2) were characterized by measurements of dc electric conductivity and the Seebeck coefficient in the 300-600 K range. The LaCrO₄ and NdCrO4 were found to be n-type semiconductors, while commonly known monazite- or zircon-type oxides are insulators. In mixed valence compounds of Cr-V and Cr-VI, $Nd_{1-x}Ca_xCrO_4$ (x = 0.1, 0.2), hole hopping conduction arising from the mixed valency was also observed. The $Nd_{1-x}Ca_xCrO_4$ (x = 0.1, 0.2) compounds obeyed Curie-Weiss behavior above the Neel temperature, and the observed magnetic moments for the Cr-V ions were in good agreement with the theoretical values. Experimental results and the calculated spin densities by the UHF method indicated that most of the unpaired electrons from Cr-V were localized on Cr atoms. The ab initio MO calculations for CrO₄³⁻ clusters in NdCrO₄ revealed that the SOMO is the degenerate d pi* state and that the LUMO is the p sigma* state (O 2p origin): the SOMO forms the degenerate states at the top of the valence band and the LUMO forms a wide conduction band. For NdCrO4 and LaCrO₄ the electronic conduction mechanism as semiconductors was explained by the band model. For $Nd_{1-x}Ca_xCrO_4$ (x = 0.1, 0.2) electronic conduction was described by the band model combined with hopping conduction of holes in degenerate d pi* states. It is concluded that the electronic conductivity of these compounds is caused by an intermixing of the ligand-to-metal charge-transfer (LMCT) state into the ionic configuration.

Synthesis, Structure and Defects of Rare Earth Chromates(V), RE_{0.9}CrO_{3.85} (RE=Gd, Yb and Y)

Y. Aoki and H. Konno

J. Mater. Chem., 11, 1458-1464 (2001)

Single phase zircon type rare earth (REIII) chromates(V), containing GdIII, YbIII and Y^{III} ions, were synthesized by pyrolysis of the precursors prepared from the mixed solutions of RE^{III} and Cr^{VI} in the ratio of RE/Cr = 0.90/1.00. With other RE/Cr ratios, RE/Cr greater than or equal to 0.95 or RE/Cr less than or equal to 0.85, the pyrolysis products contained a secondary phase of RE₂O₃ or Cr₂O₃. The composition of the compounds was determined to be RE_{0.9}CrO_{3.85} by chemical analyses, with small standard deviations. The ESR spectrum of Y_{0.9}CrO_{3.85} was typical of Cr^{V} ions in solids with g = 1.968 and $\Delta H = 140$ mT, and did not show the signals of Cr^{II} or Cr^{III}. These compounds have a defect structure which differs from other zircon type compounds containing REIII of larger ionic radius than GdIII. The detailed structure was determined by the powder X-ray Rietveld method. The measured densities suggested that the defect structure is RE_{0.9}(CrO₄)^{0.85}(CrO₃)^{0.15} (RE = Gd, Yb and Y). Apparently this structure contains CrO₃, with a dangling bond. Based on the structural analyses and ab initio MO calculations, these species might be stabilized by forming Cr₂O₇ (CrO₃-O-CrO₃) units in RE_{0.9}CrO_{3.85} due to the oxygen sharing between CrO₃, and the neighboring CrO₄ tetrahedron. The present results conclude that the phase diagram of rare earth chromate(V) series reported so far should be corrected so that the compounds containing Gd^{III} and smaller ions have the defect zircon type structure.

Carbonization and Graphitization of the Kapton-type Polyimide Film with Boron-bearing Functional Groups

H. Konno, K. Shiba, Y. Kaburagi, Y. Hishiyama and M. Inagaki

Carbon, 39, 1731-1740 (2001)

Kapton-type polyimide film having boron-bearing functional groups in the molecule was synthesized and its carbonization/graphitization behavior was investigated by XPS, SEM, XRD, Raman spectrometry, and the measurements of electronic properties. It was found that >B-N< bonds started to form in the films around 800°C, and these bonds were broken above 1200°C and boron atoms started to substitute carbon atoms in the turbostratic structure. Graphitization was recognized at 2600°C for both boron-doped and undoped films but the boron-doped film had smaller Lc by XRD and more disordered structure which was revealed by Raman spectroscopy. The electronic measurements confirmed that boron could be substituted even in turbostratic structure. The boron-doped film formed at 2600°C showed two-carrier (holes and electrons) type conduction similar to HOPG, but hole carriers were predominant to electrons because of the doping of boron. The boron doping decreases d(002) of graphite film but it does not contribute to the development of graphite structure and reduces electric conduction.

Formation of β -SiC from Exfoliated Graphite and Silicone

H. Konno, T. Kinomura and M. Aramata

Carbon, 39, 2380-2382 (2001)

A simple method to form fine β -SiC powder was developed. Two types of low molecular weight silicone and a platinum catalyst were taken in the interlayer spacing of exfoliated graphite by sorption, and they were polymerized at 300°C in air. By heating this precursor at 1500-1600°C for 1 h in flowing argon, micrometer-sized β -SiC powder was formed.

Structure of EuCrO₄ and Its Electronic and Magnetic Properties

H. Konno, Y. Aoki, Z. Klencsár, A. Vértes, M. Wakeshima, K. Tezuka and Y. Hinatsu

Bull. Chem. Soc. Jpn., 74, 2335-2341 (2001)

Single phase zircon type EuCrO₄ (S.G. I4(1)/amd) was synthesized and the structure including atomic positions was precisely determined by X-ray Rietveld refinement. The electronic and magnetic properties of the compound were studied based on the electric conductivity, Seebeck coefficient, Raman spectroscopy, Mossbauer spectroscopy, magnetic susceptibility, and specific heat. The CrO₄³ tetrahedra in EuCrO₄ were slightly elongated compared with that in NdCrO₄, which caused splitting of the degenerated vibration modes of CrO_4^{3-} , $\nu(2)$ and $\nu(3)$, in the Raman spectra. The Eu-151 Mossbauer spectra showed not a trace of the Eu(II) species in the compounds measured in the present work. The Debye temperature, $\theta(D)$, estimated from Mossbauer spectra suggested that the vibrational state of Eu(III) in EuCrO₄ was similar to that in the perovskite-type EuCrO₃. However, the isomer shift of Mossbauer spectra revealed that the electron density of the 6s orbital of Eu(III) in EuCrO4 was very low and almost the same as that in the zircon type EuVO₄, that is, Eu(III) in these compounds has highly ionic character, whereas the electron density of the 6s orbital of Eu(III) in EuCrO₃ was higher and nearly the same as that in Eu₂O₃. EuCrO₄ was found to be an n-type semiconductor similar to NdCrO₄, while zircon type REMO₄ (RE: rare earth metal(III); M: V, P, As, etc.) are insulators. Magnetic susceptibility and specific heat measurements showed that antiferromagnetic transitions took place at around 15 K and was solely due to Cr(V) from the magnetic entropy value of 5.54 J mol⁻¹ K-I

Nanocrystalline Manganese-Molybdenum-Tungsten Oxide Anodes for Oxygen Evolution in Seawater Electrolysis

H. Habazaki, T. Matsui, A. Kawashima, K. Asami, N. Kumagai and K. Hashimoto

Scripta Mater., 44, 1659-1662 (2001).

(Mn_{1-x-v}Mo_xW_v)O_{2+x+v} ternary oxides, anodically deposited on IrO₂-coated titanium substrate in 0.4M MnSO₄ solutions containing various concentrations of Na₂MoO₄ and Na₂WO₄, have a γ-MnO₂ structure with grain sizes of about 10 nm. The nanocrystalline oxides containing less than 10 at% molybdenum and tungsten in cationic percentage reveal an oxygen evolution efficiency of almost 100%, which is higher than $(Mn_{1-x}W_x)O_{2+x}$ oxides without molybdenum. The anodic activity of the ternary oxides is also slightly higher than (Mn_{1-x}Mo_x)O_{2+x} oxides oxygen evolution efficiency of tungsten. The high without (Mn_{0.89}Mo_{0.05}W_{0.06})O_{2.11} oxide maintained during prolonged electrolysis, and even after the electrolysis for 2000 h, the oxide anode shows an oxygen evolution efficiency of 99.7%.

Composition and Structure of Enriched Alloy Layers in Filmed Al Alloys Studied by Medium-Energy Ion Scattering

P. Bailey, P. Skeldon, T.C.Q. Noakes, G.E. Thompson, M. Sakairi, H. Habazaki and K. Shimizu

Surf. Interface Anal., 31, 480-483 (2001).

The topmost 20 nm of an electropolished Al-1 at.% Cu alloy has been investigated at sub-nanometre resolution using medium-energy ion scattering. Differences in the composition and depth of the enriched Cu layer are observed. Most significantly, the enriched layer contains regions of differing structure and/or lattice orientation with Cu atoms located in distinct ordered regions, consistent with the presence of Cu-rich clusters, Surface-segregated Si and Cu are observed and CI and Cu are found in the oxide.

Advanced Materials for Global Carbon Dioxide Recycling

K. Hashimoto, H. Habazaki, M. Yamasaki, S. Meguro, T. Sasaki, H. Katagiri, T. Matsui, K. Fujimura, K. Izumiya, N. Kumagai and E. Akiyama

Mater. Sci. Eng. A304-306, 88-96 (2001).

CO₂ emission increase inducing global Warming occurs mostly with the growth of the economic activity. Global CO2 recycling can prevent global warming and supply abundant renewable energy. Global CO₂ recycling consists of three district. The electricity is generated by solar cells on deserts. At coasts close to the deserts, the electricity is used for hydrogen production by seawater electrolysis and hydrogen is used for methane production by the reaction with CO₂. Methane (CH₄) is liquefied and transported to energy consuming districts where after CH4 is used as a fuel CO₂ is recovered, liquefied and transported to the coasts close to the deserts. Key materials necessary for the global CO2 recycling are the anode and cathode for seawater electrolysis and the catalyst for CO₂ conversion. All of them have been tailored by us. Amorphous and nanocrystalline nickel alloys are active cathodes for hydrogen production in seawater electrolysis. Anodically deposited nanocrystalline Mn-Mo and Mn-W oxides are the unique substance which can evolve oxygen with 100% efficiency without evolving chlorine in seawater electrolysis. Amorphous Ni-Zr alloys are excellent precursors of catalysts for conversion of CO₂ into CH₄ by the reaction with hydrogen at 1 atm. A prototype CO₂ recycling plant to supply clean energy preventing global warming has been built on the roof of our Institute (IMR) in 1996 using these key materials and has been operating successfully.

Compositional and Morphological Imaging of Laser Irradiated Human Teeth by Low Vacuum SEM, Confocal Laser Scanning Microscopy and Atomic Force Microscopy

F. Watari

J.Materials Science in Medicine 12, 189-194 (2001)

Enamel and dentin of human teeth irradiated by CO₂ laser were investigated by confocal laser scanning microscopy (CLSM), low vacuum scanning electron microscopy (WET-SEM) and atomic force microscopy(AFM). Optical tomographic imaging by CLSM, compositional imaging based on atomic number effect of reflected electrons by WET-SEM, high resolution observation of surface morphology by AFM were done for both the irradiated and non-irradiated area of the same specimen throughout. The crystals of about 50 μ m length and the bright spots were observed by CLSM at the bottom of the cavity induced by laser irradiation. They turned out from the observation by WET-SEM as the acicular crystals with the cross section of an irregularly hexagonal shape situated parallel and perpendicular, respectively, to the inner surface of the cavity. The thickness of the thermally deteriorated zone of the cavity was about 25μ m. The crystals unidirectionally grown up to the size of several hundreds nm were also observed by AFM, while the apatite crystallites of 50-150nm were recognized all over in non-irradiated area. All the results suggest that after instantaneous melting at the surface of teeth by CO2 laser shot the crystals of calcium phosphate were recrystalized and grown to a large size. The compositional imaging in addition to morphological observation was useful to obtain the information of the change in materials induced by laser irradiation.

Gradient Tissue Reaction Induced by Functionally Graded Implant

F. Watari, A. Yokoyama, H. Matsuno, R. Miyao, M. Uo, Y. Tamura, T. Kawasaki, M. Omori and T. Hirai

Ceramic Transaction 114, 73-80 (2001)

An animal implantation test was done to investigate the influence of FGM implant on the response of tissue. The Ti/Co FGM of cylindrical shape with the gradually changed Co concentration from pure Ti to pure Co in the longitudinal direction was implanted in soft tissue of rats. The thickness of the fibrous connective tissue formed around implant was increased gradiently with Co concentration. The FGM with the graded composition from pure Ti to Ti-20%hydroxyapatite (Ti/20HAP) implanted in bone marrow of rabbits showed that new bone formation in direct contact to the implant surface increased with HAP content. The Ti/100HAP FGM implanted in bone marrow of rats showed the similar results. These results demonstrated that the tissue reaction, either biocompatibility in soft tissue or osteogenesis in hard tissue, occurred over a gradient on the order of millimeters in response to the graded structure of FGM.

Tissue Reaction around Metal Implants Observed by X-ray Scanning Analytical Microscope

M.Uo, F. Watari, A. Yokoyama, H. Matsuno, T. Kawasaki

Biomaterials, 22, 677-685 (2001)

The soft tissues which implanted with Cu, Ni, Fe, Ag, Ti, Ni-Ti, SUS304 and SUS316 wires were studied with XSAM and histological observation and the relationship between the distribution of dissolved metal elements and the tissue response was evaluated. The distribution of dissolved Cu, Ni and Fe was clearly observed by XSAM. The severe tissue damages were observed around Ni and Cu implants. The tissue around the Fe implant was not damaged severely. The esimated concentration in surrounding tissue by XSAM was 10-20mM for Ni and Cu in approximately and Fe concentration was considered as ten times higher. Therefore, the order of toxicity of these elements in same concentration was estimated as Ni, Cu and Fe. For Ag, Ti, Ni-Ti, SUS304 and SUS316 implants, significant distribution and severe tissue damage was not observed. The XSAM was useful for the study of dissolution and distribution property of highly toxic and chemically unstable metal implants in the soft tissue.

Visualization and Detectability of Rarely Contained Elements in Soft Tissue by X-ray Scanning Analytical Microscopy and Electron Probe Micro Analysis

M.Uo, F.Watari, A.Yokoyama, H.Matsuno, T.Kawasaki

Biomaterials, 22, 1787-1794 (2001)

The detectability of rarely contained elements in soft tissue was compared between the X-ray scanning analytical microscope (XSAM) and the electron probe micro analysis (EPMA). The mapping images of Ca, S and P in normal soft tissue of rat and dissolved Ni in Ni implanted soft tissue could be obtained by XSAM and EPMA. The EPMA was more sensitive in detection of P, while the XSAM was superior in Ca, S and Ni mapping. The high detectability of XSAM for heavier elements was explained by the large volume of characteristic X-rays generation in XSAM and low attenuations of the characteristic X-rays from heavier elements. The XSAM could provide the clearer mapping images for heavier elements whose concentration was low without radiation damage of specimens.

Biocompatibility and Osteogenesis of Refractory Metal Implants, Titanium, Hafnium, Niobium, Tantalum and Rhenium

H.Matsuno, A.Yokoyama, F.Watari, M.Uo, T.Kawasaki

Biomaterials, 22, 1283-1262 (2001)

To evaluate the biocompatibility of refractory metals, titanium, hafnium. niobium, tantalum and rhenium were implanted in rats, and histological observation and elemental mapping were performed by X-ray scanning analytical microscope (XSAM) and electron probe microanalyzer (EPMA). The titanium, hafnium, niobium, tantalum and rhenium wires were implanted in the subcutaneous tissue of the abdominal region and in femoral bone marrow of rats for either 2 or 4 weeks. No inflammatory response was observed around the implants, and all the implants were encapsulated with thin fibrous connective tissue. No dissolution of these metals was detected by XSAM in the soft tissue. Histological examination of the hard tissue showed that the amount of new bone formation decreased slightly from the 2nd to the 4th week after implantation, and that the percentage of bone in contact with the implant increased markedly over the same period. No dissolution of these metals was detected by EPMA in the hard tissue. The Ca and P intensities in the mapping images of newly formed bone were higher after 4 weeks than those after 2 weeks, which suggests that the newly formed bone continued to mature from 2 to 4 weeks after implantation.

These results indicate that titanium, hafnium, niobium, tantalum and rhenium have good biocompatibility and affinity for osteogenesis.

The Size Dependences and Vital Reaction against Minute Particles of Titanium in vivo and in vitro

R Kumazawa, F Watari, Y. Totsuka

The Journal of Japanese Society of Dental Materials and Devices, 26 (2001)

To examine the effect of titanium fine particles, animal experiments (for $1\sim 30$ weeks) and cell functional test (TNF- α , and superoxide anion release) were done. The animal experiments showed that each particle was englobed by fibrous connective tissue for the Ti particles ($40,150\,\mu$ m), whereas Ti particles ($1\sim 3,10\,\mu$ m) smaller than the inflammatory cells were englobed by connective tissue for their agglomeration and this occurred after endocytosed by inflammatory cells for $1\sim 3\,\mu$ m particles. Cell functional test using human neutrophils revealed that fine particles of Ti stimulated cells and increased the release of superoxide anion and TNF- α . Thus, fine particles of Ti smaller than cell size may cause stronger inflammatory reaction.

Fabrication of a Functionally Graded Dental Composite Resin Post and Core by Laser Lithography and Finite Element Analysis of its Stress Relaxation Effect on Tooth Root

S.Matsuo, F.Watari, N.Ohata

Dental Materials Journal, 20, 257-74 (2001)

Laser lithography was applied for Computer Aided Design and Computer Aided Manufacturing (CAD/CAM) fabrication of dental prostheses made of composite resin. First, the conditions to obtain the optimum resolution for photo-curing were determined, and then a composite resin full crown was fabricated by laser lithography. Second, a functionally graded composite resin post and core which had gradient elasticity in the post, was manufactured by the gradual change in the filler contents of the composite resin. Finally, stress analysis of the functionally graded post and core was performed by a two-dimensional finite element method. This demonstrated the effects of reducing the stress concentration around the apex of the post.

Radiation Effects of Carbon Ions and Gamma Ray on UDMA Based Dental Resin

S. Haque, S. Takinami, F. Watari, M.H. Khan and M. Nakamura

Dental Materials J. 20(4), 325-338 (2001)

The radiation effects on the mechanical and physical properties of photo-polymerized UDMA resin without filler was investigated by various mechanical tests and spectroscopic measurements. The radiation sources were carbon ion (12C ion) and gamma ray (γ -ray). With 640 Gy of 12C ion radiation, Vickers hardness increased by about 40%, the degree of abrasion decreased by 30%, and the flexural strength increased by 20%. With the same dose of γ - ray radiation, only Vickers hardness increased by 19%. The spectra taken by the Fourier Transform Infrared Spectrometer (FT-IR), Raman spectroscopy, and Fluorescence spectrophotometer showed little change in the peak configuration and background intensities. The relative degree of conversion (DC) of carbon double bonds by radiation to the state of non-radiated samples were estimated by FT-IR. Spectroscopic results were indicative for the formation of cross-linking between carbon chains. Cross-linking of carbon molecules induced by radiation might be one of the reasons for the improved mechanical properties of UDMA resin.

Effect of Cooling Rates on Microstructures of Binary Sn-Ag Solder

T. Kobayashi, J. Tanaka, S. Hayashi, T. Takashima and T. Narita

ICEP,.66-, (2001)

Microstructures of Sn- (2.0, 3.5, and 5.0) mass % Ag solders solidified with cooling rates of 0.015, 12, 48, and 132 K/s were investigated using field emission scanning electron microscope, scanning laser microscope and electron probe micro analyzer. By furnace cooling of 0.015 K/s, a full lamellae structure was obtained for the Sn-3.5Ag, and the primary β -Sn and Ag₃Sn along with lamellae structures were observed for the Sn-2.0Ag and 5.0Ag solders, respectively. With cooling rates higher than 12 K/s the Sn-3.5Ag solder has a primary β -Sn in addition to a lamellae structure. The area fraction of the primary β -Sn phase was between 0.60 and 0.50. For the Sn-5.0Ag solder the Ag₃Sn, β -Sn, and lamellae structure were appeared at cooling rate of 12 K/s. A coupling model could be applied for appearance of the β -Sn for the Sn-3.5 and -5.0Ag when solidified with cooling rates higher than 12 K/s. (Japanese)

Aging Behavior of a Sn-Bi Eutectic Solder at Temperatures between 233 and 373 K

J.N.Hu, H.Tanaka and T.Narita

Materials Transactions, 42, 769-775 (2001)

The hardness of a Sn-Bi eutectic solder was measured as a function of aging time at 233, 298, 323, and 373 K for up to 15.4 Ms, and the time dependence of the hardness could be divided into three stages. At 373 K the hardness decreased up to 259.2 ks (the initial stage) and then increased between 259.2 ks and 1.8 Ms (the transient stage), and beyond 1.8 Ms (the final stage) the hardness tended to decrease gradually. These critical times, 259.2 ks and 1.8 Ms at 373 K, shifted to later at 323 and 298 K, while at 233 K there was little change in the hardness up to about 1 Ms after which hardness decreased rapidly. At an aging temperature of 373 K the area fractions and widths of the Sn and Bi layers in the lamellae structure as well as their lattice constants were determined by microstructural observation, electron probe microanalysis, and X-ray diffraction analysis. The decrease in hardness in the initial aging stage may be due to the disappearance of Bi particles, followed by dissolusion of Bi into the Sn matrix. The rapid increase in hardness in the transient stage could arise from changes in the Sn content in the Bi phase. The decrease in hardness in the final stage could be mainly caused by coarsening the lamellar structure and increases in the area fraction of Sn phase.

Isothermal Solidification Behavior During the Transient Liquid PhaseBonding Process of Nickel Using Binary Filler Metals

T.Shinmura, K.Ohsasa and T.Narita

Materials Transactions, 42, 292-297 (2001)

Transient liquid phase (TLP) bonding process of Ni using Ni-11.0mass%P binary filler metal was simulated by using a mathematical model based on diffusion analysis. In the model, diffusion-controlled transformation was assumed, and the base metal dissolution in the early stage and the subsequent isothermal solidification stage of the TLP bonding process were simulated. The calculated width of the eutectic structure at the bonding region agreed well with the experimental result and showed the validity of the model. In order to obtain the condition to reduce isothermal solidification time, the effect of factors, such as the width of filler metal, diffusivity of solute element in Ni and partition coefficient of element, were investigated by numerical simulation. The simulation showed that isothermal solidification time remarkably decreases with increasing partition coefficient of solute element. In order to confirm the numerical prediction, the TLP bonding experiment of Ni using Cu filler metal was carried out (the partition coefficient of Cu in Ni is close to unity). The experimental result showed that Cu filler metal remarkably shortened the isothermal solidification time and showed the validity of the prediction. (English)

Numerical Simulation of Solidification for Aluminum Base Multi-Component Alloy

K.Ohsasa

Journal of Phase Equilibria 22, 498-503 (2001)

Solidification simulation of an aluminum-base multi-component alloy was carried out by a method combining thermodynamic analysis using Thermo-Calc and heat transfer calculation. An Al-9.5%Si-3%Cu-1%Mg-0.8%Fe aluminum-base multi-component alloy was used for the simulation. The effect of latent heat on the heat transfer calculation was considered by using the enthalpy method. The temperature-enthalpy curves for both an equilibrium state and nonequilibrium state assuming no diffusion in solid were calculated by using the Thermo-Calc. A small casting with a cylindrical shape was used for the heat transfer simulation. The vertical cross section of the casting was divided into rectangular grids, and the enthalpy change of each grid was numerically calculated. The calculated enthalpies in the grids were converted for each time step into temperatures by using the temperature-enthalpy curve. A casting experiment was carried out under the same conditions as those of the simulation, and the calculated cooling curves obtained under the nonequilibrium condition agreed with the experimental ones. (English)

Application of Thermodynamics Analysis to the Heat Transfer Simulation for Multi-Component Alloy Casting

K.Ohsasa

7th Asian Foundry Congress, The Foundrymen's Assotiation, 495-501 (2001)

Solidification simulation of an aluminum-base multi-component alloy was carried out by a method combining thermodynamic analysis using Thermo-Calc and heat transfer calculation. An Al-Si-Cu-Mg-Fe aluminum-base multi-component alloy was used for the simulation. The effect of latent heat on the heat transfer was considered by using the enthalpy calculation temperature-enthalpy curves for both an equilibrium state and nonequilibrium state assuming no diffusion in solid were calculated by using the Thermo-Calc. small casting with a cylindrical shape was used for the heat transfer simulation. The vertical cross section of the casting was divided into rectangular grids, and the enthalpy change of each grid was numerically calculated. The calculated enthalpies in the grids were converted for each time step into temperatures by using the temperature-enthalpy curve. A casting experiment was carried out under the same conditions as those of the simulation, and the calculated cooling curves obtained under the nonequilibrium condition agreed with the experimental ones. Furthermore, the solidification sequence of the multi-component alloy was by using Thermo-Calc, and the calculated solidification behavior of calculated the alloy agreed well with the result of the quenching experiment and demonstrates the efficiency of the thermodynamic calculation for predicting the solidification behavior of aluminum base multi-component alloys. (English)

